The Influence of Rotational Joint Damping In Plane Frames

by

Marino Nader

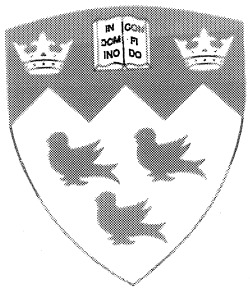

Department of Civil Engineering and Applied Mechanics
McGill University, Montreal, Canada

A thesis submitted to the Faculty of Graduate Studies and Research
in partial fulfillment of the requirements for the degree of
Doctor of Philosophy in Engineering

ABSTRACT

This thesis is concerned with the investigation of the influence of damping on the frequencies of plane frames in the presence of rotational joint damping. Usually damping is ignored in dynamic analysis of structures, or is taken into account using the simple concept of Rayleigh damping. However, damping is always present, and must be considered for a realistic analysis of structures, especially if a matching is desired with frequencies obtained from vibration testing of the structure. In the thesis, the view point is adopted that the damping is caused mainly by the relative slip of the joined parts at various joints of the structure. The slip may either be translational or rotational. However, it appears that purely translational slip is not as significant as that caused by relative rotation of members at a joint. The thesis considers frames in which joints are not perfectly rigid, and hence allow relative rotation of members meeting at the joint. The resistance to the relative rotation is modeled by (1) assigning rotational stiffness to the joints, and (2) by assigning rotational damping coefficients to the joints. The damping is considered to be of the viscous variety, so that the damping moments are proportional to the rotational velocities at the joint.

The resulting problem for free vibrations is a complex-valued eigenvalue problem. The thesis investigates this problem analytically, experimentally and numerically. Exact free vibration analyses were performed for straight beams with translational and rotational dampers at the ends. Experiments were conducted on a simple frame to determine the effect of joint damping on its in-plane frequencies. A finite element program was constructed to determine frequencies of general plane frames in the presence of rotational joint damping.

Résumé

Cette thèse présente une recherche portant sur l'influence de l'amortissement sur les fréquences des cadres en présence d'amortissement de rotation aux joints. Normalement on ne tient pas compte des amortissements dans une analyse dynamique des structures, si ce n'est par le concept d'amortissement de Rayleigh. Toutefois, l'amortissement est toujours présent et doit être pris en considération pour une analyse réaliste des structures surtout si on souhaite obtenir un résultat correspondant aux fréquences obtenues lors des tests de vibration de la structure. Dans cette thèse on considère que l'amortissement provient surtout du glissement se produisant aux parties jointes à plusieurs joints de la structure. Il peut s'agir d'un glissement de translation ou encore de rotation. Il semble toutefois qu'un simple glissement de translation ne soit pas aussi important qu'un glissement de rotation des membrures à un joint. Cette thèse porte sur les cadres dans lesquels les joints ne sont pas parfaitement rigides et permettent donc une certaine rotation des membrures aux joints. On crée un modèle de résistance relative à la rotation en donnant (1) des rigidités de rotation et (2) des coefficients d'amortissement de rotation aux joints. L'amortissement est considéré de type visqueux afin que le moment de glissement soit proportionnel à la vitesse de rotation aux joints.

Le problème résultant des vibrations libres est un problème aux valeurs propres (eigen-value) Dans cette thèse on étudie le problème de façon analytique, expérimentale et numérique. Des analyses précises de vibration libre sont faites pour des poutres droites avec des amortisseurs de translation et de rotation aux extrémités. Des expériences ont été faites sur un cadre simple afin de déterminer l'effet de l'amortissement aux joints sur les fréquences dans le plan du cadre. Un programme d'éléments finis a été créé afin de déterminer les fréquences des cadres en présence d'amortissement de rotation aux joints.

ACKNOWLEDGMENTS

The author would like to thank his research advisor Professor S. C. Shrivastava for all the guidance, encouragement, and support he gave him to pursue this project as a Ph.D. thesis. Prof. Shrivastava devoted copious amounts of his valuable time for all the questions the author had.

Thanks are due to Dr. W. Zheng, Manager, Structures Group, Canadian Space Agency, St. Hubert, Quebec for making available the facilities of the Structures Laboratory of the Agency, and for providing partial financial support. The author would also like to thank Dr. Y. Soucy of the Structures Group for the experimental training he gave to the author.

The author would like to extend special thanks to his parents who were very supportive for the completion of his graduate studies.

TABLE OF CONTENTS

LIST OF MAJOR SYMBOLS

A	=	cross- section area
B_1	=	EI = bending rigidity
B_2	=	$EA = B_1/r^2$ = axial rigidity
c	=	the velocity of sound along the beam length
E	=	Young's modulus
f	=	time dependent force in a SDOF system
F	=	force amplitude
I	=	area moment of inertia
I_m	=	mass moment of inertia
k	=	spring constant
k_{jx}, k_{jy}, k_{jz}	=	joint stiffness at joint j
k_A	=	spring constant of joint A
$[k_{\mathrm{i}}]$	=	global stiffness matrix of element i
$[k_A]$	=	rotation stiffness matrix of joint A
$[K]$	=	global stiffness matrix
$[K^J]$	=	global stiffness matrix for all rotational joints
$[K^M]$	=	member stiffness matrix
L	=	member length
m	=	the number of members meeting at a rotational joint
m	=	mass in a SDOF system
$[m_{\mathrm{i}}]$	=	global mass matrix of element i
M	=	bending moment
M_{Ai}	=	resisting moments applied by the spring to member i at joint A
M'_{Ai}	=	resisting moments applied by the damper to member i at joint A
M_j^L	=	moment at LHS of node j
M_i^R	=	moment at RHS of node i
$\{M^J\}$	=	vector of resisting moments applied by the springs to members
$\{M'^J\}$	=	vector of resisting moments applied by the dampers to members
$[M]$	=	global mass matrix
$[M^M]$	=	member mass matrix
n	=	number of joints

$N(x)$	=	axial force
N_i^R	=	axial force at RHS of node i
N_j^L	=	axial force at LHS of node j
p_1, p_2	=	complex conjugate roots of the characteristic equation
r	=	radius of gyration
$[t_j]$	=	joint transfer matrix at joint j in global co-ordinate system
T_i^M	=	kinetic energy of member i
$[T_j]$	=	joint transfer matrix at joint j in local co-ordinate systems
$[T_{ji}]$	=	6×6 member transfer matrix
u_A	=	x direction translation at joint A
$\dot{u}_A$	=	x direction velocity at joint A
u	=	longitudinal displacement in a beam
U	=	strain energy
U	=	amplitudes of axial displacements
U_A	=	strain energy of joint A
U_j^L	=	axial displacement at LHS of node j
U_i^M	=	strain energy of member i
U_i^R	=	axial displacement at RHS of node i
v_A	=	y direction translation at joint A
$\dot{v}_A$	=	y direction velocity at joint A
V	=	shear force
V_j^L	=	shear force at the LHS of node j
V_i^R	=	shear force at the RHS of node i
w	=	transverse displacement in a beam
W	=	amplitudes of transverse displacements
W_j^L	=	amplitudes of transverse displacements at LHS of node j
W_i^R	=	amplitudes of transverse displacements at RHS of node i
x_0	=	initial displacement
$\dot{x}_0$	=	initial velocity
x	=	displacement of mass in a SDOF system
$\dot{x}$	=	velocity of mass in a SDOF system
$\ddot{x}$	=	acceleration of mass in a SDOF system
x_c	=	complementary function
x_p	=	particular solution
X_p	=	static deflection

$\{X\}$	=	frequency response vector
$\{y\}$	=	$\begin{bmatrix} \{x(t)\} \\ \{\dot{x}(t)\} \end{bmatrix}$
α_{ij}	=	frequency response functions
α_i, α_j	=	inclinations with respect to global X axis
$\{\Delta\}$	=	vector of all global displacement and rotation
$\{\Delta^J\}$	=	vector of the global DOF of all rotational joints
$\{\dot{\Delta}^J\}$	=	velocity vector of the global DOF of all rotational joints
$\{\ddot{\Delta}\}$	=	acceleration vector of the global DOF
C_A	=	rotational damping constant of joint A
$[C^J]$	=	global damping matrix for all rotational joints
γ	=	phase angle
ϵ	=	strain
$\zeta\dot{\omega}$	=	damping component of the complex frequency
θ	=	slope or rotation
θ_{Ai}	=	counterclockwise rotation of member i at joint A
$\dot{\theta}_{Ai}$	=	counterclockwise rotational velocity of member i at joint A
θ_i^R	=	slope at RHS of node i
θ_j^L	=	slope at LHS of node j
λ	=	eigenvalue of damped system
λ_r	=	$-C_r + \sqrt{-1}\omega_{dr}$
λ_{r+1}	=	$\overline{\lambda}_r$, conjugate of λ_r
$\overline{\lambda}_r$	=	$-C_r - \sqrt{-1}\omega_{dr}$
μ	=	eigenvalue of undamped system
ξ	=	x/L. a non-dimensional variable of position
$\{\phi\}$	=	mode shape vector of damped system
$\{\phi_1\}$	=	mode shape vector of undamped system
$\{\psi_i\}$	=	mass-normalized mode shape vector i
ω	=	natural frequency
ω_d	=	damped natural frequency
Ω	=	driving frequency

Table of Conversion Factors

Quantity	Conversion from Imperial to SI
Length	$1\text{in} = 0.0254\,\text{m}$
Maas	$1\text{ slug} = 14.594\,\text{kg}$
Density	$1\text{ slug/ft}^3 = 515.38\,\text{kg/m}^3$
Force	$1\text{ lb} = 4.4482\,\text{N}$
Stress	$1\text{ psi} = 6894.8\,\text{N/m}^2\text{(Pa)}$

LIST OF FIGURES

LIST OF TABLES

CHAPTER 1

INTRODUCTION

1.1 Introduction to the Topic

Structural analysis using the FE method has become very widely spread for its efficiency and affordability. However, it does not precisely analyze the real physical structure due to many inaccuracies, especially when the structure is subjected to dynamic loading, in which case the discrepancies might increase. These data inaccuracies are due to lack of the physical information, for example, boundary conditions, material properties or material imperfections, imprecise dimensional data, inappropriate damping representation, and inadequate joints modeling. Finite element codes also do not provide consistent modeling options. For example, NASTRAN uses the lumped or coupled mass matrices for beam elements although, usually, consistent mass matrices are used in other finite element codes.

On the other hand, in experimental structural dynamics the data are necessarily incomplete due to the inadequacy of measurements arising from limitations on resources and available equipment. Rotational degrees of freedom (DOF) are usually not measured so that the number of DOF in the analysis are always greater than the measured ones. This spatial incompleteness eventually requires reduction of the analytical data or the expansion of the measured ones by some means. The measured data may contain signal processing errors such as aliasing and leakage. In addition, systematic errors like insufficient rigidity of supports or absence of perfect free-free conditions are present. These errors may cause difficulty in obtaining reliable data for comparison with FE results.

In space structures the mass of the payload plays an important role for mission suitability. The design objective is to construct a mass-efficient structure which can be relied upon to deliver the desired performance in space. This objective requires extensive analyses

under different loading conditions, which in turn demands a realistic finite element modeling of the structure. The validity of such a finite element model is established by laboratory testing of some prototypes of the structure with the expectation that the measured response is predictable by the constructed model within an acceptance criterion. This acceptance criterion may, for example, require that for a finite element model to be acceptable there be a reasonable ($\pm$ 5 %) match between say the first ten predicted and measured frequencies. Such a stringent criterion will usually necessitate a repeated refinement, i.e. updating, of the FE model by considering all possible sources of discrepancies in the model. In civil engineering structures, the effect of damping is usually not a major issue. However, it can be important in the case of earthquake resistant design of structures.

Damping is often ignored in finite element modeling of a structure. Therefore, logically, one cannot expect realistic predictions from such a FE model unless the structure has no damping. A common source of damping in frame structures is due to relative motion, i.e. slippage, of members meeting at a joint. It has been observed experimentally that more than 50 % of damping occurs at the structural joints [1, 2]. Thus, to account for damping in frame structures, modeling of joint damping in FE models is an obvious necessity. It also follows that in frame structures, the large axial stiffness of beams and columns would significantly inhibit translational slip at the joints. Hence it appears that rotational slip and hence rotational damping is the more likely mechanism of energy dissipation in frame structures [1, 2]. The thrust of this thesis is to include this latter type of damping in the updating of the FE models of the structures.

When damping is taken into account in dynamic analysis of structure, it is usually done by using the concept of Rayleigh damping or proportional damping, i.e. by assuming the damping matrix to be proportional to the mass and stiffness matrices. In other words, damping is characterized by using just two proportionality constants [3] regardless of how complex the structure is. This concept, although popular for its mathematical convenience, cannot be expected to represent the damping characteristics of a structure in a physically meaningful way. Almost all FE codes provide the option of using proportional damping.

In view of the experimental evidence pointing to the importance of energy dissipation at joints [1, 2], the objective of this thesis is to investigate the effect of rotational joint damping on the vibrational characteristics of frame structures. Three aspects have been

pursued in this thesis (i) theoretical – to demonstrate by exact analysis the effect of rotational joint damping on the frequencies of simple structures, for example, beams and simple 2 D frames, (ii) experimental – to validate the theoretical conclusions and, (iii) numerical – to implement the theory in a general finite element program. For simplicity the attention will be restricted to the viscous variety of damping.

Needless to say, although this research was undertaken with the main motivation of updating of the finite element models of space structures it has wide applicability to all structures wherever joint damping is important be it in civil, mechanical, or aerospace structures.

1.2 General Literature Review

Damping is a very large field. There are many papers written on various aspects of this field (see section 1.3). However, the subject of this thesis, i.e. The Influence of Rotational Joint Damping In Plane Frames, is a specialized field with little previous work. The most pertinent references which the author could locate are by Beards, [1, 2]. The first paper: "The Damping of Structural Vibration by Rotational Slip in Joints" was published in 1977, and the second paper: "Damping in Structural Joints", was published in 1985. Both papers describe the experimental work proving that dissipation of energy takes places mostly at the joints by virtue of slip and friction. In the second paper it is stated that, "... about 90% of the total damping in a structure originates in the joints....". The papers are qualitative, with no formulation for structural analysis. It appears that such analyses are not available even now. This lack of quantitative analysis provides the motivation to investigate the effect of joint damping in theoretical and structural FE analyses.

Experimental modal analysis plays an essential part in updating of the FE models. There is considerable knowledge on the subject of modal analysis. The classical paper on this subject is by Bishop and Gladwell [4]. This pioneering work has been followed in more recent times by Ewins [5] and his associates [6]. In the updating of FE models the calculated frequencies and mode shapes are correlated with those obtained experimentally. Checks on the appropriateness of the frequency match are performed by computing the Modal Assurance Criteria (MAC) matrix [7, 8]. This computation involves both the analytical and the experimental mode shapes. A diagonal MAC value close to 1 indicates strong correlation between the modes. A further correlation check is the Pseudo

Orthoganality Check (POC). The POC is based on the orthogonality of the mass-normalized modes [7, 9]. The correlation is considered good if the off-diagonal terms of the POC matrix are less than 0.05 and diagonal values higher than 0.95 [10,11]. POC requires reduction of the mass matrix to the size of the experimental modes. This reduction is achieved by the SEREP formula [7].
The correlation techniques mentioned above form the basis for decisions on updating of the FE models. The various parameters which can be modified for updating are discussed in the book by Friswell and Mottershead [10]. Damping is noticeably absent from these parameters.

1.3 Bibliography On Damping

As mentioned before the topic of damping is an extensive one. There are a number of references which the reader may consult, some of which are listed in the Bibliography section at the end of the thesis. These references, athough important from the general point of view, are not directly connected to this thesis. The sole reason for giving this list is to give the reader an idea about the diversity of the subject matter.

1.4 Thesis Overview

The thesis comprises of seven chapters:

Chapter 1 is the present chapter which introduces the subject and its significance in structural dynamics, especially in relation to updating of FE models of space structures. It also gives a review of the most relevant literature on this topic.

Chapter 2 presents the theoretical background of the lumped mass dynamic systems for single degree of freedom (SDOF) and multi degree of freedom (MDOF) systems for undamped and damped free vibration. It also presents the forced vibration of these systems under harmonic excitations. The ensuing mathematical problem leads to a generalized eigenvalue problem for undamped cases, and to a quadratic eigenvalue problem for damped ones. The chapter is slanted to the theory of experimental modal analysis.

Chapter 3 deals with the exact free vibration analysis of a cantilever beam with rotational or translational dampers present at the "free" end. This chapter illustrates the significance of rotational damping on the frequencies of such structures.

Chapter 4 describes the experiment on a simple frame conducted by the author at the Structures Laboratory of the Canadian Space Agency (CSA).

Chapter 5 deals with the exact theoretical frequency analysis of straight and bent beams. The method of analysis is based on the transfer matrix approach. It calculates the exact frequencies of the frame tested at the CSA described in chapter 4. It establishes benchmark frequencies which can be used for validating FE results.

Chapter 6 formulates the FE implementation of the theory for taking into account the finite rotational joint stiffness and joint rotational damping. Three frames of increasing complexity were analyzed by a general MatLab program constructed by the author. Extensive verification of the obtained results was performed by constructing independent Mathematica programs for the damped cases and also by using the NASTRAN finite element package for the undamped cases.

Chapter 7 highlights the principal findings of the research, and suggests topics for further investigation.

1.5 Originality of Contributions

The major original contributions reported in this thesis are as follow:

- The concept of rotational joint damping was introduced in the dynamic analysis of frame structures. To the author's knowledge the implementation of this concept for updating of 2D frames has not been presented in the literature.

- An original experiment was designed for a 2D frame structure to test the influence of rotational joint damping.

- The construction and validation of a finite element program incorporating the rotational joint damping concept, and calculating for plane frame structures the complex damped frequencies and the associated mode shapes.

CHAPTER 2

SINGLE AND MULTI-DEGREE-OF-FREEDOM SYSTEMS

The purpose of this chapter is to present the theory of vibration of discrete systems defined by masses interconnected by linear elastic springs and linear viscous dashpots. Free as well as forced vibrations are considered. The theory is well known [5], but is presented here for completeness and easy reference, and for emphasizing the role of damping which has the most bearing on the subject matter of this thesis.

First free vibrations of a single-degree-of-freedom (SDOF) system, without and with damping, are considered. Then, forced vibrations are considered, but only for harmonic applied forces as being relevant to the thesis. The theory is then extended to free and forced vibrations of multi degree of freedom (MDOF) systems with and without damping.

2.1 Vibrations of a Damped and Undamped SDOF System

The SDOF system is the simplest form of spatial representation of a structure. It can be represented by the mechanical model of Fig. 2.1. It consists of a rigid body of mass m, connected to a fixed support by a spring of constant k, and a dashpot of damping coefficient C. It slides on a frictionless surface. Let $x(t)$ be the displacement of the mass from its equilibrium position, $\dot{x}(t)$ its velocity, and $f(t)$ the external force acting on it at time t.

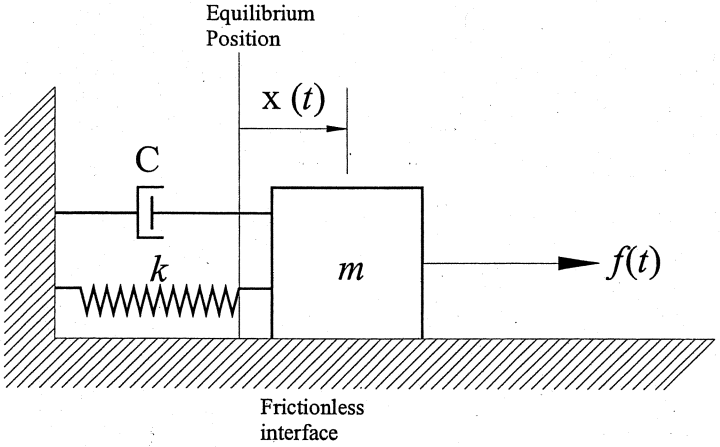

Fig. 2.1: Single degree of freedom system.

The extension of the spring is $x(t)$ and the force exerted on the mass is $-k\,x(t)$. The damping force $-C\,\dot{x}(t)$ is of the viscous variety, proportional to the velocity and provided (conceptually) by a dashpot filled with a fluid of viscosity C. The free body

diagram of the mass leads to the following ordinary differential equation of motion for the displacement $x(t)$:

$$m\,\ddot{x}\,(t) + C\,\dot{x}\,(t) + k\,x(t) = f(t) \tag{2.1}$$

The solution consists of the sum of a complementary function obtained by solving the equation with $f(t) = 0$, and a particular solution with $f(t) \neq 0$.

(a) Complementary Function

In the absence of any applied force, the equation to be solved is

$$m\,\ddot{x}\,(t) + C\,\dot{x}\,(t) + k\,x(t) = 0. \tag{2.2}$$

It is called the homogeneous equation, and its solution, $x_c(t)$, is known as the complementary function. Substitution of a solution form $x_c(t) = Ae^{pt}$ gives the characteristic equation

$$mp^2 + Cp + k = 0 \tag{2.3}$$

which determines its two roots as

$$p_1,\, p_2 = -\frac{C}{2m} \pm i\sqrt{\frac{k}{m} - \frac{C^2}{4m^2}}. \tag{2.4}$$

Introducing the symbols

$$\zeta\omega = \frac{C}{2m}, \omega^2 = \frac{k}{m},\ \omega_d^2 = \omega^2 - \zeta^2\omega^2,\ C_{\text{cr}} = \sqrt{4km} \tag{2.5}$$

the two roots can be expressed as

$$p_1,\, p_2 = -\zeta\omega \pm i\omega_d \tag{2.6}$$

and therefore the complementary function as

$$x_c(t) = A_1 e^{-(\zeta\omega - i\omega_d)t} + A_2 e^{-(\zeta\omega + i\omega_d)t} \tag{2.7}$$

where A_1 and A_2 are arbitrary constants. The symbol ω is called the natural frequency of the system, and the symbol $\zeta\omega$ stands for the damping coefficient. Both of these quantities are characteristic of the system and can be varied independently. However, $\omega_d = \omega\sqrt{1-\zeta^2}$ is a quantity dependent on ω and $\zeta\omega$.

For an under-damped system, defined by $C < C_{cr}$ or $\zeta < 1$, ω_d is real and is called the damped frequency. For such cases, the solution is oscillatory with decaying amplitude:

$$x_c(t) = e^{-\zeta\omega t}(A\cos\omega_d t + B\frac{\sin\omega_d t}{\omega_d}) \tag{2.8}$$

where A and B are arbitrary constants.

For a critically damped system, defined by $C = C_{cr}$ or $\zeta\omega = \omega$, one finds $\omega_d = 0$; the solution looses its oscillatory characteristic by assuming the form

$$x_c(t) = e^{-\zeta\omega t}(A + Bt). \tag{2.9}$$

For an over-damped system, $C > C_{cr}$ or $\zeta\omega > \omega$, $\sqrt{\omega^2 - \zeta\omega^2}$ becomes purely imaginary equal to $i\omega_d$, and correspondingly the solution is again non-oscillatory, of the form

$$x_c(t) = e^{-\zeta\omega t}(A\cosh\omega_d t + B\frac{\sinh\omega_d t}{\omega_d}) \tag{2.10}$$

As a conclusion, we can say that the free vibration response of a damped single degree of freedom (SDOF) system is oscillatory only if the damping is below its critical value. Conversely, we may think of the critical damping as the dividing line between the oscillatory and non oscillatory behaviours of the system when it is excited by some initial input of energy via initial displacement or initial velocity.

(b) Particular Solution for a Harmonic Applied Force

Consider the mass to be acted upon by a harmonic force $f(t) = Fe^{i(\Omega t - \gamma_f)}$, of frequency Ω and amplitude F. The constant γ_f, called the initial phase, is related to the position of force peaks on the time scale. The peaks occur at $t = \dfrac{\gamma_f + n\pi}{\Omega}$ where n is an integer. For simplicity we take $\gamma_f = 0$ which only means a shift of time origin. For $\Re e Fe^{i\Omega t} = F\cos\Omega t$, the response is the real part of the solution $\Re e\ x_p(t)$.

When damping is absent, i.e., when $\zeta\omega = 0$, the response is always oscillatory. For $\Omega \neq \omega$, it is expressible as:

$$x_p(t) = \alpha F e^{i\Omega t},\ \text{with}\ \alpha = \alpha(\Omega) = \frac{1/m}{\omega^2 - \Omega^2} = \frac{1}{2\omega m}\{\frac{1}{\omega + \Omega} + \frac{1}{\omega - \Omega}\} \tag{2.11}$$

where $\alpha = \alpha(\Omega)$, being a function of Ω, is known as the frequency response function (FRF). Equivalently we may write, using the polar representation of a complex number

$$x_p(t) = X_p e^{i(\Omega t - \gamma)},\ \text{with}\ X_p = F\|\alpha\| = F\frac{1/m}{\sqrt{(\omega^2 - \Omega^2)^2}}\ \text{and} \tag{2.12}$$

$$\gamma = \arg(\alpha) = \tan^{-1}\frac{\mathfrak{Im}(\alpha\}}{\mathfrak{Re}(\alpha)} = 0 \text{ for } \Omega < \omega \text{ and } \gamma = \pi \text{ for } \Omega > \omega.$$

X_p is always positive, and the sign change in the response is accounted for by change in the phase angle γ. At $\Omega = 0$, the applied force is static and the response is $X_p = \frac{F}{k}$ = the static deflection. For, $\Omega < \omega$, i.e., for driving frequencies smaller than the natural frequency, the response $x_p(t)$ is oscillatory and in phase with the force, $\gamma = 0$. On the other hand, for driving frequencies greater than the natural frequency, $\Omega > \omega$, the response $x_p(t)$ is out of phase, $\gamma = \pi$.

When $\Omega = \omega$, the solution changes to

$$x_p(t) = X_p\, e^{i(\Omega t - \gamma)} \text{ with } X_p = \frac{F}{m}\frac{t}{2\omega} \text{ and } \gamma = \pi/2 \tag{2.13}$$

which shows that at $\Omega = \omega$, the amplitude $X_p = \frac{F}{m}\frac{t}{2\omega}$ of the response oscillations grows unbounded, proportionally with time t. This growth in time is called resonance. We say that resonance occurs in absence of damping when the driving frequency coincides with the natural frequency of the system.

When damping is present, $\zeta\omega \neq 0$, the response $x_p(t)$ to $f(t) = Fe^{i\Omega t}$ may be expressed as

$$x_p(t) = \alpha\, f(t) = \alpha F e^{i\Omega t} \tag{2.14}$$

where α, the frequency response function (FRF), is now a complex valued function of Ω:

$$\alpha = \alpha(\Omega) = \frac{1/m}{\omega^2 - \Omega^2 + 2i\zeta\omega\Omega} \tag{2.15}$$

Equivalently, we may write, using the polar form of a complex number

$$x_p(t) = X_p e^{i(\Omega t - \gamma)} \tag{2.16}$$

where the amplitude X_p and the phase γ and their connection to the FRF are given by

$$X_p = F \times \text{magnitude of } \alpha = F\frac{1/m}{\sqrt{(\omega^2 - \Omega^{2)^2} + 4\zeta^2\omega^2\Omega^2}}, \tag{2.17}$$

$$\gamma = \text{phase difference} = \arg(\alpha) = \tan^{-1}\frac{2\zeta\omega\Omega}{(\omega^2 - \Omega^2)} \tag{2.18}$$

Equation (2.16) shows that damping causes a time lag $\frac{\gamma}{\Omega}$ in the response peaks relative to the force peaks. This shift determined experimentally can give information on damping of the system. Equation. (2.18) shows that γ varies from 0 to π, as Ω sweeps from 0 to ∞. At $\Omega = \omega$, $\gamma = \pi/2$ regardless of the damping.

Due to damping, X_p remains bounded for all Ω. It can be easily shown that the maximum amplitude X_p as a function of Ω occurs at $\Omega = \sqrt{\omega^2 - 2\zeta\omega^2}$, i.e. at a frequency less than the resonance frequency and $X_p(\max) = \frac{F}{k}\frac{\omega}{2\zeta\omega\sqrt{1-\zeta\omega^2/\omega^2}}$. Exactly at the resonance frequency $\Omega = \omega$, we have $x_p(t) = X_p\, e^{i(\Omega t - \alpha - \pi/2)}$ with $X_p = \frac{F}{k}\frac{\omega}{2\zeta\omega}$. The complete solution of the equation of motion, for $f(t) = F\cos\Omega t$, is

$$x(t) = Ae^{-\zeta\omega t}\cos\omega_d t + Be^{-\zeta\omega t}\frac{\sin\omega_d t}{\omega_d} + X_p\cos(\Omega t - \gamma). \tag{2.19}$$

where X_p and γ are different functions of Ω depending upon $\omega^2 - \Omega^2$ being positive, zero, or negative as described above. Initial displacement x_0 and initial velocity $\dot{x}_0$ determine the arbitrary constants A and B to yield the complete solution as

$$x(t) = e^{-\zeta\omega t}\{x_0 - X_p\cos\gamma\}\cos\omega_d t + e^{-\zeta\omega t}\{\dot{x}_0 + \zeta\omega A - \Omega X_p\sin\gamma\}\frac{\sin\omega_d t}{\omega_d} + X_p\cos(\Omega t - \gamma). \tag{2.20}$$

If the interest is focussed on longtime response, $t \gg \frac{1}{\zeta\omega}$, the terms with exponential decay approach zero, and then effectively $x(t) = X_p\cos(\Omega t - \gamma)$. This part of the response in (2.17) is called the steady-state response.

To reiterate their importance to this thesis, we recall the relations of the response amplitude X_p and phase angle γ to the frequency response function α(FRF)

$$\frac{X_p}{F} = \|\alpha\| = \left\|\frac{1/m}{\omega^2 - \Omega^2 + 2i\zeta\omega\Omega}\right\| = \frac{1/m}{\sqrt{(\omega^2-\Omega^2)^2 + 4\zeta\omega^2\Omega^2}}$$
$$\gamma = \arg(\alpha) = \tan^{-1}\frac{-\mathfrak{Im}\,\alpha}{\mathfrak{Re}\,\alpha} = \tan^{-1}\frac{2\zeta\omega\Omega}{\omega^2 - \Omega^2} \tag{2.21}$$

One can determine $\|\alpha\|$ experimentally by plotting X_p/F data as a function of Ω in a vibration test, and may estimate, by curve fitting Eq. (2.21) to these data, the natural frequency ω and the damping coefficient $\zeta\omega$ of the SDOF system.

2.2 Vibrations of an Undamped MDOF System

We first present the easier case of vibrations of an undamped multi-degree-of-freedom system. The general equations of motion of a MDOF system, with no damping, can be written in the matrix form as

$$[M]\{\ddot{x}(t)\} + [K]\{x(t)\} = \{F(t)\} \tag{2.22}$$

where $[M] = n \times n$ size mass matrix, $[K] = n \times n$ size stiffness matrix, $\{x\} = n \times 1$ size vector of displacements, $\{F\} = n \times 1$ size vector of applied forces. In index notation, using the summation convention, the above equation is expressible as

$$M_{ij}\ddot{x}_j(t) + K_{ij}x_j(t) = F_i(t) \tag{2.23}$$

where i and j range from 1 to n.

2.2.1 Free Undamped Vibrations of a MDOF System

Consider first free undamped vibrations. Then, there are no applied forces, i.e. $\{F\} = 0$. Hence, the motion is started by imparting initial displacements $\{x_0\}$, or equivalently a strain energy $\frac{1}{2}\{x_0\}^T[K]\{x_0\}$, and velocities $\{\dot{x}_0\}$ to the masses, or equivalently a kinetic energy $\frac{1}{2}\{\dot{x}_0\}^T[M]\{\dot{x}_0\}$. The equations of motion, as a statement of the conservation of the initially supplied total energy, are

$$[M]\{\ddot{x}(t)\} + [K]\{\dot{x}(t)\} = \{0\} \tag{2.24}$$

For a solution we assume

$$\{x\} = \{\phi\}e^{i\omega t} \tag{2.25}$$

where ω is a natural frequency of vibration, and $\{\phi\}$ is the corresponding mode shape. When substituted in Eq. (2.24) it is found that

$$[-\omega^2[M] + [K]]\{\phi\} = \{0\} \tag{2.26}$$

For a solution of the assumed type, $\{\phi\} \neq \{0\}$, ω^2 must be a root of the equation

$$\det[-\omega^2[M] + [K]] = \{0\} \tag{2.27}$$

called the frequency equation. This is a polynomial equation of nth degree in ω^2, and has consequently $2n$ real roots $\pm\omega_i$, some of which may be repeated roots. We arrange frequencies in ascending order so that ω_1 is the lowest (i.e., fundamental) frequency and

ω_n is the highest frequency. For each $\pm\omega_i$ so found, we can obtain a mode shape vector $\{\phi_i\}$ by solving $[-\omega_i^2[M] + [K]]\{\phi_i\} = \{0\}$. Thus, for distinct ω_i^2 and ω_j^2 we have

$$\begin{aligned}[-\omega_i^2[M] + [K]]\{\phi_i\} &= \{0\} \\ [-\omega_j^2[M] + [K]]\{\phi_j\} &= \{0\}\end{aligned} \tag{2.28}$$

The symmetries of both $[M]$ and $[K]$ lead to the orthogonality conditions for the modes:

$$\{\phi_i\}^T[M]\{\phi_j\} = \overline{m}_i\delta_{ij} \tag{2.29}$$

where δ_{ij} is the Kronecker delta, $\delta_{ij} = 1$ for $i = j$ and $\delta_{ij} = 0$ for $i \neq j$. Introducing mode shapes $\{\psi_i\}$ scaled as

$$\{\psi_i\} = \frac{1}{\sqrt{\overline{m}_i}}\{\phi_i\} \tag{2.30}$$

the orthogonality condition is simplified to become

$$\{\psi_i\}^T[M]\{\psi_j\} = \delta_{ij} \tag{2.31}$$

The mode shapes $\{\psi_i\}$ are called mass-normalized mode shapes. Using these mode shapes, the second orthogonality condition is found as

$$\{\psi_i\}^T[K]\{\psi_j\} = \omega_i^2\delta_{ij} \tag{2.32}$$

The orthogonality relations (2.31) and (2.32) are useful in solving forced vibration problems as will be shown below. The general solution of Eq. (2.24) can therefore be expressed as

$$\begin{aligned}\{x_c\} = c_1\{\psi_1\}\cos\omega_1 t + c_2\{\psi_2\}\cos\omega_2 t + \ldots c_n\{\psi_n\}\cos\omega_n t \\ + d_1\{\psi_1\}\sin\omega_1 t + d_2\{\psi_2\}\sin\omega_2 t + \ldots d_n\{\psi_n\}\sin\omega_n t\end{aligned} \tag{2.33}$$

where c_1, c_2, $\ldots c_n$ and d_1, d_2, $\ldots d_n$ are arbitrary constants to be determined from the imposed initial displacements and velocities: $\{x_0\} = x\{0\}$ and $\{\dot{x}_0\} = \dot{x}\{0\}$. We have

$$\{x_0\} = c_1\{\psi_1\} + c_2\{\psi_2\} + \ldots c_n\{\psi_n\} = \sum_{k=1}^{n} c_k\{\psi_k\} \tag{2.34}$$

$$\{\dot{x}_0\} = \omega_1 d_1\{\psi_1\} + \omega_2 d_2\{\psi_2\} + \ldots \omega_n d_n\{\psi_n\} = \sum_{k=1}^{n} \omega_k d_k\{\psi_k\} \tag{2.35}$$

Then, using the orthogonality of the modes, we find

$$c_k = \{\psi_k\}^T[M]\{x_0\} \text{ and } d_k = \frac{\{\psi_k\}^T[M]\{\dot{x}_0\}}{\omega_k} \tag{2.36}$$

The complementary solution can therefore be written as

$$\{x_c\} = [\cos\omega_1 t\,\{\psi_1\}\{\psi_1\}^T + \cos\omega_2 t\{\psi_2\}\{\psi_2\}^T + \ldots\cos\omega_n t\{\psi_n\}\{\psi_n\}^T][M]\{x_0\}$$

$$+ [\sin\omega_1 t\frac{\{\psi_1\}\{\psi_1\}^T}{\omega_1} + \sin\omega_2 t\frac{\{\psi_2\}\{\psi_2\}^T}{\omega_2} + \ldots\sin\omega_n t\frac{\{\psi_n\}\{\psi_n\}^T}{\omega_n}][M]\{\dot{x}_0\} \tag{2.37}$$

Succinctly, we may write the above as

$$\{x_c\} = \sum_{k=1}^{n}\{A_k\}\cos\omega_k t + \sum_{k=1}^{n}\{B_k\}\frac{\sin\omega_k t}{\omega_k} \tag{2.38}$$

where

$$\{A_k\} = \{\psi_k\}\{\psi_k\}^T[M]\{x_0\},\ \{B_k\} = \{\psi_k\}\{\psi_k\}^T[M]\{\dot{x}_0\} \tag{2.39}$$

It is clear from the above equation that an energy input may excite all the modes. The single-degree-of-freedom solution, $x_c = x_0\cos\omega_1 t + \dot{x}_0\frac{\sin\omega_1 t}{\omega_1}$, is recovered by substituting $\psi_1 = 1/\sqrt{m}$, $\psi_j = 0$ for $j \neq 1$, $[M] = m$.

2.2.2 Forced Undamped Vibrations

The equations of motion for forced vibration is

$$[M]\{\ddot{x}(t)\} + [K]\{\dot{x}(t)\} = \{F(t)\} \tag{2.40}$$

We restrict consideration to the loading of the type

$$\{F(t)\} = \{F\}e^{i\Omega t} \tag{2.41}$$

which implies that all loads are harmonic and are applied with a common frequency Ω and common phase angle $\gamma_f = 0$. $\{F\}$ is therefore the vector of force magnitudes which may be different for each degree of freedom. For such a loading we expect the response to be harmonic of the same frequency Ω. Thus we assume

$$\{x\} = \{X\}e^{i\Omega t} \tag{2.42}$$

Substitution of (13) and (14) in (12) gives the matrix equation

$$[-\Omega^2[M] + [K]]\{X\} = \{F\} \tag{2.43}$$

The objective is to find $\{X\}$ given $\{F\}$. We determine $\{X\}$, not by numerical inversion, but by using the orthogonality properties of the mode shapes $[Ewing]$. Let $\{X\}$ be expressed as a linear combination of mode shapes :

$$\{X\} = \{\psi_1\}Y_1 + \{\psi_2\}Y_2 + \ldots\{\psi_n\}Y_n = [\psi_1\, \psi_2 \ldots\ \psi_n]\{Y\} = [\psi]\{Y\} \tag{2.44}$$

or in index notation

$$X_i = \psi_{ij}Y_j \tag{2.45}$$

where ψ_{ij} = the i^{th} element of the j^{th} mode shape. Determining $\{Y\}$ determines $\{X\}$. Substituting equation (2.44) in equation (2.43) and pre multiplying the whole equation by $[\psi]^T$, we obtain

$$[-\Omega^2[\psi]^T[M][\psi] + [\psi]^T[K][\psi]]\{Y\} = [\psi]^T\{F\} \tag{2.46}$$

which by virtue of the orthogonality of the mass-normalized mode shapes gives

$$\left[-\Omega^2 + \omega_i^2\right]\{Y\} = [\psi]^T\{F\} \tag{2.47}$$

$$\{Y\} = \left[\frac{1}{\omega_i^2 - \Omega^2}\right][\psi]^T\{F\} \tag{2.48}$$

where $\left[\frac{1}{\omega_i^2 - \Omega^2}\right]$ is a diagonal matrix. Since $\{X\} = [\psi]\{Y\}$, we obtain

$$\{X\} = [\psi]\left[\frac{1}{\omega_i^2 - \Omega^2}\right][\psi]^T\{F\} \tag{2.49}$$

In index notation, this result can be expressed as

$$X_i = \psi_{ij}\frac{\delta_{jk}}{\omega_j^2 - \Omega^2}\psi_{mk}F_m \tag{2.50}$$

When expanded, we find for a typical i

$$X_i = \{\frac{\psi_{i1}\psi_{11}}{\omega_1^2 - \Omega^2} + \frac{\psi_{i2}\psi_{12}}{\omega_2^2 - \Omega^2} + \ldots\frac{\psi_{in}\psi_{1n}}{\omega_n^2 - \Omega^2}\}F_1 + \{\frac{\psi_{i1}\psi_{21}}{\omega_1^2 - \Omega^2} + \frac{\psi_{i2}\psi_{22}}{\omega_2^2 - \Omega^2} + \ldots\frac{\psi_{in}\psi_{2n}}{\omega_n^2 - \Omega^2}\}F_2$$

$$+ \ldots\{\frac{\psi_{i1}\psi_{n1}}{\omega_1^2 - \Omega^2} + \frac{\psi_{i2}\psi_{n2}}{\omega_2^2 - \Omega^2} + \ldots\frac{\psi_{in}\psi_{nn}}{\omega_n^2 - \Omega^2}\}F_n \tag{2.51}$$

Writing the above equation as $X_i = \alpha_{ij}(\Omega)F_j$, we identify

$$\alpha_{ij}(\Omega) = \{\frac{\psi_{i1}\psi_{j1}}{\omega_1^2 - \Omega^2} + \frac{\psi_{i2}\psi_{j2}}{\omega_2^2 - \Omega^2} + \cdots \frac{\psi_{in}\psi_{jn}}{\omega_n^2 - \Omega^2}\} = \sum_{p=1}^{n} \frac{\psi_{ip}\psi_{jp}}{\omega_p^2 - \Omega^2} \tag{2.52}$$

as the $n \times n$ frequency response functions (FRF) for an undamped n-degree-of-freedom system. A typical term in $\alpha_{ij}(\Omega)$, say the pth term, is the product of the pth elements of ith and jth normalized eigen-vectors. Each FRF assumes an infinite value when the driving frequency Ω coincides with any of the natural frequencies ω_p. The graph of any $\alpha_{ij}(\Omega)$ as a function of Ω will have n peeks at values of $\Omega = \omega_i$ $(i = 1, 2, 3, \ldots n)$. For the case of a single-degree-of-freedom system, the FRF is $\alpha_{11} = \dfrac{1/m}{\omega_1^2 - \Omega^2}$, the same as obtained directly in section 2.1.

2.3 Damped Vibrations of MDOF System

This subsection is important for this thesis. The equations of motion of a multi-degree-of-freedom system with viscous damping can be written in the matrix form as

$$[M]\{\ddot{x}(t)\} + [C]\{\dot{x}(t)\} + [K]\{x(t)\} = \{F(t)\} \tag{2.53}$$

where $[C] = n \times n$ size damping matrix. In index notation, the above equation is

$$M_{ij}\ddot{x}_j(t) + C_{ij}\dot{x}_j(t) + K_{ij}x_j(t) = F_i(t) \tag{2.54}$$

The application to a particular physical system (for example a cantilever beam) would require definition of its mass density, the stiffness, and the damping coefficients. Rotational joint damping can also be included into the $[C]$ matrix (see Chapter 6). The particular values of the material properties can be obtained from experiments or handbooks. Different materials have different damping coefficients, i.e. steel, concrete (cracked or uncracked) and wood all have different coefficients of damping, stiffnesses and mass densities.

2.3.1 Force-free damped vibrations

We first find the solution for force-free damped vibrations, when $F_i(t) \equiv 0$, i.e., for

$$[M]\{\ddot{x}(t)\} + [C]\{\dot{x}(t)\} + [K]\{x(t)\} = \{0\} \tag{2.55}$$

This form of the matrix eigenvalue problem, for a general damping matrix $[C]$, does not admit a solution for which modes are orthogonal. Following Ewins [5] and Mia and Silva [6] we therefore recast the above equation in a manner that entails orthogonality. We write the above equation as the following $2n$ equations:

$$\begin{bmatrix} [C] & [M] \\ [M] & [0] \end{bmatrix} \begin{bmatrix} \{\dot{x}(t)\} \\ \{\ddot{x}(t)\} \end{bmatrix} + \begin{bmatrix} [K] & [0] \\ [0] & -[M] \end{bmatrix} \begin{bmatrix} \{x(t)\} \\ \{\dot{x}(t)\} \end{bmatrix} = \begin{bmatrix} 0 \\ 0 \end{bmatrix} \tag{2.56}$$

where the second matrix equation is in fact an identity. The expanded matrix equation may be written as

$$[A]\{\dot{y}\} + [B]\{y\} = \{0\} \tag{2.57}$$

where

$$[A] = \begin{bmatrix} [C] & [M] \\ [M] & [0] \end{bmatrix}, [B] = \begin{bmatrix} [K] & [0] \\ [0] & -[M] \end{bmatrix}, \text{ and } \{y\} = \begin{bmatrix} \{x(t)\} \\ \{\dot{x}(t)\} \end{bmatrix} \tag{2.58}$$

This device renders $[A]$ and $[B]$ to be symmetric matrices, and the mode shapes of the modified system orthogonal. We assume a solution in the form

$$\{y\} = \{\phi\}e^{pt} \tag{2.59}$$

which requires that p be the roots of the frequency equation

$$\det[p[A] + [B]] = 0 \tag{2.60}$$

which is a polynomial equation of degree $2n$ in p with real coefficients. Accordingly, $\overline{p}$, the conjugate of p is also a root. Additionally, if the mode shape corresponding to p_1 is $\{\phi_1\}$ then that corresponding to $p_2 = \overline{p}_1$ is $\{\phi_2\} = \{\overline{\phi}_1\}$. The orthogonality conditions follow from the symmetry of $[A]$ and $[B]$, so that for distinct roots p_i and p_j the corresponding mode shapes obey

$$\{\phi_i\}^{\mathrm{T}}[A]\{\phi_j\} = a_j\delta_{ij} \tag{2.61}$$

Introducing normalized mode shapes as

$$\{\psi_i\} = \frac{1}{\sqrt{a_i}}\{\phi_i\} \tag{2.62}$$

the orthogonality conditions are then expressible as

$$\{\psi_i\}^{\mathrm{T}}[A]\{\psi_j\} = \delta_{ij} \text{ and } \{\psi_i\}^{\mathrm{T}}[B]\{\psi_j\} = -p_i\delta_{ij} \tag{2.63}$$

We leave the free damped vibration at this stage, and consider the forced damped vibrations of multi-degree-of-freedom systems as more relevant to the present work.

2.3.2 Forced damped vibrations

The pertinent equations of motion driven by sinusoidal forces of the same frequency Ω and same phase ($\gamma_f = 0$) but possibly different amplitudes are

$$\begin{bmatrix} [C] & [M] \\ [M] & [0] \end{bmatrix} \begin{bmatrix} \{\dot{x}(t)\} \\ \{\ddot{x}(t)\} \end{bmatrix} + \begin{bmatrix} [K] & [0] \\ [0] & -[M] \end{bmatrix} \begin{bmatrix} \{x(t)\} \\ \{\dot{x}(t)\} \end{bmatrix} = \begin{bmatrix} \{F\} \\ \{0\} \end{bmatrix} e^{i\Omega t} \tag{2.64}$$

which alternatively are expressible as

$$[A]\{\dot{y}\} + [B]\{y\} = \{F\}e^{i\Omega t} \tag{2.65}$$

Note that $\begin{bmatrix} \{F\} \\ \{0\} \end{bmatrix}$ has been redefined as $\{F\}$. Letting $\{y\} = \{Y\}e^{i\Omega t}$, we find

$$i\Omega[A]\{Y\} + [B]\{Y\} = \{F\} \tag{2.66}$$

For inversion, i.e., to find $\{Y\}$ given $\{F\}$, we use the orthogonality conditions. First, we introduce a $2n \times 1$ vector $\{Z\}$ in terms of which

$$\{Y\} = [\psi]\{Z\} \tag{2.67}$$

Finding $\{Z\}$is equivalent to finding $\{Y\}$. We can now write

$$i\Omega[A][\psi]\{Z\} + [B][\psi]\{Z\} = \{F\}, \text{ or} \tag{2.68}$$

$$i\Omega[\psi]^T[A][\psi]\{Z\} + [\psi]^T[B][\psi]\{Z\} = [\psi]^T\{F\} \tag{2.69}$$

which by virtue of the orthogonality of mode shapes enables us to write

$$\{Y\} = [\psi]\left[\frac{1}{i\Omega - p}\right][\psi]^T\{F\} \tag{2.70}$$

in which the matrix $\left[\frac{1}{i\Omega - p}\right]$ is diagonal of order $2n$. In index notation

$$Y_r = \psi_{rj}\frac{\delta_{jk}}{i\Omega - p_j}\psi_{mk}F_m \tag{2.71}$$

where the indices range from 1 to $m = 2n$. Explicitly one has

$$Y_r = \{\frac{\psi_{r1}\psi_{11}}{i\Omega - p_1} + \frac{\psi_{r2}\psi_{12}}{i\Omega - p_2} + \ldots\frac{\psi_{rn}\psi_{1m}}{i\Omega - p_m}\}F_1 + \{\frac{\psi_{r1}\psi_{21}}{i\Omega - p_1} + \frac{\psi_{r2}\psi_{22}}{i\Omega - p_2} + \ldots\frac{\psi_{rn}\psi_{2m}}{i\Omega - p_m}\}F_2$$

$$+ \ldots\{\frac{\psi_{r1}\psi_{n1}}{i\Omega - p_1} + \frac{\psi_{r2}\psi_{n2}}{i\Omega - p_2} + \ldots\frac{\psi_{rn}\psi_{mm}}{i\Omega - p_m}\}F_n \tag{2.72}$$

Since the roots p_r are in conjugate pairs, and so are the mode shapes $\{\psi_r\}$, we can write by combining the conjugate pairs

$$Y_r = \{\frac{i\Omega(\psi_{i1}\psi_{11} + \overline{\psi}_{i1}\overline{\psi}_{11}) - \overline{p}_1\psi_{i1}\psi_{11} - p_1\overline{\psi}_{i1}\overline{\psi}_{11}}{-\Omega^2 - i(p_1 + \overline{p}_1)\Omega + p_1\overline{p}_1}$$

$$+ \frac{i\Omega(\psi_{r2}\psi_{12} + \overline{\psi}_{r2}\overline{\psi}_{12}) - \overline{p}_2\psi_{r2}\psi_{12} - p_2\overline{\psi}_{r2}\overline{\psi}_{12}}{-\Omega^2 - i(p_2 + \overline{p}_2)\Omega + p_2\overline{p}_2} + \ldots \frac{i\Omega(\psi_{rn}\psi_{1n2} + \overline{\psi}_{rn}\overline{\psi}_{1n}) - \overline{p}_n\psi_{rn}\psi_{1n} - p_n\overline{\psi}_{rn}\overline{\psi}_{1n}}{-\Omega^2 - i(p_n + \overline{p}_n)\Omega + p_n\overline{p}_n}\}F_1$$

$$+ \{\frac{i\Omega(\psi_{r1}\psi_{21} + \overline{\psi}_{r1}\overline{\psi}_{21}) - \overline{p}_1\psi_{r1}\psi_{21} - p_1\overline{\psi}_{r1}\overline{\psi}_{21}}{\Omega^2 - i(p_1 + \overline{p}_1)\Omega + p_1\overline{p}_1} + \frac{i\Omega(\psi_{r2}\psi_{22} + \overline{\psi}_{r2}\overline{\psi}_{22}) - \overline{p}_2\psi_{r2}\psi_{22} - p_2\overline{\psi}_{r2}\overline{\psi}_{22}}{-\Omega^2 - i(p_2 + \overline{p}_2)\Omega + p_2\overline{p}_2}$$

$$+ \ldots \frac{i\Omega(\psi_{rn}\psi_{2n} + \overline{\psi}_{rn}\overline{\psi}_{2n}) - \overline{p}_n\psi_{rn}\psi_{2n} - p_n\overline{\psi}_{rn}\overline{\psi}_{2n}}{-\Omega^2 - i(p_n + \overline{p}_n)\Omega + p_n\overline{p}_n}\}F_2 + \ldots\{\frac{i\Omega(\psi_{r1}\psi_{n1} + \overline{\psi}_{r1}\overline{\psi}_{n1}) - \overline{p}_1\psi_{r1}\psi_{n1} - p_1\overline{\psi}_{r1}\overline{\psi}_{n1}}{-\Omega^2 - i(p_1 + \overline{p}_1)\Omega + p_1\overline{p}_1}$$

$$+ \frac{i\Omega(\psi_{r2}\psi_{n2} + \overline{\psi}_{r2}\overline{\psi}_{n2}) - \overline{p}_2\psi_{r2}\psi_{n2} - p_2\overline{\psi}_{r2}\overline{\psi}_{n2}}{-\Omega^2 - i(p_2 + \overline{p}_2)\Omega + p_2\overline{p}_2} + \ldots \frac{i\Omega(\psi_{rn}\psi_{nn} + \overline{\psi}_{rn}\overline{\psi}_{nn}) - \overline{p}_n\psi_{rn}\psi_{nn} - p_n\overline{\psi}_{rn}\overline{\psi}_{nn}}{-\Omega^2 - i(p_n + \overline{p}_n)\Omega + p_n\overline{p}_n}\}F_n \tag{2.73}$$

Denoting

$$p_k, \overline{p}_k = -\zeta\omega_k \pm i\omega_{kd} \text{ so that } p_k + \overline{p}_k = -2\zeta\omega_k,\ p_k\overline{p}_k = \omega_k^2 = \zeta\omega_k^2 + \omega^2{}_{kd} \tag{2.74}$$

we can write the above as the double sum

$$Y_r = \sum_{k=1}^{n}\{\sum_{s=1}^{n}\frac{i\Omega(\psi_{rs}\psi_{ks} + \overline{\psi}_{rs}\overline{\psi}_{ks}) - \overline{p}_k\psi_{rs}\psi_{ks} - p_k\overline{\psi}_{rs}\overline{\psi}_{ks}}{-\Omega^2 + 2i\Omega\,\zeta\omega_k + \omega_k^2}\}F_k = \sum_{j=1}^{n}\alpha_{rk}F_k \tag{2.75}$$

$$\text{where } \alpha_{rk} = \alpha_{rk}(\Omega) = \sum_{s=1}^{n}\frac{i\Omega(\psi_{rs}\psi_{ks} + \overline{\psi}_{rs}\overline{\psi}_{ks}) - \overline{p}_k\psi_{rs}\psi_{ks} - p_k\overline{\psi}_{rs}\overline{\psi}_{ks}}{-\Omega^2 + 2i\Omega\,\zeta\omega_k + \omega_k^2} \tag{2.76}$$

When damping is absent, $\zeta\omega_k = 0$, $\overline{p}_k = -p_k = -i\omega_k$ and $\overline{\psi}_{rs}\overline{\psi}_{ks} = -\psi_{rs}\psi_{ks}$ and it can be shown that Eqs. (2.76) reduce to those for the undamped system, Eq. (2.52).

From the relation postulated between $\{y\}$ and $\{x\}$ and $\{\dot{x}\}$, the displacements are

$$x_m = Y_m\, e^{\Omega t} \text{ for } m = 1 \text{ to } n \tag{2.77}$$

and the velocities are

$$\dot{x}_m = Y_m\, e^{\Omega t} \text{ for } m = n+1 \text{ to } 2n. \tag{2.78}$$

Alternatively, but less preferably, from Eq. (2.77)

$$\dot{x}_m = i\Omega Y_m\, e^{\Omega t} \tag{2.79}$$

for $m = 1$ to n. This latter equality implies $Y_{n+r} = i\Omega Y_r$, $r = 1$ to n.

Equations (2.76) are the basic equations by which a damped structural dynamic system is represented. Software, e.g., LMS CADA-X [12] fit the experimental data on the basis of

the above theoretical model. The reader is referred to Ewins [5] and Mia and Silva [6] for the extraction methods for determining frequencies, mode shapes and damping coefficients from experimental data.

2.4 Example: Forced Vibrations with General Viscous Damping

The above formulas appear quite theoretical and complicated. As an aid in understanding their significance we present a concrete example. Consider a two-degree-of-freedom system ($n = 2$) defined by:

$$[M] = \begin{bmatrix} 6 & 2 \\ 2 & 8 \end{bmatrix} \text{kg}, \; [C] = \begin{bmatrix} 2 & 2 \\ 2 & 4 \end{bmatrix} \text{N} \cdot \text{s/m}, \; [k] = \begin{bmatrix} 2000 & 800 \\ 800 & 1200 \end{bmatrix} \text{N/m},$$
$$\{F\} = \begin{bmatrix} 1 \\ 1 \end{bmatrix} e^{i\Omega t} \text{N} \tag{2.80}$$

Thereby, in accordance with the above explained theory:

$$[A] = \begin{bmatrix} 2 & 2 & 6 & 2 \\ 2 & 4 & 2 & 8 \\ 6 & 2 & 0 & 0 \\ 2 & 8 & 0 & 0 \end{bmatrix}, [B] = \begin{bmatrix} 2000 & 800 & 0 & 0 \\ 800 & 1200 & 0 & 0 \\ 0 & 0 & -6 & -2 \\ 0 & 0 & -2 & -8 \end{bmatrix} \tag{2.81}$$

The roots of $\det[pA + B] = 0$ and the corresponding normalized eigenvectors $\{\psi_i\}$ are:

$$p_1 = -0.178023 - 10.9232i, \; \{\psi_1\} = \begin{bmatrix} -0.0249 - 0.0237i \\ 0.0555 + 0.0557i \\ -0.2544 + 0.2765i \\ 0.5983 - 0.6170i \end{bmatrix}$$

$$p_2 = -0.178023 + 10.9232i, \; \{\psi_2\} = \begin{bmatrix} -0.0249 + 0.0237i \\ 0.0555 - 0.0557i \\ -0.2544 - 0.2765i \\ 0.5983 + 0.6170i \end{bmatrix}$$

$$p_3 = -0.185613 - 18.3046i, \; \{\psi_3\} = \begin{bmatrix} -0.04583 - 0.04648i \\ -0.0047 - 0.003i \\ -0.8424 + 0.8477i \\ -0.0593 + 0.0879i \end{bmatrix}$$

$$p_4 = -0.185613 + 18.3046i, \; \{\psi_4\} = \begin{bmatrix} -0.04583 + 0.04648i \\ -0.0047 + 0.003i \\ -0.8424 - 0.8477i \\ -0.0593 - 0.0879i \end{bmatrix} \tag{2.82}$$

Although not used in the sequel it should be noted that the lower half of each eigenvector, ψ_i, is equal to the upper half multiplied by the complex eigenvalue p_i. This fact is apparent from the last of equations (2.58) and equation (2.59). The order in which frequencies are listed is from the lowest to the highest. Note that the absolute value of $\|p_1\| = \|p_2\| = 10.9247$ rad/s, and $\|p_3\| = \|p_4\| = 18.3055$ rad/s

The FRFs α_{jk} can now be calculated from the formula derived previously:

$$\alpha_{jk} = \frac{\psi_{j1}\psi_{k1}}{i\Omega - p_1} + \frac{\psi_{j2}\psi_{k2}}{i\Omega - p_2} + \frac{\psi_{j3}\psi_{k3}}{i\Omega - p_3} + \frac{\psi_{j4}\psi_{k4}}{i\Omega - p_4} \tag{2.83}$$

where j ranges from 1 to 4, and k from 1 to 2. As an example we note that $\psi_{j3}\psi_{k3}$ denotes multiplication of the third elements of the jth and kth normalized column vectors. Also recall that the first two values of j, $j = 1, 2$ correspond to displacement response, while the latter two, $j = 3, 4$, correspond to velocity response. For the present example the FRF for displacements are :

$$\begin{aligned}
\alpha_{11} &= \frac{0.0000597 - 0.001181i}{i\Omega + 0.178 - 10.92i} + \frac{0.0000597 + 0.001181i}{i\Omega + 0.178 + 10.92i} + \frac{0.0000597 + 0.004261i}{i\Omega + 0.186 - 18.30i} + \frac{0.0000597 - 0.00426i}{i\Omega + 0.186 + 18.30i} \\
\alpha_{12} &= \frac{-0.0000657 + 0.0027i}{i\Omega + 0.178 - 10.92i} + \frac{-0.0000657 - 0.0027i}{i\Omega + 0.178 + 10.92i} + \frac{0.0000657 - 0.000372i}{i\Omega + 0.186 - 18.30i} + \frac{0.0000657 + 0.000372i}{i\Omega + 0.186 + 18.30i} \\
\alpha_{12} &= \frac{-0.0000657 + 0.0027i}{i\Omega + 0.178 - 10.92i} + \frac{-0.0000657 - 0.0027i}{i\Omega + 0.178 + 10.92i} + \frac{0.0000657 - 0.000372i}{i\Omega + 0.186 - 18.30i} + \frac{0.0000657 + 0.000372i}{i\Omega + 0.186 + 18.30i} \\
\alpha_{22} &= \frac{-0.000012 - 0.00619i}{i\Omega + 0.178 - 10.92i} + \frac{-0.000012 + 0.00619i}{i\Omega + 0.178 + 10.92i} + \frac{0.000012 - 0.000031i}{i\Omega + 0.186 - 18.30i} + \frac{0.000012 + 0.000031i}{i\Omega + 0.186 + 18.30i}
\end{aligned} \tag{2.84}$$

The FRF for velocities are found as

$$\begin{aligned}
\alpha_{31} &= \frac{0.012897 + 0.000862i}{i\Omega + 0.1780 - 10.923i} + \frac{0.012897 - 0.000862i}{i\Omega + 0.1780 + 10.923i} + \frac{0.078017 - 0.000302i}{i\Omega + 0.1856 - 18.3046i} + \frac{0.078017 + 0.000302ii}{i\Omega + 0.1856 + 18.3046i} \\
\alpha_{32} &= \frac{-0.02953 - 0.0012i}{i\Omega + 0.1780 - 10.923i} + \frac{-0.02953 + 0.0012i}{i\Omega + 0.1780 + 10.923i} + \frac{0.006805 + 0.00127i}{i\Omega + 0.1856 - 18.3046i} + \frac{0.006805 - 0.00127i}{i\Omega + 0.1856 + 18.3046i} \\
\alpha_{41} &= \frac{-0.02953 - 0.0012i}{i\Omega + 0.1780 - 10.923i} + \frac{-0.02953 + 0.0012i}{i\Omega + 0.1780 + 10.923i} + \frac{0.006805 + 0.00127i}{i\Omega + 0.1856 - 18.3046i} + \frac{0.006805 - 0.00127i}{i\Omega + 0.1856 + 18.3046i} \\
\alpha_{42} &= \frac{0.0676 + 0.00971i}{i\Omega + 0.1780 - 10.923i} + \frac{0.0676 - 0.00971i}{i\Omega + 0.1780 + 10.923i} + \frac{0.000572 + 0.000224i}{i\Omega + 0.1856 - 18.3046i} + \frac{0.000572 - 0.000224i}{i\Omega + 0.1856 + 18.3046i}
\end{aligned} \tag{2.85}$$

It is to be noted that $\alpha_{21} = \alpha_{12}$ and $\alpha_{41} = \alpha_{32}$ in accordance with the expected symmetry. The displacements can be computed as

$$x_1 = (\alpha_{11}F_1 + \alpha_{12}F_2)e^{i\Omega t},\ x_2 = (\alpha_{21}F_1 + \alpha_{22}F_2)e^{i\Omega t} \tag{2.86}$$

and the velocities as

$$\dot{x}_1 = (\alpha_{31}F_1 + \alpha_{32}F_2)e^{i\Omega t},\ \dot{x}_2 = (\alpha_{41}F_1 + \alpha_{42}F_2)e^{i\Omega t} \tag{2.87}$$

Since $\dot{x}_1 = i\Omega x_1$ and $\dot{x}_2 = i\Omega x_2$, we find that

$$\alpha_{31} = i\Omega\alpha_{11},\ \alpha_{32} = i\Omega\alpha_{11},\ \alpha_{41} = i\Omega\alpha_{21},\ \text{and}\ \alpha_{42} = i\Omega\alpha_{22}, \tag{2.88}$$

Thus, the FRFs for velocities may be obtained from those for displacements.

The simplified expressions are

$$\alpha_{11}(\Omega) = \frac{0.0258259 + 0.000119466i\Omega}{-\Omega^2 + 2\times 0.178023\, i\Omega + 10.9246^2} + \frac{0.15599 - 0.000119466i\Omega}{-\Omega^2 + 2\times 0.185613\, i\Omega + 18.3073^2} \tag{2.89}$$

Similarly, one obtains

$$\alpha_{12}(\Omega) = \alpha_{21}(\Omega) = -\frac{0.059113 + 0.000131477i\Omega}{-\Omega^2 + 2\times 0.178023\, i\Omega + 10.9246^2} + \frac{0.0136605 + 0.000131477i\Omega}{-\Omega^2 + 0.371226i\Omega + 18.3073^2} \tag{2.90}$$

$$\alpha_{22}(\Omega) = \frac{0.135211 - 0.0000238626i\,\Omega}{-\Omega^2 + 2\times 0.178023\, i\Omega + 10.9246^2} + \frac{0.0011530 + 0.0000238626i\Omega}{-\Omega^2 + 0.371226i\Omega + 18.3073^2} \tag{2.91}$$

The graphs of the three FRFs are shown below. They all have peak amplitudes near the undamped resonant frequencies $\omega_1 = 10.9246$ rad/s, and $\omega_2 = 18.3073$ rad/s. The graph for the point receptance $\alpha_{11}(\Omega)$, Fig. 2.2, clearly shows the anti-resonant frequency between the two resonant frequencies; the anti-resonant frequencies are those at which a point receptance (here α_{11}) becomes zero. Theoretically, for a point receptance $\alpha_{kk}(\Omega)$, an anti-resonance must follow a resonance. The graph for the transfer receptance $\alpha_{12}(\Omega)$, Fig. 2.3 is also quite consistent in showing a minimum between the resonances. However, the graph of the point receptance $\alpha_{22}(\Omega)$, Fig. 2.4 is misleading in that the peak around ω_2 is not pronounced and might not be recognized as a resonance peak in an experimental situation. This underscores the fact that some FRFs are better indicators of resonance frequencies than others. Therefore, in experiments, one should look at as many FRFs as possible to discern all resonance frequencies in a given frequency range.

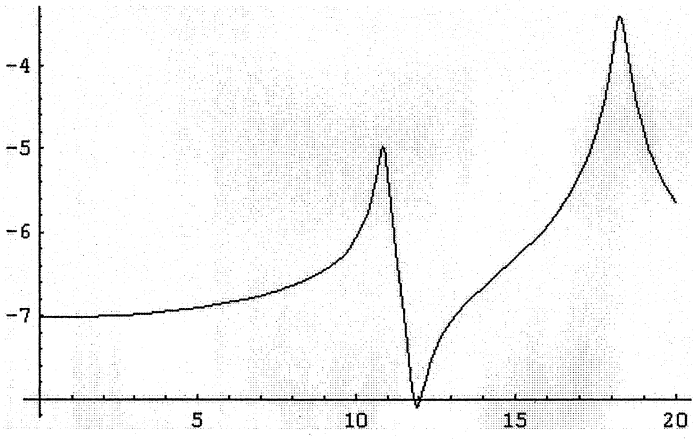

Fig.2.2: FRF α_{11} ordinate versus Ω

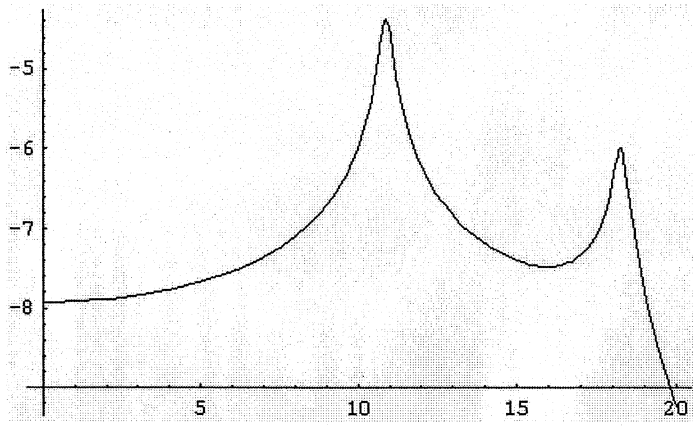

Fig.2.3: FRF α_{12} ordinate versus Ω

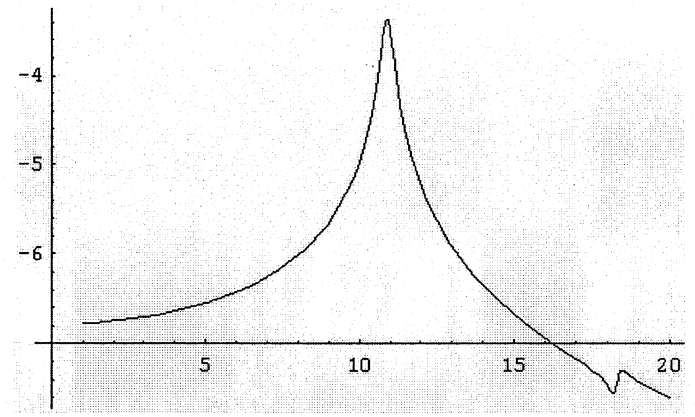

Fig.2.4: FRF α_{22} ordinate versus Ω

We may verify the above solution with that obtained by direct matrix inversion of

$$\begin{bmatrix} -6\Omega^2 + 2i\Omega + 2000 & -2\Omega^2 + 2i\Omega + 800 \\ -2\Omega^2 + 2i\Omega + 800 & -8\Omega^2 + 4i\Omega + 1200 \end{bmatrix} \begin{bmatrix} x_1 \\ x_2 \end{bmatrix} = \begin{bmatrix} F_1 \\ F_2 \end{bmatrix} \tag{2.92}$$

Taking $F_1 = 1,\ F_2 = 0,$ Creamer's rule of solving simultaneous equations gives

$$\alpha_{11} = \frac{-8\Omega^2 + 4i\Omega + 1200}{\Delta},\ \alpha_{12} = -\frac{-2\Omega^2 + 2i\Omega + 800}{\Delta} \tag{2.93}$$

where $\Delta = 44\Omega^4 - 32i\Omega^3 - 20004\Omega^2 + 7200i\Omega + 1760000$ (2.94)

is the determinant of the matrix in (2.83). Then, by taking $F_1 = 0,\ F_2 = 1,$ one obtains

(2.95)

$$\alpha_{21} = \alpha_{12} \text{ and } \alpha_{22} = \frac{-6\Omega^2 + 2i\Omega + 2000}{\Delta}$$

The above expressions for α_{ij} can be cast in the form of summation of quadratic partial fractions, equations (2.80) to (2.82). More easily, by summing the partial fractions, it can be shown that equations (2.80) to (2.82) reduce identically to those above, thereby confirming the correctness of the previous method. For example, equation (2.80) becomes

$$\alpha_{11} = \frac{0.15599 - 0.000119466i\Omega}{(\Omega^2 - 2 \times 0.178023\, i\Omega - 10.9246^2)(\Omega^2 - 2 \times 0.185613\, i\Omega - 18.3073^2)} = \frac{27.2727 + 0.0909 - 0.1818\Omega^2}{\Delta/44} \tag{2.96}$$

exactly equal to the expression for α_{11} in (2.84) above.

CHAPTER 3

THE INFLUENCE OF JOINT DAMPING ON A BEAM

In the previous chapter discrete systems were discussed to give the reader some background about structural dynamics of such systems, particularly with regard to the effect of viscous damping. In this chapter vibration of one-dimensional continuous systems, i.e. beams, is discussed, including the effect of viscous damping at beam joints.

As indicated in the Introduction, damping is often neglected in finite element analyses. We therefore have a situation in which we may be trying to correlate the undamped frequencies of the analyses with the damped frequencies of the real structure. The goal of this research, as previously stated, is to investigate the effect of damping in updating FE models. There are many sources of damping, but, as previously emphasized, a significant source is that due to slip which may occur at joints of the structure [1, 2]. The following analyses illustrate the joint damping effects with reference to a cantilever beam in which the free end is attached to (1) a translational damper, Fig. 3.1 and (2) a rotational damper, Fig. 3.2.

3.1 Free Vibration of a Cantilever Beam

It will be shown in Chapter 5 that the equation governing the transverse displacement of a freely vibrating elastic beam of uniform properties, neglecting the rotary inertia term, is

$$EI\frac{\partial^4 w}{\partial x^4} + \rho A\frac{\partial^2 w}{\partial t^2} = 0 \tag{3.1}$$

where $EI =$ bending rigidity, $\rho =$ mass density per unit volume, $A =$ area of cross section, $x =$ length coordinate, $t =$ time variable, and $w \equiv w(x,t) =$ the transverse deflection. The adopted sign convention is that positive x is rightward, positive deflection w is upward, positive slope $\dfrac{\partial w}{\partial x}$ is counterclockwise, positive bending moment M is of the sagging kind, and positive shear gives a counterclockwise rotation to an infinitesimal beam element. The Bernoulli-Euler kinematic assumption and small strain linear elastic behaviour lead to

$$M = EI\frac{\partial^2 w}{\partial x^2} \text{ and } V = -EI\frac{\partial^3 w}{\partial x^3}. \tag{3.2}$$

A solution of (3.1) for free vibration is sought in the form

$$w(x,t) = \phi(x)e^{i\omega t} \tag{3.2}$$

where $\phi = \phi(x)$ is the mode shape corresponding to frequency ω. Substitution of this into the above equation leads to

$$\frac{d^4\phi}{dx^4} - \frac{\rho A\omega^2}{EI}\phi = 0 \tag{3.3}$$

The solution of (3.3) is expressible as

$$\phi(x) = A\cos\alpha x + B\sin\alpha x + C\cosh\alpha x + D\sinh\alpha x \tag{3.4}$$

$$\text{where } \alpha = \left(\frac{\rho A\omega^2}{EI}\right)^{1/4} \text{ or, equivalently, } \omega = \alpha^2\sqrt{\frac{EI}{\rho A}} \tag{3.5}$$

The boundary conditions determine the corresponding natural frequencies of the beam. We consider two cases in which damping acts at the end $x = L$ of a cantilever beam fixed at $x = 0$.

3.1.1 Translational Damper at $x = L$

The boundary conditions at the fixed end require vanishing of displacement and slope, i.e.

$$w(0,t) = \frac{\partial w}{\partial x}(0,t) = 0 \text{ at } x = 0 \tag{3.6}$$

The boundary conditions at the other end require the shear force to be equal to the reactive viscous force from the dash-pot, and vanishing of the bending moment, i.e.

$$V(L,t) = -EI\frac{\partial^3 w}{\partial x^3}(L,t) = -C_s\frac{\partial w}{\partial t}(L,t),\ M = EI\frac{\partial^2 w}{\partial x^2}(L,t) = 0 \tag{3.7}$$

These boundary conditions imply fixed support at $x = 0$. At the end $x = L$, the beam is moment free but is attached to a dash-pot, Fig. 3.1.

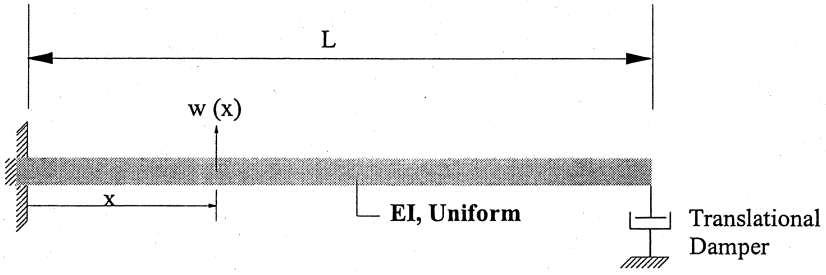

Fig. 3.1: Cantilever beam with a vertical damper at free end.

The solution form $w(x,t) = \phi\ e^{i\omega t}$ where ω is a natural frequency and $\phi = \phi(x)$ is the corresponding mode shape requires satisfaction of the following conditions

$$\phi = \frac{d\phi}{dx} = 0 \text{ at } x = 0 \text{ and} \tag{3.8}$$

$$EI\frac{d^3\phi}{dx^3} = i\omega C_s\phi,\ EI\frac{d^2\phi}{dx^2} = 0 \text{ at } x = L \tag{3.9}$$

The conditions at $x = 0$ render $C = -A$ and $D = -B$, and the solution becomes

$$\phi(x) = A(\cos\alpha x - \cosh\alpha x) + B(\sin\alpha x - \sinh\alpha x) \tag{3.10}$$

The conditions at $x = L$ require

$$\begin{aligned} &A\{\sin\alpha L - \sinh\alpha L - \frac{i\omega C_s}{EI\alpha^3}(\cos\alpha L - \cosh\alpha L)\} \\ &- B\{\cos\alpha L + \cosh\alpha L + \frac{i\omega C_s}{EI\alpha^3}(\sin\alpha L - \sinh\alpha L)\} = 0 \end{aligned} \tag{3.11}$$

$$A(\cos\alpha L + \cosh\alpha L) + B(\sin\alpha L + \sinh\alpha L) = 0 \tag{3.12}$$

For a nontrivial solution of these two equations, meaning that both A and B are not zero, the determinant of the matrix of the coefficients of A and B must be zero. This condition then produces the frequency equation;

$$1 + \cosh\alpha L\cos\alpha L + \frac{i\omega C_s}{EI\alpha^3}(\sin\alpha L\cosh\alpha L - \cos\alpha L\sinh\alpha L) = 0, \text{ or} \tag{3.13}$$

$$1 + \cosh\alpha L\cos\alpha L + \frac{iC_s}{\alpha L}\sqrt{\frac{L^2}{EI\rho A}}(\sin\alpha L\cosh\alpha L - \cos\alpha L\sinh\alpha L) = 0, \text{ or} \tag{3.14}$$

$$\frac{i}{C_s}\sqrt{\frac{EI\rho A}{L^2}} \times \alpha L(1 + \cosh\alpha L\cos\alpha L) - (\sin\alpha L\cosh\alpha L - \cos\alpha L\sinh\alpha L) = 0 \tag{3.15}$$

The computed frequency values for a particular choice of properties will be shown later. We however note that if $C_s = 0$, the frequency equation is the well-known

$$1 + \cosh\alpha L\cos\alpha L = 0 \tag{3.16}$$

for a beam fixed at $x = 0$ and free at $x = L$. The first, i.e. the fundamental frequency is

$$\omega_1 = (\frac{0.597\pi}{L})^2\sqrt{\frac{EI}{\rho A}} \tag{3.17}$$

whereas the higher frequencies ($n > 1$) are given to a very good approximation by [13]

$$\omega_n = (\frac{(2n-1)\pi}{2L})^2\sqrt{\frac{EI}{\rho A}},\ n = 2,\ 3, 4,\ \ldots \tag{3.18}$$

Now when $C_s = \infty$, then the frequency equation is that of a beam fixed at $x = 0$ and supported at $x = L$:

$$\sin \alpha L \cosh \alpha L - \cos \alpha L \sinh \alpha L = 0. \tag{3.19}$$

The natural frequencies for such a beam are [13]

$$\omega_1 = (\frac{1.2498\,\pi}{L})^2\sqrt{\frac{EI}{\rho A}}\ , \text{and}\ \omega_n = (\frac{(4n+1)\pi}{4L})^2\sqrt{\frac{EI}{\rho A}},\ \text{for}\ n = 2,\ 3, 4,\ \ldots \tag{3.20}$$

If C_s is different from zero or infinity, the natural frequencies ω are complex:

$$\omega = \omega_d + i\zeta\omega \tag{3.21}$$

with real (oscillatory) part ω_d and imaginary (damping) part $\zeta\omega$, which must be positive for energy absorbing damping. In an experimental situation it is the damped frequencies ω_d which are measured, while in analysis damping is usually neglected in determining the natural frequencies. The usual presumption is that damping is small, and should not affect the undamped frequencies significantly.

The frequency equation is now split into two equations, one pertaining to the real part of the equation being zero and the other requiring the imaginary part to be zero. The solutions of the two simultaneous transcendental equations thus obtained yield ω_d and the corresponding $\zeta\omega$ of the complex frequencies.

3.1.2 Rotational Damper at $x = L$

In this case the end at $x = L$ is free against displacement but constrained against rotation by a rotational damper. Therefore, the boundary conditions on $w(x, t)$, as shown in Fig. 3.2, are

$$w(0, t) = \frac{\partial w}{\partial x}(0, t) = 0 \text{ at } x = 0, \text{ and} \tag{3.22}$$

$$V = -EI\frac{\partial^3 w}{\partial x^3}(L,t) = 0, M = EI\frac{\partial^2 w}{\partial x^2}(L,t) = -C_r\frac{\partial^2 w}{\partial t \partial x}(L,t) \tag{3.23}$$

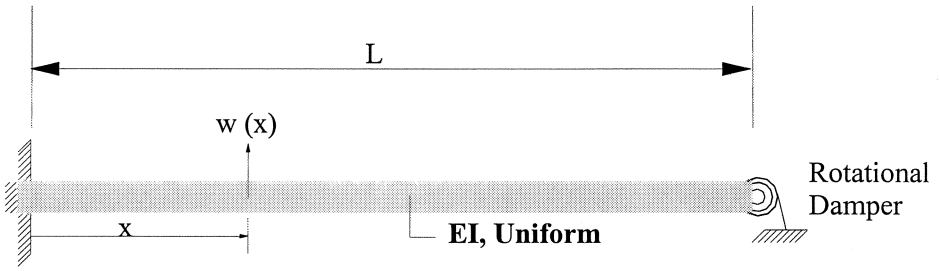

Fig. 3.2: Cantilever beam with a rotational damper at free end.

The boundary conditions on $\phi(x)$ are

$$\phi = \frac{d\phi}{dx} = 0 \text{ at } x = 0, \text{ and} \tag{3.24}$$

$$EI\frac{d^3\phi}{dx^3} = 0,\ EI\frac{d^2\phi}{dx^2} = -i\omega C_r\frac{d\phi}{dx} \tag{3.25}$$

These boundary conditions now require

$$\begin{aligned} -A[\cos\alpha L + \cosh\alpha L + \frac{i\omega C_r}{EI\alpha^3}(\sin\alpha L + \sinh\alpha L)] \\ -B[\sin\alpha L + \sinh\alpha L - \frac{i\omega C_r}{EI\alpha^3}(\cos\alpha L - \cosh\alpha L)] = 0 \end{aligned} \tag{3.26}$$

$$A(\sin\alpha L - \sinh\alpha L) - B(\cos\alpha L + \cosh\alpha L) = 0 \tag{3.27}$$

Vanishing of the determinant of the matrix of the coefficients A and B in the two equations produces the frequency equation for this case as

$$1 + \cos\alpha L\cosh\alpha L + \frac{i\omega C_r}{EI\alpha}(\sin\alpha L\cosh\alpha L + \cos\alpha L\sinh\alpha L) = 0, \text{ or} \tag{3.28}$$

$$i\frac{\sqrt{EI\rho A}}{C_r}(1 + \cosh\alpha L\cos\alpha L) - (\sin\alpha L\cosh\alpha L + \cos\alpha L\sinh\alpha L) = 0 \tag{3.29}$$

We note that if $C_r = 0$, the frequency equation becomes

$$1 + \cosh\alpha L\cos\alpha L = 0 \tag{3.30}$$

which is again that for a cantilever beam fixed at $x = 0$ and free at $x = L$. If, on the other hand, $C_r = \infty$, then the frequency equation becomes that of a beam fixed at $x = 0$ and supported against rotation but free to translate at $x = L$:

$$\sin \alpha L \cosh \alpha L + \cos \alpha L \sinh \alpha L = 0. \tag{3.31}$$

The frequencies for such a beam are

$$\omega_1 = (\frac{0.7528\pi}{L})^2 \sqrt{\frac{EI}{\rho A}} \text{ , and } \omega_n = (\frac{(4n-1)\pi}{4L})^2 \sqrt{\frac{EI}{\rho A}}, \text{ for } n = 2, 3, 4, \ldots \tag{3.32}$$

Again if C_r is different from zero or infinity, the natural frequencies ω are complex similar to the case of displacement damping.

3.2 Frequency Comparison

To see the effect of the two types of damping, we work out a specific example of a cantilever beam. The beam properties in Imperial units are taken as (for conversion to SI units see the Conversion Table):

Length $L = 1$ft, Area of cross-section $A = 1\,\text{in}^2 = 1/144\,\text{ft}^2$, $I = 1/12\,\text{in}^4 = (1/12)^5\text{ft}^4$

Density $\rho = 15.528\,\text{slug/ft}^3$, $E = 29 \times 10^6\text{psi} = 4176\ \times 10^6\text{lb/ft}^2$

The undamped fundamental frequencies for the three ideal cases are found as

$\omega_1(C_s = C_r = 0) = 220.86\,\text{Hz}$, $\omega_1(C_s = \infty) = 967.95\,\text{Hz}$, $\omega_1(C_r = \infty) = 351.18\,\text{Hz}$

The values corresponding to "infinite" damping (the last two cases) are not used in the following as they only give an indication on the upper limit of the increased frequencies due to damping. Only the frequencies of the standard fixed-free cantilever beam with no damping (the first case) are used as reference.

Parametric studies for various values of C_s and C_r were performed. Table 3.1 comprising of 4 smaller tables displays these studies for the first five frequencies. The smaller tables list the frequencies for damping values of $C_s = 12.5,\ 25, 37.5$ units (lb.sec/ft.), ∞ and of $C_r = 15,\ 30,\ 45$ units (lb.sec/ft), ∞. The damping renders the frequencies to be complex $\omega = \omega_d + \zeta\omega i$ with modulus $\|\omega\| = \sqrt{\omega_d^2 + \zeta^2\omega^2}$. Only the oscillatory part ω_d is used for comparison, as it makes physical sense to do so. The damping part indicates the decrement of the amplitudes of vibration, i.e., a higher $\zeta\omega$ value means faster decrease of the amplitude with time.

Undamp Frequency	Transl. Damp. $C_s = 12.5$	% Diff.	Rot. Damp.$C_r = 7.5$	% Diff
ω	$\omega = \omega_d + \zeta\omega i$	Disp.Damper	$\omega = \omega_d + \zeta\omega i$	Rot. Damper
220.86 Hz	$218.022 + 37.03i$	-1.28	$228.03 + 43.31i$	$+3.25$
1394.29 Hz	$1381.37 + 36.85i$	-0.93	$1718.24 + 305.93i$	$+23.230$
3873.04 Hz	$3872.51 + 36.88i$	-0.014	$4573.32 + 334.82i$	$+18.08$
7591.15 Hz	$7590.16 + 36.89i$	-0.013	$8631.26 + 344.66i$	$+13.70$
12548.62 Hz	$12547.9 + 36.89i$	-0.006	$13915.8 + 348.81i$	$+10.90$

Undamp Frequency	Transl. Damp. $C_s = 25$	% Diff.	Rot. Damp.$C_r = 15$	% Diff
ω	$\omega = \omega_d + \zeta\omega i$	Disp.Damper	$\omega = \omega_d + \zeta\omega i$	Rot. Damper
220.86 Hz	$209.34 + 74.83i$	-5.22	$265.60 + 83.70i$	$+20.26$
1394.29 Hz	$1374.99 + 73.43i$	-1.38	$1854.83 + 175/63i$	$+33.03$
3873.04 Hz	$3868.62 + 73.62i$	-0.11	$4658.59 + 175.70i$	$+20.28$
7591.15 Hz	$7587.33 + 73.69$	-0.05	$8693.73 + 176.74i$	$+14.52$
12548.62 Hz	$12545.7 + 73.73i$	-0.02	$13965.3 + 177.19\,i$	$+11.29$

Undamp Frequency	Transl. Damp. $C_s = 37.5$	% Diff.	Rot. Damp.$C_r = 22.5$	% Diff
ω	$\omega = \omega_d + \zeta\omega i$	Disp.Damper	$\omega = \omega_d + \zeta\omega i$	Rot. Damper
220.86 Hz	$193.03 + 114.25i$	-12.60	$310.63 + 77.59i$	$+40.65$
1394.29 Hz	$1364.16 + 109.39i$	-2.16	$1879.02 + 118.87i$	$+34.77$
3873.04 Hz	$3862.12 + 110.08i$	-0.28	$4674.08 + 117.98i$	$+20.68$
7591.15 Hz	$7582.61 + 110.34i$	-0.11	$8705.19 + 118.32i$	$+14.68$
12548.62 Hz	$12542.0 + 110.47i$	-0.053	$13974.4 + 118.45i$	$+11.36$

Undamp Frequency	Transl. Damp. $C_s = \infty$	% Diff.	Rot. Damp.$C_r = \infty$	% Diff
ω	$\omega = \omega_d + \zeta\omega i$	Disp.Damper	$\omega = \omega_d + \zeta\omega i$	Rot. Damper
220.86 Hz	0	-100	$351.89 + 0i$	$+59.33$
1394.29 Hz	$968.07 + 0i$	-30.57	$1897.80 + 0i$	$+36.11$
3873.04 Hz	$3137.16 + 0i$	-19.00	$4686.37 + 0i$	$+21.0$
7591.15 Hz	$6545.43 + 0i$	-13.78	$8714.32 + 0i$	$+14.80$
12548.62 Hz	$11193.1 + 0i$	-10.80	$13981.6 + 0i$	$+11.42$

Table 3.1 Frequency comparison for the two types of damping of a cantilever beam.

Consider first the variation in frequencies due to changes in C_s values. It is apparent that as C_s increases, the frequencies decrease. For example, the oscillatory part of the first frequency decreases from 220.86 to 218.02 to 209.34 to 193.03 as C_s increases from 0 to 12.5 to 25 to 37.5 units. The percentage decrease $(\omega_d - \omega)/\omega \times 100$ is greater for the lower few frequencies. It is interesting to note that the damping part of the complex frequency increases with increase in damping, and is approximately the same for all five frequencies for a specified $C_s$value. This means that all modes are attenuated significantly with almost the same factor.

For C_s values varying from 37.5 units to very high values it is found (although not shown here), that at some value of C_s the oscillatory part of the first frequency becomes zero. After which a further increase in the C_s value yields only a decreasing imaginary first frequency, meaning that the motion is no longer periodic. For very large C_s value, $C_s = \infty$, the first frequency is rendered zero, and the hitherto second frequency becomes the first frequency of a beam fixed at $x = 0$, and simply supported at $x = L$. Thus the listed non-zero frequencies for the $C_s = \infty$ case are those for a such beam, Eq. (3.20)

Table 3.1 also shows the variation in the first five damped frequencies for C_r values varying from 7.5 to 15 to 22.5 units (lb.ft.sec) to ∞. In contrast to the previous translational damping case, it is seen that the oscillatory parts of all frequencies continue to increase (rather than decrease) with the increase of C_r values. At $C_r = \infty$, the frequencies are those of a beam fixed at $x = 0$, and fixed against rotation but free in displacement at $x = L$ given by Eq. (3.32). The percentage increase in frequencies $(\omega_d - \omega)/\omega \times 100$ are significant for all five frequencies, indicating that the rotational damping is more pervasive, not confined to only first few frequencies. However, the fact remains that generally the lower frequencies experience greater increases. The damping part of the frequency here has a similar kind of character as for the translational damping case. Except for the first frequency, all other frequencies are attenuated by approximately the same factor.

It is apparent from the above comparison that the effects of rotational damping are quite different in character than those due to translational damping.

CHAPTER 4

THE EXPERIMENT

In space-related applications, as mentioned earlier, the structure has to be tested under dynamic loading to verify the theoretical model used in its analysis and design. Over-design is not permitted with a high safety allowance as often done in civil engineering structures. In aerospace structures the mass has to be minimized by an efficient design. Experimental modal analysis has to be performed to ensure safety of the structure.

One can perform dynamic analysis using either commercial software like NASTRAN [14] or by developing MatLab [15] or Mathematica programs [16] for taking into account special circumstances, like those in the present thesis. The analytical results should however be supported by experiments. Consequently, a series of experiments was conducted at the Canadian Space Agency (CSA) laboratories. The experiments were performed using the signal conditioning and data acquisition system operating with LMS-CADA-X modal analysis software [12].

It should, however, be noted that the experimental part of the investigation was not the main thrust of this work. The experiments were performed by the author at the CSA as a guest researcher, with little authority. As well, the limitations of the equipment, resources, and time hindered an in-depth experimental investigation. This chapter therefore provides a rather brief summary of the experimental work. The value of the work reported herein lies mainly in the fact that this was the first time these original experiments were attempted. It is expected that the difficulties encountered in designing and conducting them will prove valuable to other researchers in the future.

4.1 The test Specimen

The specimen constructed for the experimental study was a simple 2D aluminum frame consisting of two columns (i.e. vertical members) and one beam (i.e. a horizontal member). The dimensions of the specimen frame in xy plane are shown in Fig. 4.1. The beam is lapped on to the columns by bolts. The holes for the bolts are provided in 3×3 configuration as shown. This configuration gives the flexibility to join the beam by 1, 2, 4

or 9 bolts at each corner. The frame was tested for motion in the xy plane. However, the eccentricity introduced by the lapping (i.e. offsetting) of the beam over the columns rendered the frame to be a slightly non-symmetric structure with respect to the xy plane passing through the column centerlines. A second set of columns or a beam might have been used to make the structure symmetric. But, this added stiffness would have increased the frequencies of the structure rendering them more difficult to measure with the available equipment. The presence of this eccentricity, however, did not have any significant effect on the xy plane frequencies which are of interest here, in view of the near absence of any out-of-plane motion during testing. The beam length measured from the centerlines of the columns was 15 inches (0.381 m). The lengths of the column measured from the centerline of the beam was 15 inches (0.381 m) but which additionally had 1/2 in (12.7 mm) length for clamping it to the foundation of the test bed, which rendered the effective length of the column to be 15 in (0.381 m). As shown, the width of the members is 3 in (76.2 mm) and the thickness of the frame in the z direction is 1/8 in ($\approx$ 3.2 mm).

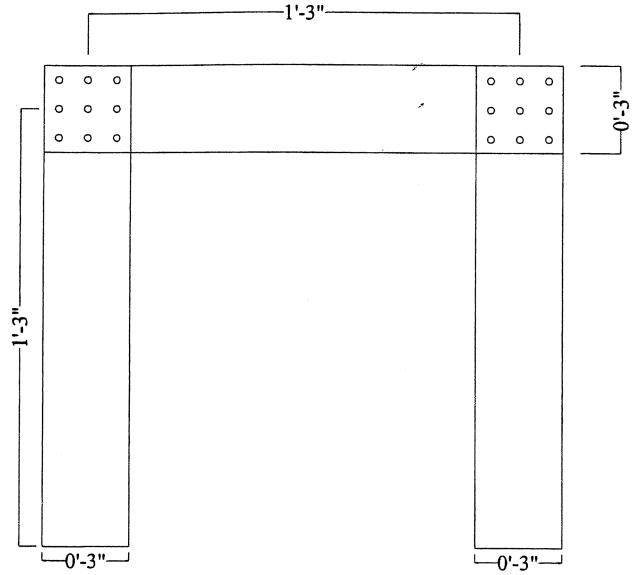

Fig. 4.1: The 2 D frame

The properties common to all three aluminum members were:

Length $L = 15$ in (381 mm), Width = 3 in (76.2 mm), Thickness = 0.125 in (3.2 mm)
Area $A = 0.375\,\text{in}^2$ ($0.242 \times 10^{-3}\text{m}^2$), Moment of Inertia $I = 0.28125\text{in}^4$
($117 \times 10^{-9}\text{m}^4$), Density $\rho = 5.4\,\text{slugs/ft}^3$ ($2768\,\text{kg/m}^3$), Young's Modulus
$E = 10.4 \times 10^6\text{psi}$ ($71.7 \times 10^9\,\text{Pa}$).

4.2 The test set up

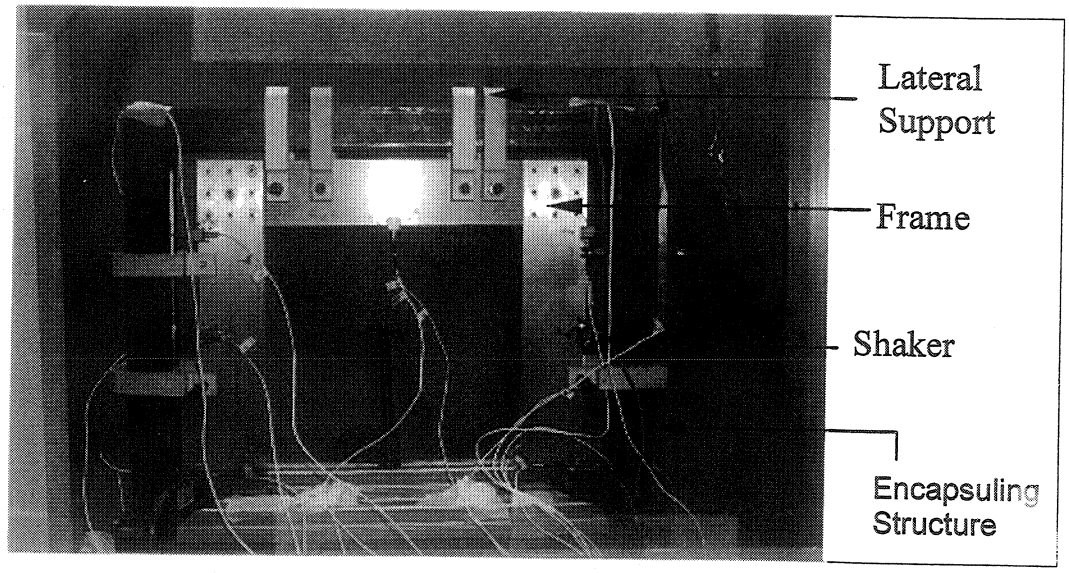

Fig. 4.2: The main frame structure.

4.2.1 The joint

The most significant element of the experiment is the joint. It is clear that the joint damping will depend on the way it is constructed. The type of the joint will dictate the amount of damping arising from friction between the surfaces or from material viscosity. A bolted joint can be expected to have much more damping than a welded one because of the amount of slip occurring in the joint as it opens and closes during vibrations. The number of bolts in a joint and the torque used to tighten them will also affect the overall joint damping. A welded joint, on the other hand, may only have micro slip within its parts which may not contribute much to damping.

In this experiment, the beam and the columns were not welded, but bolted as shown in Fig. 4.3 and 4.4. In order to experiment with different bolting configurations, the common member widths was chosen to yield a joint of sufficiently large area to accommodate as many as nine bolts. A width of 3 inches compared to a length dimension of 15 inches was deemed sufficient for this purpose.

Bolt configurations of 1, 2, 4, or 9 bolts were tested, with different bolt materials and different bolting torques. Actually twelve experiments were performed for the purpose of this thesis. Table 4.1 lists the specific combinations used in the tests.

Bolts	Material	Torque (in.lb)
1, 2, 4, 9	Steel	2
1, 2, 4, 9	Steel	5
1, 2, 4, 9	Plastic	2

Table 4.1: Bolts configurations.

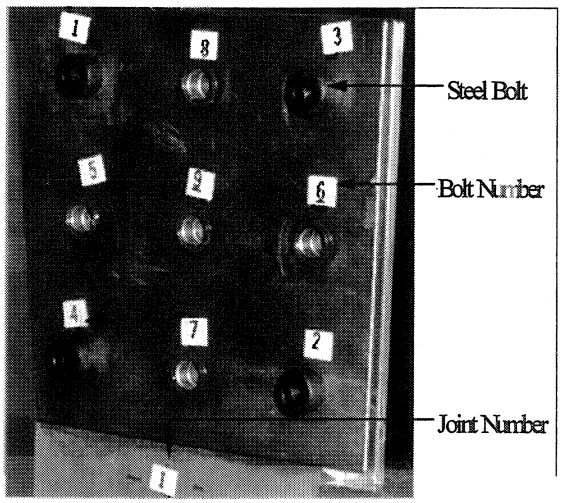

Fig. 4.3 The Joint with the steel Bolts.

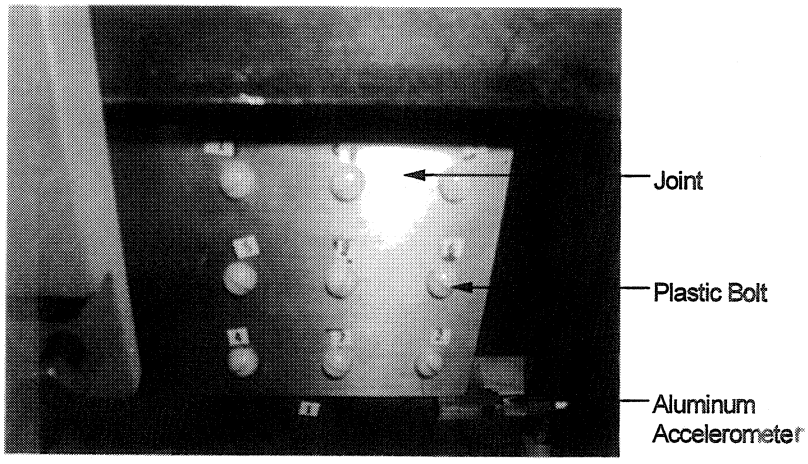

Fig. 4.4: The joint with plastic bolts.

4.3 Fixity

To ensure valid experimental results, the 2-D frame was fixed to a sufficiently rigid metal foundation. For this purpose, three holes were drilled widthwise at the bottom of each leg. The legs were lowered into the recesses of symmetrically placed clamps. The legs were then bolted to the clamps through the three holes, and the clamps were bolted to the steel base. This arrangement of providing fixity of the columns to the base was tested experimentally by obtaining FRF of the base plate alone, which was found to be small (close to zero) as it should be for a "rigid" foundation. Thereafter, FRF curves were obtained for the attached frame with accelerometers placed at points close to the connecting bolts. The difference between the two FRF curves was found to be negligible (less than 2%), thus proving the absence of any significant slip between the base plate and the columns.

4.4 Prevention of out-of-plane displacements

Since the objective of the test was to obtain influence of joint damping in the xy motion of the frame and since the frame was flexible in the out-of-plane direction, it was necessary to constrain it against motion in that direction. The main structure was therefore encapsulated by a stronger structure that provided lateral support against the out-of-plane motion. The set up for encapsulating the 2D frame is indicated in Fig. 4.1. The lateral supports were in the form of screwable Teflon-tipped contacts protruding from the encapsulating frame. These permitted almost frictionless sliding of the contacting surfaces of the beam and of the columns of the frame, and thus preventing it from out-of-plane vibration and at the same time permitting unhindered in-plane motion. This arrangement also helped minimize the effect of the slight asymmetry of the constructed frame.

4.5 Positioning of the accelerometers

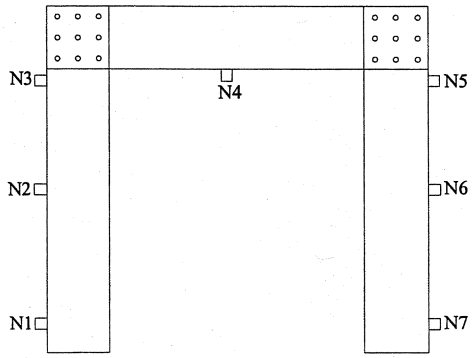

Fig. 4.5: The numbering of the accelerometers.

The monitoring of in-plane motion required that the accelerometers be attached to the sides of the frame as shown in Fig. 4.5 by the square symbols and names N1, N2, ...N7. The small (1/8 in) thickness of the frame made it necessary to employ special attachments to affix the accelerometers. The number of the accelerometers and their positions were considered to be adequate to capture the mode shapes and hence the frequencies of the frame. Figure 4.2 shows the leads from the accelerometers to the data acquisition system.

4.6 Position of the shaker

For exciting the frame with random burst input, a shaker was installed and attached as shown in Fig. 4.2. The shaker was hung using bungee chords to allow for free vibration of the frame. The attachment between the shaker and the frame was done through a stringer. The stringer was leveled and placed to be in the same xy plane as the frame to ensure in-plane excitation of the frame.

4.7 Data acquisition

For data acquisition, the LMS-CADA-X [12] software was employed. The motion of the accelerometers produces electrical signals that are sent to the signal conditioners, and then to the data acquisition system. The signals are converted from analog to digital and are then communicated to the computer for data analysis. Figure 4.6 shows the tower housing the data acquisition system with its components identified.

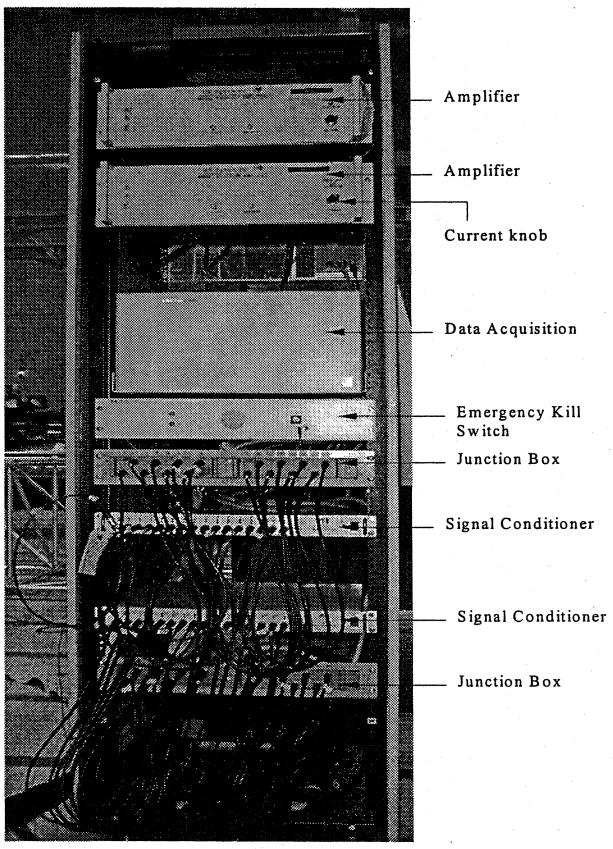

Fig 4.6: The control tower housing the data acquisition system.

4.8 Verification of experimental results

The experimental results were checked, as soon as they were obtained, and before they were processed to avoid errors in the correlation between the experimental and numerical analyses. Figure 4.7 shows the FRF of the frame obtained from different accelerometers, N2, ...N6, all of which could detect in-plane motion as well as out-of-plane motion. The graphs corresponding to node 5 show the recorded in-plane and the out-of-plane motions, clearly indicating that the out-of-plane (z-direction) motion was small.

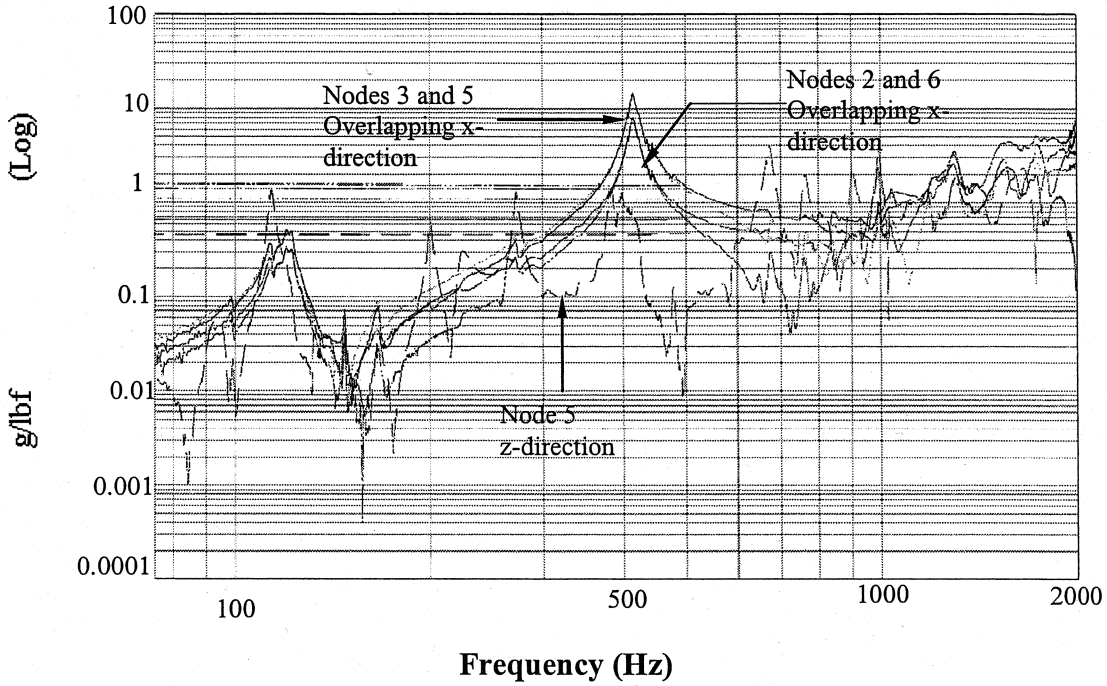

Fig. 4.7: FRF for each individual accelerometer (N2, N3, N5 and N6).

The figure also shows that for the most part of the FRF for nodes N3 and N5 coincide as expected because they are placed in parallel columns at the same height shown in Fig. 4.5. The same can be said about the FRF of nodes N2 and N6. The overall average results of the frame is obtained by the LMX software as shown in Fig. 4.8 (Note that the displacements of N1 and N7 are close to zero since they are both near the base). N4 is not included in Fig. 4.7 since it does not measure the horizontal (x-displacement) but only the vertical (y-displacement).

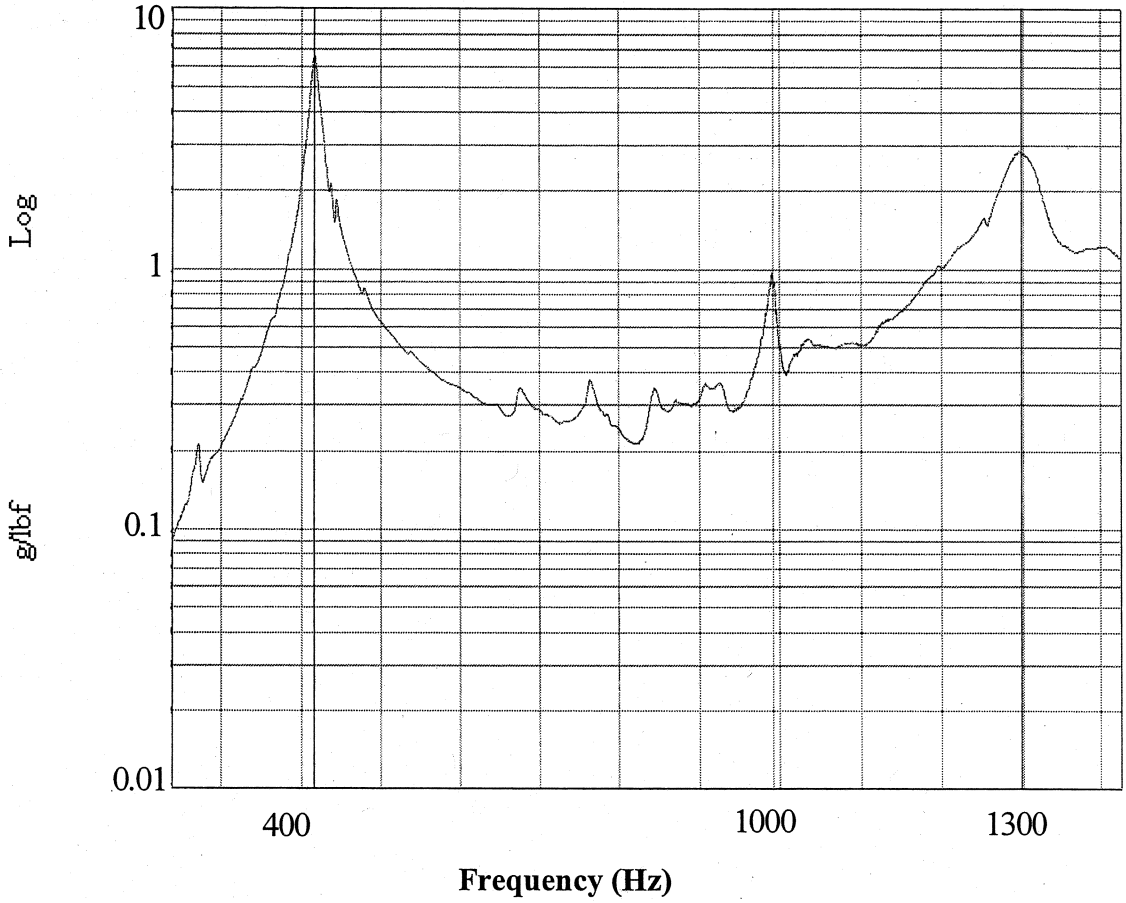

Fig. 4.8: The average of FRFs of N2, N3, N5 and N6.

At this stage the frequencies corresponding to the peaks or resonant frequencies are registered and their mode shapes are obtained as well. Unfortunately, the equipment used in this experiment was inadequate to measure the rotational mode shapes of the structure. Moreover, the system is limited to measuring with good accuracy frequencies less than 2000 Hz. This limitation of the equipment resulted in the fact that only two frequencies could be measured. Table 4.2 shows the measured frequencies.

	1	2	3	4	5	6
	Exp. (Hz)	Modal	Exp. (Hz)	Modal	Exp. (Hz)	Modal
Bolt Nos.	Trq = 2 (inlb)	Damping	Trq = 5 (inlb)	Damping	Trq = 2 (inlb)	Damping
	(Steel)		(Steel)		(Plastic)	
1	415.21	0.0223	416.55	0.0162	413.41	0.0135
	1302.64	0.0229	1286.64	0.0229	1292.31	0.0235
2	413.31	0.0222	423.60	0.0170	417.07	0.0126
	1321.96	0.0132	1341.09	0.0132	1324.06	0.0113
4	419.13	0.0216	424.17	0.0218	421.66	0.0160
	1335.26	0.0156	1355.81	0.0149	1345.09	0.0116
9	411.30	0.0200	415.45	0.0213	421.98	0.0140
	1336.98	0.0154	1353.33	0.0142	1345.92	0.0113

Table 4.2: Frequency values for steel and plastic bolts configurations.

The modal damping determined experimentally and shown in the above table gives an indication of rather low damping in the tested frame. An interpretation of these damping values in terms of rotational damping, is not straight forward, and was considered beyond the scope of this limited experimental investigation.

Regarding comparison with the computed frequencies, Table 4.3 shows that the experimental frequencies, taken as the averages of the measured frequencies for each mode, are fairly close to the ones obtained by NASTRAN considering no damping. This indicates that the experiments were performed rather accurately. They achieved the expected dynamic behaviour with a discrepancy in the measured frequencies of about 7%. compared to the computed undamped values, which is quite acceptable.

Logically, the measured frequencies ought to be lower than the NASTRAN frequencies since the latter are for undamped and rigid jointed frame. However, one finds that the first measured frequency is higher than that of NASTRAN. On the other hand, the second measured frequency is lower than the NASTRAN value, which is expected for a damped structure. If one disregards the possibility of experimental error in the second case then this frequency would correspond to a combination of some joint stiffness and rotational damping as is shown in Chapter 6.

Average Exp.	NASTRAN	Diff
(Hz)	No damp	%
418	389.8	− 6.7
1328	1421.4	+ 7.0

Table 4.3: Comparison of the experimental frequencies with calculated ones.

Coming back to Table 4.2, it can be seen that generally (allowing for the experimental discrepancies) the higher number of bolts in the two joints increases the frame frequencies, columns 1, 3 and 5. This is more true for the second frequency than for the first one indicating less experimental error in the determination of the second frequency. Also, as expected, the higher torque increased the frequency (columns 3 in comparison to column 1). Thus, it is evident, that the higher number of bolts and the higher torque increased the stiffness of the frame.

When the plastic bolts are used, the frequencies are generally higher than their steel counterpart for the same amount of torque, column 5 versus column 1 . This increase is rather surprising in view of the lower modulus of plastic bolts, and correspondingly the lower pinching forces exerted by the bolts on the joined parts. However, the possibility exists that the plastic bolts provide a higher damping and therefore resulting in higher frequencies. A further experimental investigation along the present lines, using steel and plastic bolts, would be useful in proving this observation conclusively.

In conclusion, this limited number of experiments were successful in achieving their primary purposes of demonstrating the effect of joint damping on the frequencies of the tested frame. Availability of equipment with higher measurement capacity would have made it possible to capture more frequencies. Obviously, for future investigation, many improvements can be made in the design and construction of the present experiments, to obtain a greater number of in-plane frequencies.

CHAPTER 5

FREE VIBRATION OF A BEAM WITH INCLINED SEGMENTS

The purpose of this section is to derive the exact frequencies and mode shapes of a beam, or a bent with various straight but inclined segments. The specific problem is to determine the exact frequencies and mode shapes of the frame for which experimental frequencies were obtained. The analysis method presented below uses the concept of transfer matrices [17]. This method produces the exact benchmark frequencies which can be used for determining the goodness of approximate frequencies obtained by the finite element method.

5.1 Transfer Matrix of a Straight Beam Segment

The exact transfer matrix of a straight beam element of uniform section can be derived by solving the differential equations of motion expressed in terms of transverse displacement $w(x,\ t)$ and longitudinal displacement $u(x,\ t)$ where x is the coordinate along the beam centroidal axis and t denotes the time coordinate. We assume that xy plane is a principal plane of the beam. Positive $w(x, t)$ and positive $u(x,\ t)$ are in positive directions of the x and y axes.

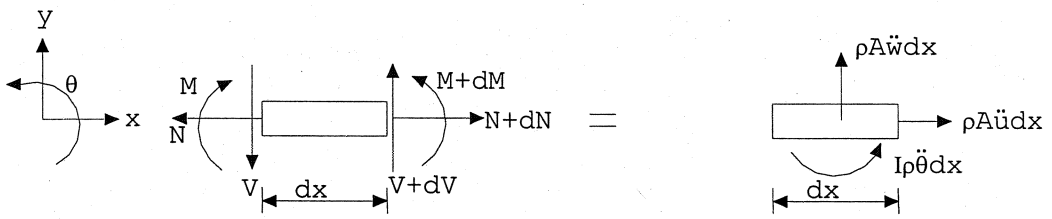

Fig. 5.1: The free body diagram of a beam element in motion

With reference to Fig. 5.1, the equations of motion in the xy plane, involving shear force $V = V(x)$, bending moment $M = M(x)$, and axial force $N = N(x)$ are

$$\frac{\partial V}{\partial x} = A\rho\frac{\partial^2 w}{\partial t^2}, \tag{5.1}$$

$$\frac{\partial M}{\partial x} + V = \rho I\frac{\partial^2}{\partial t^2}(\frac{\partial w}{\partial x}), \tag{5.2}$$

$$\frac{\partial N}{\partial x} = A\rho\frac{\partial^2 u}{\partial t^2} \tag{5.3}$$

where in view of their tensor character the internal moment and forces, M, V, and N are positive as shown. ρ stands for the mass per unit volume, A denotes the cross-sectional area, and I is the area moment of inertia about the centroidal principal axis. The rotation of the cross section, in accordance with Bernoulli-Euler hypothesis is taken equal to the slope, $\theta = \frac{\partial w}{\partial x}$. The assumption of small rotations ($\frac{\partial w}{\partial x} \ll 1$) leads to the strain expression $\epsilon = \frac{\partial u}{\partial x} - y\frac{\partial^2 w}{\partial x^2}$, and that of linear elastic isotropic material to

$$M = -\int \sigma y \, dA = -\int E\epsilon y \, dA = \int E\frac{\partial^2 w}{\partial x^2} y^2 \, dA = EI\frac{\partial^2 w}{\partial x^2}, \text{ and} \tag{5.4}$$

$$N = \int \sigma \, dA = \int E\epsilon dA = EA\frac{\partial u}{\partial x} \tag{5.5}$$

where E is Young's modulus. Consequently, the equations of motion can be written as

$$EI\frac{\partial^4 w}{\partial x^4} + A\rho\frac{\partial^2 w}{\partial t^2} - \rho I\frac{\partial^2}{\partial t^2}(\frac{\partial^2 w}{\partial x^2}) = 0 \text{ and} \tag{5.6}$$

$$EA\frac{\partial^2 u}{\partial x^2} - A\rho\frac{\partial^2 u}{\partial t^2} = 0 \tag{5.7}$$

If ω denotes a natural frequency, then free vibrations with this frequency requires

$$w(x,t) = W(\xi)\, e^{i\omega t},\ u(x,t) = U(\xi)\, e^{i\omega t} \tag{5.8}$$

in which $\xi = x/L$ is a non-dimensional variable and $W(\xi)$ and $U(\xi)$ are amplitudes of transverse and axial displacements, respectively. The differential equations become

$$\frac{d^4 W}{d\xi^4} - \alpha^4 W + \frac{\alpha^4 r^2}{L^2}\frac{\partial^2 W}{\partial \xi^2} = 0 \text{ and} \tag{5.9}$$

$$\frac{d^2 U}{d\xi^2} + \beta^2 U = 0 \tag{5.10}$$

wherein

$$\beta = \frac{L\omega}{c},\ \alpha^4 = \frac{AL^4\rho}{EI}\omega^2 = \frac{L^2\omega^2}{c^2}(\frac{L}{r})^2 = (\frac{\beta L}{r})^2,\ c^2 = \frac{E}{\rho},\ r = \sqrt{I/A}. \tag{5.11}$$

Symbol c stands for the velocity of sound along the beam length, and r denotes the radius of gyration of the beam cross-section. The roots m of the characteristic equation for $W(\xi)$ are

$$m^2 = \alpha^2\{ -\frac{\alpha^2 r^2}{2L^2} \pm \sqrt{1+(\frac{\alpha^2 r^2}{2L^2})^2}\ \}. \tag{5.12}$$

Now, if the attention is restricted to those natural frequencies $\omega \ll \frac{2c}{r}$, or equivalently $\frac{\alpha^2 r^2}{2L^2} \ll 1$, then for such cases, $m^2 \approx \pm\alpha^2$ and the rotary inertia term in the differential equation for $W(\xi)$ may be considered negligible, so that in effect $\frac{\partial M}{\partial x} + V = 0$ or $V = -EI\frac{\partial^3 w}{\partial x^3}$. The general solution can then be expressed as

$$W(\xi) = K_1 \sin\alpha\xi + K_2 \cos\alpha\xi + K_3 \sinh\alpha\xi + K_4 \cosh\alpha\xi \tag{5.13}$$

$$U(\xi) = C_1 \sin C\xi + C_2 \cos C\xi \tag{5.14}$$

involving arbitrary constants K_1, K_2, K_3, K_4 and C_1, C_2 to accommodate specified boundary conditions on bending moment M, shear force V, axial force N, slope $\frac{dW}{d\xi}$, and displacements W and U at left ($\xi = 0$) and at right ($\xi = 1$) ends.

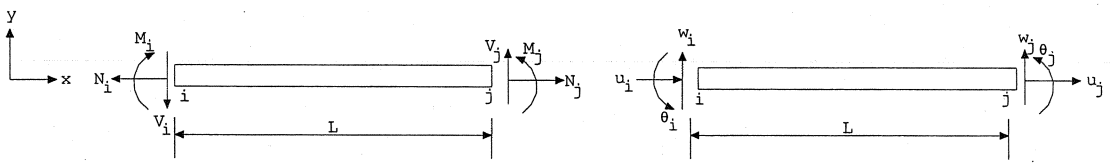

Fig. 5.2: Positive sign convention for positive quantities at nodes i and j.

Denoting the beam end joints as i and j, the quantities at the right of joint i (or left of member $i-j$), positive as shown in Fig. 5.2, are

$$W_i^R = (K_2 + K_4) \tag{5.15}$$

$$\theta_i^R = \frac{dW}{Ld\xi} = \frac{\alpha}{L}(K_1 + K_3) \tag{5.16}$$

$$V_i^R = -\frac{EI}{L^3}\frac{d^3W}{d\xi^3}\Big|_{\xi=0} = \frac{EI\alpha^3}{L^3}(K_1 - K_3), \tag{5.17}$$

$$M_i^R = \frac{EI}{L^2}\frac{d^2W}{d\xi^2}\Big|_{\xi=0} = -\frac{EI\alpha^2}{L^2}(K_2 - K_4), \tag{5.18}$$

These give

$$K_1 = \frac{1}{2\alpha}(L\theta_i^R + \frac{L^3}{EI\alpha^2}V_i^R),\ K_2 = \frac{1}{2}(W_i^R - \frac{L^2}{EI\alpha^2}M_i^R) \tag{5.19}$$

$$K_3 = \frac{1}{2\alpha}(L\theta_i^R - \frac{L^3}{EI\alpha^2}V_i^R),\ K_4 = \frac{1}{2}(W_i^R + \frac{L^2}{EI\alpha^2}M_i^R) \tag{5.20}$$

and hence

$$W(\xi) = \frac{\cos\alpha\xi + \cosh\alpha\xi}{2}W_i^R + \frac{\sin\alpha\xi + \sinh\alpha\xi}{2}\frac{L}{\alpha}\theta_i^R + \frac{\sin\alpha\xi - \sinh\alpha\xi}{2}\frac{L^3}{EI\alpha^3}V_i^R - \frac{\cos\alpha\xi - \cosh\alpha\xi}{2}\frac{L^2}{EI\alpha^2}M_i^R \tag{5.21}$$

The quantities at the left of joint j (or right of member $i-j$) are therefore

$$W_j^L = W\big|_{\xi=1} = \frac{\cos\alpha + \cosh\alpha}{2}W_i^R + \frac{\sin\alpha + \sinh\alpha}{2}\frac{L}{\alpha}\theta_i^R + \frac{\sin\alpha - \sinh\alpha}{2}\frac{L^3}{EI\alpha^3}V_i^R - \frac{\cos\alpha - \cosh\alpha}{2}\frac{L^2}{EI\alpha^2}M_i^R \tag{5.22}$$

$$\theta_j^L = \frac{dW}{Ld\xi}\Big|_{\xi=1} = -\frac{(\sin\alpha - \sinh\alpha)}{2}\frac{\alpha}{L}W_i^R + \frac{(\cos\alpha + \cosh\alpha)}{2}\theta_i^R + \frac{(\cos\alpha - \cosh\alpha)}{2}\frac{L^2}{EI\alpha^2}V_i^R + \frac{(\sin\alpha + \sinh\alpha)}{2}\frac{L}{\alpha EI}M_i^R \tag{5.23}$$

$$V_j^L = -\frac{EI}{L^3}\frac{d^3W}{d\xi^3}\Big|_{\xi=1} = -\frac{(\sin\alpha + \sinh\alpha)}{2}\frac{EI\alpha^3}{L^3}W_i^R + \frac{(\cos\alpha - \cosh\alpha)}{2}\frac{EI\alpha^2}{L^2}\theta_i^R + \frac{(\cos\alpha + \cosh\alpha)}{2}V_i^R + \frac{(\sin\alpha - \sinh\alpha)}{2}\frac{\alpha}{L}M_i^R \tag{5.24}$$

$$M_j^L = \frac{EI}{L^2}\frac{d^2W}{d\xi^2}\Big|_{\xi=1} = -\frac{(\cos\alpha - \cosh\alpha)}{2}\frac{EI\alpha^2}{L^2}W_i^R - \frac{(\sin\alpha - \sinh\alpha)}{2}\frac{EI\alpha}{L}\theta_i^R - \frac{(\sin\alpha + \sinh\alpha)}{2}\frac{L}{\alpha}V_i^R + \frac{(\cos\alpha + \cosh\alpha)}{2}M_i^R \tag{5.25}$$

For longitudinal vibrations, the solution of $\frac{d^2U}{d\xi^2} + C^2U = 0$ can be written as

$$U(\xi) = U_i^R\cos C\xi + \frac{LN_i^R}{CEA}\sin C\xi \tag{5.26}$$

where U_i^R and N_i^R are respectively the axial displacement and axial force at $\xi = 0$. These quantities at end $\xi = 1$ are

$$U_j^L = U_i^R \cos C + \frac{LN_i^R}{CEA} \sin C, \text{ and } N_j^L = -U_i^R \frac{CEA}{L} \sin C + N_i^R \cos C \tag{5.27}$$

The connection between the quantities at the two joints of a member $i - j$, right of joint i to those at the left of joint j can now be written via a transfer matrix as:

$$\begin{bmatrix} U_j^L \\ W_j^L \\ \theta_j^L \\ N_j^L \\ V_j^L \\ M_j^L \end{bmatrix} = \begin{bmatrix} e & 0 & 0 & \frac{Lf}{B_2 C} & 0 & 0 \\ 0 & a & \frac{Lc}{\alpha} & 0 & \frac{L^3 d}{B_1 \alpha^3} & -\frac{L^2 b}{B_1 \alpha^2} \\ 0 & -\frac{\alpha d}{L} & a & 0 & \frac{bL^2}{B_1 \alpha^2} & \frac{Lc}{B_1 \alpha} \\ -\frac{B_2}{L} Cf & 0 & 0 & e & 0 & 0 \\ 0 & -\frac{B_1 \alpha^3}{L^3} c & \frac{B_1 \alpha^2}{L^2} b & 0 & a & \frac{\alpha d}{L} \\ 0 & -\frac{B_1 \alpha^2}{L^2} b & -\frac{B_1 \alpha}{L} d & 0 & -\frac{Lc}{\alpha} & a \end{bmatrix} \begin{bmatrix} U_i^R \\ W_i^R \\ \theta_i^R \\ N_i^R \\ V_i^R \\ M_i^R \end{bmatrix} \tag{5.28}$$

where the new symbols B_1, B_2, a, b, c, d have the following definitions:

$$B_1 = EI = \text{ bending rigidity, } B_2 = EA = B_1/r^2 = \text{axial rigidity,} \tag{5.29}$$

$$a = \frac{(\cos\alpha + \cosh\alpha)}{2}, \; b = \frac{(\cos\alpha - \cosh\alpha)}{2}, \tag{5.30}$$

$$c = \frac{(\sin\alpha + \sinh\alpha)}{2}, d = \frac{(\sin\alpha - \sinh\alpha)}{2}. \tag{5.31}$$

$$e = \cos C, \; f = \sin C \tag{5.32}$$

As an immediate verification example, we note that for a cantilever beam fixed at the left joint i ($U_i^R = W_i^R = \theta_i^R = 0$) and free at the right end j ($N_j^L = V_j^R = M_j^R = 0$), the above relations become

$$\begin{bmatrix} U_j^L \\ W_j^L \\ \theta_j^L \\ 0 \\ 0 \\ 0 \end{bmatrix} = \begin{bmatrix} e & 0 & 0 & \frac{Lf}{B_2C} & 0 & 0 \\ 0 & a & \frac{Lc}{\alpha} & 0 & \frac{L^3d}{B_1\alpha^3} & -\frac{L^2b}{B_1\alpha^2} \\ 0 & -\frac{\alpha d}{L} & a & 0 & \frac{bL^2}{B_1\alpha^2} & \frac{Lc}{B_1\alpha} \\ -\frac{B_2}{L}Cf & 0 & 0 & e & 0 & 0 \\ 0 & -\frac{B_1\alpha^3}{L^3}c & \frac{B_1\alpha^2}{L^2}b & 0 & a & \frac{\alpha d}{L} \\ 0 & -\frac{B_1\alpha^2}{L^2}b & -\frac{B_1\alpha}{L}d & 0 & -\frac{Lc}{\alpha} & a \end{bmatrix} \begin{bmatrix} 0 \\ 0 \\ 0 \\ N_i^R \\ V_i^R \\ M_i^R \end{bmatrix} \tag{5.33}$$

which can be written as two decoupled matrix equations:

$$\begin{bmatrix} e & 0 & 0 \\ 0 & a & \frac{\alpha d}{L} \\ 0 & -\frac{Lc}{\alpha} & a \end{bmatrix} \begin{bmatrix} N_i^R \\ V_i^R \\ M_i^R \end{bmatrix} = \begin{bmatrix} 0 \\ 0 \\ 0 \end{bmatrix} \text{ and} \tag{5.34}$$

$$\begin{bmatrix} U_j^L \\ W_j^L \\ \theta_j^L \end{bmatrix} = \begin{bmatrix} \frac{Lf}{B_2C} & 0 & 0 \\ 0 & \frac{L^3d}{B_1\alpha^3} & -\frac{L^2b}{B_1\alpha^2} \\ 0 & \frac{bL^2}{B_1\alpha^2} & \frac{Lc}{B_1\alpha} \end{bmatrix} \begin{bmatrix} N_i^R \\ V_i^R \\ M_i^R \end{bmatrix} \tag{5.35}$$

The first is a set of homogeneous equations to determine N_i^R, V_i^R, M_i^R. The second set then yields U_i^R, W_i^R, θ_i^R. The condition for the nontrivial solution of the first set is vanishing of its determinant, which is the frequency equation for such a beam, namely:

$$e(a^2 + cd) = 0, \text{ i.e., } (1 + \cos\alpha \cosh\alpha)\cos C = 0 \tag{5.36}$$

which is a well known equation. From a similar procedure it follows that the frequency equation for a simply supported beam is $e(c^2 - d^2) \equiv \sin\alpha \sinh\alpha \cos C = 0$, whereas for a beam fixed at both ends it is $f(b^2 + cd) \equiv \sin C\,(1 - \cos\alpha\, \cosh\alpha) = 0$. Note that in all these examples, the axial vibrations of the beam are uncoupled from the transverse vibrations.

Symbolically we may write the above relations as

$$\{\Delta_j\} = [T_{ji}]\{\Delta_i\} \tag{5.37}$$

where $[T_{ji}]$ is the above 6×6 *member transfer matrix* connecting the six quantities $\{\Delta_i\}$ at end i to $\{\Delta_j\}$ at end j of the member.

5.2 Bents with Straight Segments, Joint Transfer Matrix

For a beam with segments of different section properties, and meeting at angles, we must supplement the above member transfer matrix with a *joint transfer matrix*. Additionally, we may endow the joint with desirable stiffness or flexibility properties to account for joint deformation or joint slip. Restricting to beam segments with XY plane as the common principal plane, let the local x_i axis be directed from node i to node j and let α_i be its inclination with respect to global X axis. Then the global components of the six quantities at the left of joint j, denoted by δ_j^L, are

$$\{\delta_j^L\} = [R^L{}_{\alpha_i}]\{\Delta_j\} \tag{5.38}$$

where $[R^L{}_{\alpha_i}]$ is the transformation matrix converting components of vectors in the local (member) system to those with respect to the global (joint) coordinate system. Explicitly:

$$\{\delta_j^L\} = \begin{bmatrix} u_j \\ v_j \\ \theta_j \\ F_{jx} \\ F_{jy} \\ M_{jz} \end{bmatrix} = \begin{bmatrix} \cos\alpha_i & -\sin\alpha_i & 0 & 0 & 0 & 0 \\ \sin\alpha_i & \cos\alpha_i & 0 & 0 & 0 & 0 \\ 0 & 0 & 1 & 0 & 0 & 0 \\ 0 & 0 & 0 & \cos\alpha_i & -\sin\alpha_i & 0 \\ 0 & 0 & 0 & \sin\alpha_i & \cos\alpha_i & 0 \\ 0 & 0 & 0 & 0 & 0 & 1 \end{bmatrix} \begin{bmatrix} U_j \\ W_j \\ \theta_j \\ N_j \\ V_j \\ M_j \end{bmatrix} \tag{5.39}$$

Now $\{\delta_j^R\}$, the six global components at the right of joint j, may be expressed in terms of those at the left by means of a joint transfer matrix $[t_j]$ as

$$\{\delta_j^R\} = [t_j]\{\delta_j^L\} \tag{5.40}$$

The nature of $[t_j]$ will depend upon the joint characteristics. In this work,

$$\begin{bmatrix} u_j^R \\ v_j^R \\ \theta_j^R \\ F_{jx}^R \\ F_{jy}^R \\ M_{jz}^R \end{bmatrix} = \begin{bmatrix} 1 & 0 & 0 & \frac{1}{k_{jx}} & 0 & 0 \\ 0 & 1 & 0 & 0 & \frac{1}{k_{jy}} & 0 \\ 0 & 0 & 1 & 0 & 0 & \frac{1}{k_{jz}} \\ 0 & 0 & 0 & 1 & 0 & 0 \\ 0 & 0 & 0 & 0 & 1 & 0 \\ 0 & 0 & 0 & 0 & 0 & 1 \end{bmatrix} \begin{bmatrix} u_j^L \\ v_j^L \\ \theta_j^L \\ F_{jx}^L \\ F_{jy}^L \\ M_{jz}^L \end{bmatrix} \tag{5.41}$$

where k_{jx}, k_{jy}, k_{jz} are joint stiffness at joint j against X, Y displacements and Z rotation, and where we have assumed that joint inertia forces can be neglected and hence

left and right joint forces and moments must be in equilibrium. For a perfectly stiff (i.e., rigid) joint $k_{jx} = k_{jy} = k_{jz} = \infty$, and the above matrix becomes an identity matrix.

Now if α_j is the inclination of the member spanning joints j and k, then the quantities at the right of joint j in global and local coordinates are related as

$$\{\Delta_j^R\} = \begin{bmatrix} U_j^R \\ W_j^R \\ \theta_j^R \\ N_j^R \\ V_j^R \\ M_j^R \end{bmatrix} = \begin{bmatrix} \cos\alpha_j & \sin\alpha_j & 0 & 0 & 0 & 0 \\ -\sin\alpha_j & \cos\alpha_j & 0 & 0 & 0 & 0 \\ 0 & 0 & 1 & 0 & 0 & 0 \\ 0 & 0 & 0 & \cos\alpha_j & \sin\alpha_j & 0 \\ 0 & 0 & 0 & -\sin\alpha_j & \cos\alpha_j & 0 \\ 0 & 0 & 0 & 0 & 0 & 1 \end{bmatrix} \begin{bmatrix} u_j^R \\ v_j^R \\ \theta_j^R \\ F_{jx}^R \\ F_{jy}^R \\ M_{jz}^R \end{bmatrix} \tag{5.42}$$

or symbolically as

$$\{\Delta_j^R\} = [R_{\alpha_j}]^T \{\delta_j^R\} \tag{5.43}$$

Then combining the above results we may write

$$\{\Delta_j^R\} = [T_j]\{\Delta_j^L\} \text{ where} \tag{5.44}$$

$$[T_j] = [R_{\alpha_j}]^T [t_j][R_{\alpha_i}] \tag{5.45}$$

is the joint transfer matrix. This operation is shown pictorially for the forces and moments, as well as for displacements and rotations in Figs. 5.3 and 5.4.

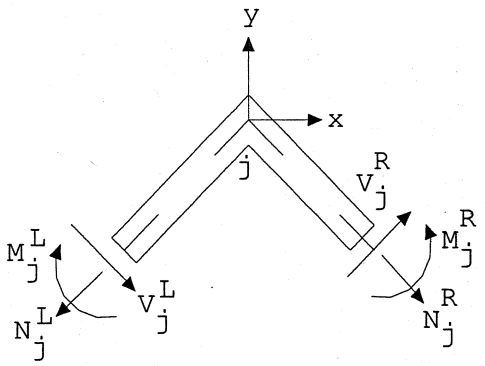

Fig. 5.3: Joint forces and moments.

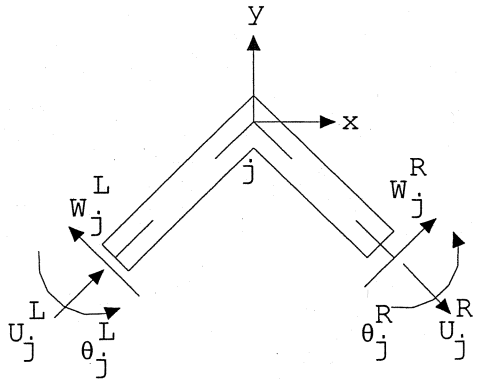

Fig. 5.4: Joint displacements and rotations.

Explicitly, the joint transfer matrix has the following form:

$$[T_j] = \begin{bmatrix} \cos(\alpha_j - \alpha_i) & \sin(\alpha_j - \alpha_i) & 0 & \frac{\cos\alpha_i\cos\alpha_j}{k_{jx}} + \frac{\sin\alpha_i\sin\alpha_j}{k_{jy}} & \frac{\sin\alpha_j\cos\alpha_i}{k_{jy}} - \frac{\sin\alpha_i\cos\alpha_j}{k_{jx}} & 0 \\ -\sin(\alpha_j - \alpha_i) & \cos(\alpha_j - \alpha_i) & 0 & \frac{\cos\alpha_j\sin\alpha_i}{k_{jy}} - \frac{\cos\alpha_i\sin\alpha_j}{k_{jx}} & \frac{\cos\alpha_i\cos\alpha_j}{k_{jy}} + \frac{\sin\alpha_i\sin\alpha_j}{k_{jx}} & 0 \\ 0 & 0 & 1 & 0 & 0 & \frac{1}{k_{jz}} \\ 0 & 0 & 0 & \cos(\alpha_j - \alpha_i) & \sin(\alpha_j - \alpha_i) & 0 \\ 0 & 0 & 0 & -\sin(\alpha_j - \alpha_i) & \cos(\alpha_j - \alpha_i) & 0 \\ 0 & 0 & 0 & 0 & 0 & 1 \end{bmatrix} \tag{5.46}$$

In this work, joint deformations are allowed in the rotational degree of freedom, but not in the translational degrees of freedom. This in effect means that $k_{jx} = k_{jy} = \infty$ always, but k_{jz} may be assigned a finite value. If in addition to the rotational stiffness k_{jz}, there is also rotational damping with coefficient C_{jz}, then

$$M_{jz}^R = C_{jz}(\dot{\theta}_j^R - \dot{\theta}_j^L) + k_{jz}(\theta_j^R - \theta_j^L) \tag{5.47}$$

Assuming harmonic vibrations with frequency ω, $\dot{\theta}_j^R = \sqrt{-1}\ \omega\theta_j^R$ and $\dot{\theta}_j^L = \sqrt{-1}\,\omega\ \theta_j^L$, the joint transformation matrix can be written as

$$[T_j] = \begin{bmatrix} \cos(\alpha_j - \alpha_i) & \sin(\alpha_j - \alpha_i) & 0 & 0 & 0 & 0 \\ -\sin(\alpha_j - \alpha_i) & \cos(\alpha_j - \alpha_i) & 0 & 0 & 0 & 0 \\ 0 & 0 & 1 & 0 & 0 & \frac{1}{k_{jz} + \sqrt{-1}\ \omega C_{jz}} \\ 0 & 0 & 0 & \cos(\alpha_j - \alpha_i) & \sin(\alpha_j - \alpha_i) & 0 \\ 0 & 0 & 0 & -\sin(\alpha_j - \alpha_i) & \cos(\alpha_j - \alpha_i) & 0 \\ 0 & 0 & 0 & 0 & 0 & 1 \end{bmatrix} \tag{5.48}$$

5.3 Exact Frequencies of a One-Story One-Bay Frame

The above formulation is now applied to determining the frequencies of vibration of the one-story frame of the experiment described in Chapter 4. The two columns and one beam of this frame have identical geometric and (Aluminum) material properties:

$$L = 15\,\text{in} = 0.381\,\text{m},\ A = \frac{1}{8} \times 3\,\text{in}^2 = 2.42 \times 10^{-4}\text{m}^2, \rho = 2768.0\,\text{kg/m}^3$$

$$I = \frac{1}{8} \times \frac{3^3}{12}\,\text{in}^4 = 117 \times 10^{-9}\text{m}^4,\ E = 10.4 \times 10^6\,\text{psi} = 71.7 \times 10^9\,\text{N/m}^2$$

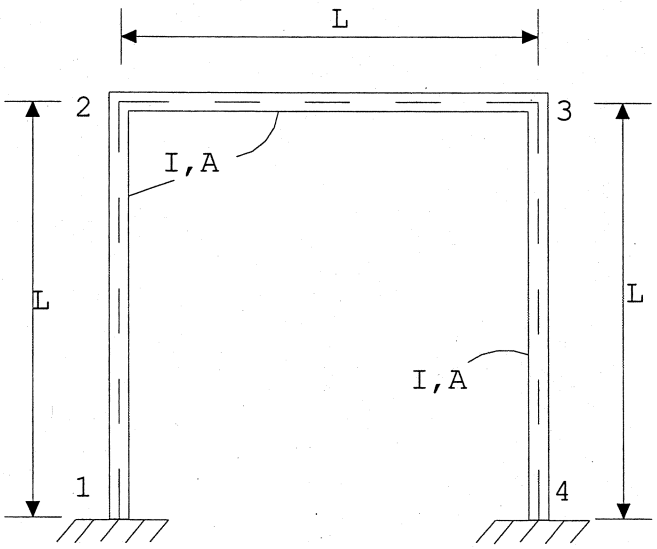

Fig. 5.5: The frame of the experiment, Chapter 4.

The four joints are named as 1, 2, 3, 4 with joints 1 and 2 considered fixed, Fig. 5.5. For joints 2 and 3, identical stiffness and damping coefficients are assumed.

The sequence of matrix multiplications giving the connection between quantities at joint 1 to those at joint 4 are:

$$\{\Delta_4\} = [T_{43}][T_3][T_{23}][T_2][T_{21}]\{\Delta_1\} \tag{5.49}$$

For the three members $\alpha_1 = 90°, \alpha_2 = 0°, \alpha_3 = -90°$, and hence $(\alpha_2 - \alpha_1) = -90°$, $(\alpha_3 - \alpha_2) = -90°$. Thereby

$$[T_2] = [T_3] = \begin{bmatrix} 0 & -1 & 0 & 0 & 0 & 0 \\ 1 & 0 & 0 & 0 & 0 & 0 \\ 0 & 0 & 1 & 0 & 0 & \dfrac{1}{k_{jz} + \sqrt{-1}\,\omega C_{jz}} \\ 0 & 0 & 0 & 0 & -1 & 0 \\ 0 & 0 & 0 & 1 & 0 & 0 \\ 0 & 0 & 0 & 0 & 0 & 1 \end{bmatrix} \tag{5.50}$$

$$[T_{21}] = [T_{32}] = [T_{43}] = \begin{bmatrix} e & 0 & 0 & \frac{Lf}{B_2C} & 0 & 0 \\ 0 & a & \frac{Lc}{\alpha} & 0 & \frac{L^3d}{B_1\alpha^3} & -\frac{L^2b}{B_1\alpha^2} \\ 0 & -\frac{\alpha d}{L} & a & 0 & \frac{bL^2}{B_1\alpha^2} & \frac{Lc}{B_1\alpha} \\ -\frac{B_2}{L}Cf & 0 & 0 & e & 0 & 0 \\ 0 & -\frac{B_1\alpha^3}{L^3}c & \frac{B_1\alpha^2}{L^2}b & 0 & a & \frac{\alpha d}{L} \\ 0 & -\frac{B_1\alpha^2}{L^2}b & -\frac{B_1\alpha}{L}d & 0 & -\frac{Lc}{\alpha} & a \end{bmatrix} \tag{5.51}$$

The sequence of matrix multiplications giving the connection between quantities at joint 1 to those at joint 4 are:

$$\{\Delta_4\} = [T_{43}][T_3][T_{23}][T_2][T_{21}]\{\Delta_1\} \tag{5.52}$$

From the resulting 6×6 matrix equation we can extract the 3×3 matrix equation by virtue of the ends 1 and 4 being fixed ends as was done previously for the beam example. The determinant of the 3×3 matrix gives the frequency equation. We refrain from writing the resulting 3×3 matrix as it is very complex with many large terms. Eventually numerical values must be substituted for calculations of the frequencies.

Although we can account for finite joint stiffness and possible rotational damping, we chose not to do so for the sake of simplicity as the calculations for these cases are very tedious involving complex numbers in a transcendental frequency equation. We confine ourselves to computing exact frequencies for the standard rigid joint case for which $k_{jz} = \infty$, $C = 0$. The first ten benchmark frequencies are shown in the following table:

No.	Exact Freq.	NASTRAN
	Hz	Hz
1	389.78	389.79
2	1421.18	1421.20
3	2287.97	2287.65
4	2504.76	2506.49
5	2759.09	2757.38
6	3588.87	3590.94
7	5016.16	5008.35
8	5745.65	5759.66
9	7300.60	7310.71
10	7796.54	7830.97

Table 5.1: Exact and NASTRAN frequencies.

For comparison NASTRAN results were obtained on the basis of 5 elements per member for the same frame (see Chapter 6). It is evident that NASTRAN results are quite good for all ten frequencies. This establishes the validity of using 5 elements per member as a good finite element division for obtaining the first 10 frequencies with sufficient accuracy.

CHAPTER 6

FREQUENCIES OF PLANE FRAMES WITH ROTATIONAL JOINT DAMPING

6.1 Introduction

This Chapter deals with determining the natural frequencies of general frame structures with viscous rotational joint damping. For simplicity, the analysis is restricted to two dimensional frames with members lying in xy plane, which is also the common principal plane for all frame members.

The analysis is complicated because any frame joint can be considered to have finite rotational stiffness as well as rotational damping. Each member meeting at such a joint may have a different rotation. Thus, if there are m members meeting at such a joint, then there are m rotations corresponding to that joint. In contrast, in the traditional method of analysis, all members meeting at a joint have the same common rotation, which is called the joint rotation. In effect, it is assumed in this latter case that the joint has infinite stiffness and no relative rotation is possible between the members meeting at the joint. Thus, in the present case of frame analysis, there can be many more degrees of freedom than in frames analyzed with the usual assumption of rigid joints.

The present theoretical formulation leads to a complex-valued quadratic eigenvalue problem with sparse damping matrix. The general problem is solved by constructing a MatLab program by appropriately choosing the subroutines required for solving the problem. Commercial finite element codes do not allow the option of modeling of damping in this way, and therefore the validation of the constructed program can only be done for cases where joints are considered rigid, and damping is neglected. This limited validation was carried out here by comparing the results from the present program with those obtained by performing analyses with the NASTRAN finite element code.

Additionally, independent Mathematica programs were constructed to verify the results obtained by the MatLab programs, using a different numerical method to solve the

quadratic eigenvalue problem. This was done for almost all cases presented in this thesis and in each case the results were found to be almost identical.

6.2 Finite Element Formulation

Similar to the standard method, the present analysis also deals with the derivation of the matrix equations for obtaining the frequencies and the corresponding mode shapes. These equations include the global stiffness matrix which now has rotational joint stiffness terms, global mass matrix with massless springs, and the global rotational joint damping matrix which is of the utmost importance for the present thesis.

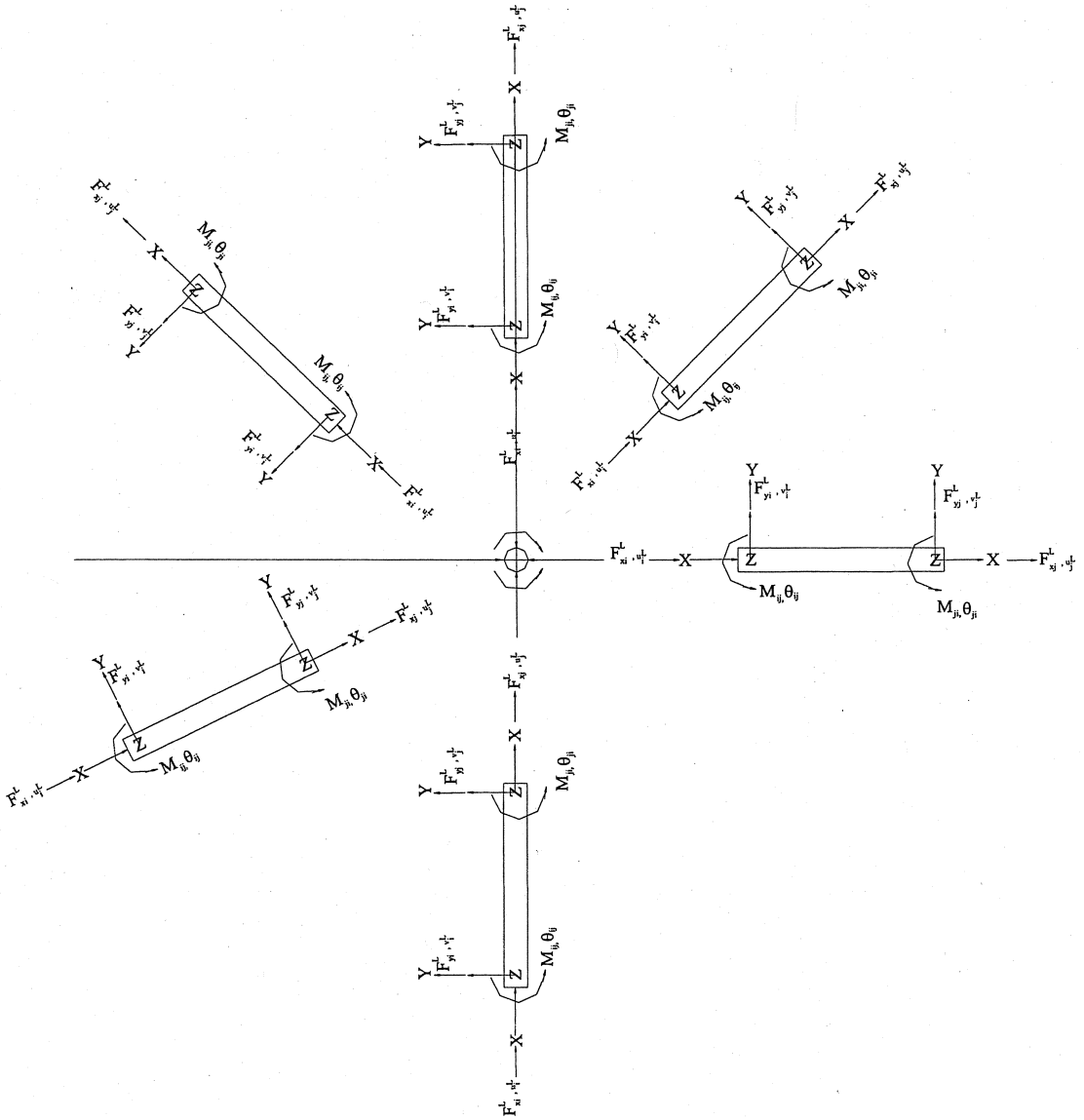

Fig. 6.1: A joint with arbitrary number of members connected to it.

Fig. 6.1 shows a typical joint to which arbitrary m members, here $m = 6$, are connected. For a simple theoretical formulation we assume that the joint is like a rotational spring with members connected to it. The spring resists rotations of connected elements relative to each other. Now, assume that each member connected to joint A undergoes a positive, i.e. counterclockwise rotation, θ_{A1}, θ_{A2}, θ_{A3}, $\ldots\theta_{Am}$. Then, the relative rotations of member 1 meeting at joint A with respect to other members are:

$$\theta_{A1} - \theta_{A2}, \theta_{A1} - \theta_{A3}, \ldots\theta_{A1} - \theta_{Am} \tag{6.1}$$

Hence, if k_A is the spring constant of joint A then the resisting moments applied by the spring to member 1 at joint A is

$$M_{A1} = k_A(\theta_{A1} - \theta_{A2}) + k_A(\theta_{A1} - \theta_{A3}) + \ldots k_A(\theta_{A1} - \theta_{Am}) \tag{6.2}$$

Similarly, the relative rotations of member 2 meeting at the same joint A are:

$$\theta_{A2} - \theta_{A1}, \theta_{A2} - \theta_{A3}, \ldots\theta_{A2} - \theta_{Am} \tag{6.3}$$

and the resisting moment applied by the spring to member 2, is

$$M_{A2} = k_A(\theta_{A2} - \theta_{A1}) + k_A(\theta_{A2} - \theta_{A3}) + \ldots k_A(\theta_{A2} - \theta_{Am}) \tag{6.4}$$

The same procedure is be applied to all the members, m meeting at the joint.

In matrix notation, the complete relations can be expressed as:

$$\begin{Bmatrix} M_{A1} \\ M_{A2} \\ . \\ M_{Am} \end{Bmatrix} = \begin{bmatrix} (m-1)\,k_A & -k_A & -k_A & \ldots & \ldots & -k_A \\ -k_A & (m-1)\,k_A & -k_A & \ldots & \ldots & -k_A \\ . & . & . & \ldots & \ldots & -k_A \\ -k_A & -k_A & -k_A & \ldots & \ldots & (m-1)\,k_A \end{bmatrix} \begin{Bmatrix} \theta_{A1} \\ \theta_{A2} \\ . \\ \theta_{Am} \end{Bmatrix} \tag{6.5}$$

Symbolically, this equation for joint A can be written as

$$\{M_A\} = [k_A]\{\theta_A\} \tag{6.6}$$

For the whole system, the above equation can be written as

$$\{M^J\} = [K^J]\{\Delta^J\} \tag{6.7}$$

where, $\{\Delta^J\}$ is the vector of the global degrees of freedom and $[K^J]$ is the assembled global stiffness matrix corresponding to the finite stiffness of joints.

$$[K^J] = [k_A] + [k_B] + \ldots \tag{6.8}$$

where, the sum extends over the joints with finite rotational stiffness and where their stiffness matrices $[k_A]$, $[k_B]$, ... have been augmented appropriately to the system size.

The similar formulation applies for damping. At joint A the relative velocities of rotation are

$$\dot{\theta}_{A1} - \dot{\theta}_{A2},\ \dot{\theta}_{A1} - \dot{\theta}_{A3}, \ldots \dot{\theta}_{A1} - \dot{\theta}_{Am} \tag{6.9}$$

Hence, if C_A is the damping constant of joint A then the resisting moments applied by the damper to member 1 at joint A is

$$M'_{A1} = C_A(\dot{\theta}_{A1} - \dot{\theta}_{A2}) + C_A(\dot{\theta}_{A1} - \dot{\theta}_{A3}) + \ldots C_A(\dot{\theta}_{A1} - \dot{\theta}_{Am}) \tag{6.10}$$

and, similarly for other members meeting at joint A. All such relations can be expressed in matrix notation as:

$$\begin{Bmatrix} M'_{A1} \\ M'_{A2} \\ . \\ M'_{Am_d} \end{Bmatrix} = \begin{bmatrix} (m-1)C_A & -C_A & -C_A & \ldots & \ldots & -C_A \\ -C_A & (m-1)C_A & -C_A & \ldots & \ldots & -C_A \\ . & . & . & \ldots & \ldots & -C_A \\ -C_A & -C_A & -C_A & \ldots & \ldots & (m-1)C_A \end{bmatrix} \begin{Bmatrix} \dot{\theta}_{A1} \\ \dot{\theta}_{A2} \\ . \\ \dot{\theta}_{Am} \end{Bmatrix} \tag{6.11}$$

or symbolically as, $\{M'_A\} = [C_A]\{\dot{\theta}_A\}$ (6.12)

For all the joints with dampers,

$$\{M'^J\} = [C^J]\{\dot{\Delta}^J\} \tag{6.13}$$

where $[C^J]$ is the assembled global damping matrix corresponding to the joints with rotational damping:

$$[C^J] = [C_A] + [C_B] + \ldots \tag{6.14}$$

where, $[C_A]$, $[C_B]$, ... are the damping matrices for individual joints augmented appropriately to the system size.

Now, consider the energies of the joints. The strain energy of the joint A is:

$$\begin{aligned} U_A = \quad & \tfrac{1}{4}k_A(\theta_{A1} - \theta_{A2})^2 + \tfrac{1}{4}k_A(\theta_{A1} - \theta_{A3})^2 + \ldots + \tfrac{1}{4}k_A(\theta_{A1} - \theta_{Am})^2 + \\ & \tfrac{1}{4}k_A(\theta_{A2} - \theta_{A1})^2 + \tfrac{1}{4}k_A(\theta_{A2} - \theta_{A3})^2 + \ldots + \tfrac{1}{4}k_A(\theta_{A2} - \theta_{Am})^2 \\ & + \ldots \end{aligned} \tag{6.15}$$

where the factor $\frac{1}{4}$ is used in place of the standard factor $\frac{1}{2}$ because the strain energies of the relative rotations have been counted twice in the above expression. This is due to the fact that the relative rotation like $(\theta_{A1} - \theta_{A2})$ is equal in magnitude to $(\theta_{A2} - \theta_{A1})$ and should not be counted twice. Obviously, the value of the strain energy is zero when the joint is considered rigid, as in the traditional method, i.e. when the relative rotations are zero or alternatively the joint stiffness is infinite.

The total energy of joint deformations for n joints is

$$U = U_A + U_B + \ldots Un = \sum_{\text{Joints}}^{n} U_j \tag{6.16}$$

In contrast to the above strain energy of the joints of the frame, their kinetic energies are taken to be zero by assuming them to be massless.

Now, consider the strain and the kinetic energies of the members. Let member 1 span between joints A and B. The finite element approximation gives the strain energy of this member as

$$[U_1^M] = \frac{1}{2} < \Delta_1 > [k_1]\{\Delta_1\} \tag{6.17}$$

and the kinetic energy as

$$[T_1^M] = \frac{1}{2} < \dot{\Delta}_1 > [m_1]\{\dot{\Delta}_1\} \tag{6.18}$$

where,

$$< \Delta_1 > = < u_A \quad v_A \quad \theta_{A1} \quad u_B \quad v_B \quad \theta_{B1} > \tag{6.19}$$

is the vector of global joint displacements and rotations corresponding to joints A and B. Note that $\theta_{A1}$is the rotation at joint A and $\theta_{B1}$is that at joint B associated with member 1. Similarly,

$$< \dot{\Delta}_1 > = < \dot{u}_A \quad \dot{v}_A \quad \dot{\theta}_{A1} \quad \dot{u}_B \quad \dot{v}_B \quad \dot{\theta}_{B1} > \tag{6.20}$$

is the vector of global joint translational and rotational velocities associated with member 1. Also

$[k_1]$ = global stiffness matrix of member 1, and

$[m_1]$= global mass matrix of member 1.

These global matrices are obtained from transforming the local stiffness and mass matrices $[k_1^L]$, $[m_1^L]$ by the usual transformation formulas

$$[k_1] = [R_1]^T[k_1^L][R_1],\ [m_1] = [R_1]^T[m_1^L][R_1] \tag{6.21}$$

where $[R_1]$ is the transformation matrix transforming vector components from the global coordinate system to the local member coordinate system.

$[k_1^L]$ and $[m_1^L]$ are standard matrices and can be found, for example in Cook [18].

$$[k_1^L] = \begin{bmatrix} \frac{EA}{L} & 0 & 0 & -\frac{EA}{L} & 0 & 0 \\ 0 & \frac{12EI}{L^3} & \frac{6EI}{L^2} & 0 & -\frac{12EI}{L^3} & \frac{6EI}{L^2} \\ 0 & \frac{6EI}{L^2} & \frac{4EI}{L} & 0 & -\frac{6EI}{L^2} & \frac{2EI}{L} \\ -\frac{EA}{L} & 0 & 0 & \frac{EA}{L} & 0 & 0 \\ 0 & -\frac{12EI}{L^3} & -\frac{6EI}{L^2} & 0 & \frac{12EI}{L^3} & -\frac{6EI}{L^2} \\ 0 & \frac{6EI}{L^2} & \frac{2EI}{L} & 0 & -\frac{6EI}{L^2} & \frac{4EI}{L} \end{bmatrix} \tag{6.22}$$

$$[m_1^L] = \rho AL \begin{bmatrix} \frac{1}{3} & 0 & 0 & \frac{1}{6} & 0 & 0 \\ 0 & \frac{13}{35} & \frac{11L}{210} & 0 & \frac{9}{70} & -\frac{13L}{420} \\ 0 & \frac{11L}{210} & \frac{L^2}{105} & 0 & \frac{13L}{420} & -\frac{L^2}{140} \\ \frac{1}{6} & 0 & 0 & \frac{1}{3} & 0 & 0 \\ 0 & \frac{9}{70} & \frac{13L}{420} & 0 & \frac{13}{35} & -\frac{11L}{210} \\ 0 & -\frac{13L}{420} & -\frac{L^2}{140} & 0 & -\frac{11L}{210} & \frac{L^2}{105} \end{bmatrix} \tag{6.23}$$

The strain and kinetic energies of the system, members as well as joints, can therefore be written as

$$\sum_{\text{members}}^{m} (T_i^M + U_i^M) + \sum_{\text{Joints}}^{n} U_j^J \tag{6.24}$$

Using the expressions derived, these can be written as:

$$\frac{1}{2} < \dot{\Delta} > [M^M]\{\dot{\Delta}\} + \frac{1}{2} < \Delta > [K^M]\{\Delta\} + \frac{1}{2} < \Delta > [K^J]\{\Delta\} \tag{6.25}$$

where,

$\{\Delta\}$ = the vector of all global displacement and rotation degrees of freedom,

$\{\dot{\Delta}\}$= the vector of all global translational and rotational velocity degrees of freedom, $[K^J]$ and, $[K^M]$ are the assembled global joint and member stiffness matrices and, $[M^M]$ is the assembled global mass matrix.

The equation of energy balance requires that the rate of change of strain and kinetic energies of the system is equal to the rate of dissipation due to damping. The rate of change of the total energy of the system is

$$\frac{d}{dt}\left[\frac{1}{2} < \dot{\Delta} > [M^M]\{\dot{\Delta}\} + \frac{1}{2} < \Delta > [K^M]\{\Delta\} + \frac{1}{2} < \Delta > [K^J]\{\Delta\}\right]$$
$$= - < \dot{\Delta} > [M'^J] = - < \dot{\Delta} > [C^J]\{\dot{\Delta}\} \tag{6.26}$$

where the term on the right side of the equation is the work of the damping moments acting at the joints through the velocities $< \dot{\Delta} >$.

This leads to,

$$< \dot{\Delta} > [M^M]\{\ddot{\Delta}\} + < \dot{\Delta} > [K^M]\{\Delta\} + < \dot{\Delta} > [K^J]\{\Delta\} = - < \dot{\Delta} > [C^J]\{\dot{\Delta}\} \tag{6.27}$$

This last equation can be interpreted as the virtual power equation involving the stiffness, damping, and inertia forces and moments of the system acting through the arbitrary velocities $< \dot{\Delta} >$. This implies the satisfaction of the following system equations:

$$[M^M]\{\ddot{\Delta}\} + [C^J]\{\dot{\Delta}\} + [K]\{\Delta\} = \{0\} \tag{6.28}$$

where $[K] = [K^M] + [K^J]$ (6.29)

The number of equations in this system is equal to

$$3n + \sum_{\text{damped joints}} (m - 1) \tag{6.30}$$

where, m is the number of members meeting at a joint with a rotational damper. In the traditional method of analysis, the system size is $3n$.

To solve this system of equations of motion, let

$$\{\Delta\} = \{\phi\}e^{\lambda t} \tag{6.31}$$

which upon substitution gives

$$\lambda^2[M]\{\phi\} + \lambda[C]\{\phi\} + [K]\{\phi\} = \{0\} \tag{6.32}$$

The common factor $e^{\lambda t}$ has been canceled out and the matrices are written without superscripts for simplicity in subsequent treatment of these equations. This above system of equations defines a quadratic eigenvalue problem. The solution of this problem involves determining the eigenvalues λ and the corresponding mode shapes $\{\phi\}$. The eigenvalues, as well as, the eigenmodes occur in pairs of complex conjugates quantities. For example,

$$\lambda_r = -C_r + i\omega_{dr},\ \lambda_{r+1} = \overline{\lambda}_r = -C_r - i\omega_{dr} \tag{6.33}$$

where, C_r and ω_{dr} are respectively, the damping factor and the frequency of the damped vibration with modes $\{\phi_r\}$ and $\{\phi_{r+1}\} = \{\overline{\phi}_r\}$.

One may solve the above system by the method shown in Chapter 2. Or, one may use the direct procedure of solving a polynomial eigenvalue problem of degree 2. Both procedures were used in this thesis for independent checks. Mathematica programs were constructed to implement the first method, whereas MatLab programs were constructed for solution by the second method.

6.2.1 The values of joint stiffness *k*

In general, the joint stiffness will depend upon the material of the joint, size of the joint and the way its is constructed (welded or bolted). The numerical value of the joint stiffness will have to be determined from experiments. The values of k were not found experimentally for this thesis. Theoretically, these values can vary from 0 (hinged joint) to ∞ (rigid joint). For the purpose of this thesis the value of k was chosen as:

$$k = \frac{5EI}{L} \tag{6.34}$$

This value was chosen in view of the fact that for a beam of length, L and bending EI, the end moments required to bend it by one radian is $\frac{EI}{L}$. A value of $\frac{5EI}{L}$ assumes that the joint is five times stiffer than the beam. This value of k is found to be reasonable in view of the results to be presented later in this chapter. In applications where length and bending vary from member to member a reference length L and reference EI will have to be chosen.

6.2.2 The values of joint damping constant C

The joint damping will depend upon the characteristics of the joint, for example the material of the joined members, the tightening torque applied to the bolts in a bolted joint, the surface conditions, etc. Ideally, the numerical value of the damping constant will have to be determined experimentally. The values of C could not be found experimentally for this thesis. Again, as for the stiffness, C values can theoretically vary from 0 to ∞. For the purpose of this thesis the value of C was selected by the following argument.

Consider a rigid bar of length L and mass M hinged at one end and free at the other, like a pendulum. Now let a rotational spring of constant k, and a rotational damper of constant C be affixed to the bar at the hinged end. The equation of free vibration of this rod is

$$I_m\ddot{\theta} + C\dot{\theta} + k\theta = 0 \tag{6.35}$$

where θ = rotation of the rod from its equilibrium position, and $I_m = \frac{1}{3}ML^2$ = mass moment of inertia of the rod about the hinge point. As a SDOF system, the frequencies of vibration is given by substituting $\theta = \Theta e^{i\omega t}$ whereupon it is found that

$$\omega = i\frac{C}{2I_m} \pm \sqrt{-\frac{C^2}{4I_m^2} + \frac{k}{I_m}} \tag{6.36}$$

At the limit of oscillatory behaviour ω is purely imaginary, which means that at such limit,

$$-\frac{C^2}{4I_m^2} + \frac{k}{I_m} = 0, \text{ or } C = \sqrt{4I_m k} \tag{6.37}$$

Now, we may take the value of $k = \dfrac{EI}{L}$ = the bending stiffness of a beam of length L, which gives

$$C = \sqrt{\frac{4}{3}MLEI} \tag{6.38}$$

In lieu of the lack of data, we take the above value of C as the rotational joint damping constant in our subsequent calculations.

6.3 Example 1: One-storey one-bay frame

To illustrate the above formulation and methods of solution, we solve the one-storey one-bay plane frame of the experiment described in Chapter 5.

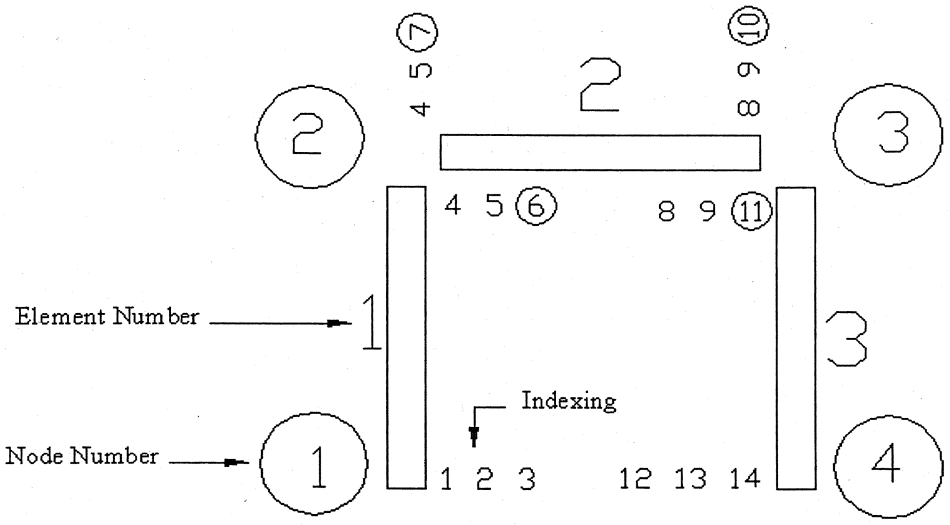

Fig. 6.2: One-storey one-bay frame of the experiment of Chapter 4

Fig. 6.2 shows the frame, the joint numbers, and the member numbers. For simplicity, the analysis considers only one finite element per member. Thus, there are 4 nodes and 3 members. Joints 1 and 4 are fixed joints, whereas, joints 2 and 3 permit relative rotations of the members joined to them. These latter joints are assumed to have rotational springs and rotational dampers. Since there are 2 members meeting at each of these joints, $m_2 = 2$ and $m_3 = 2$. The extra degrees of freedom of rotation at each of these joints are therefore, $m_2 - 1$ and $m_3 - 1$. Consequently, the total number of degrees of freedom are

$$3n + \sum_{\text{damped joints}} (m-1) = 3 \times 4 + 1 + 1 = 14. \tag{6.39}$$

The degrees of freedom are

$$\begin{aligned} < \Delta > &= < \Delta_1, \Delta_2, \Delta_3, \Delta_4, \Delta_5, \Delta_6, \Delta_7, \Delta_8, \Delta_9, \Delta_{10}, \Delta_{11}, \Delta_{12}, \Delta_{13}, \Delta_{14} > \\ &= < u_1, v_1, \theta_{11}, u_2, v_2, \theta_{21}, \theta_{22}, u_3, v_3, \theta_{32}, \theta_{33}, u_4, v_4, \theta_4 > \end{aligned} \tag{6.40}$$

Note, joints 2 and 3 have 2 degrees of rotations each. θ_{21} and θ_{22} corresponding to members 1 and 2 meeting at joint 2, and θ_{32} and θ_{33} corresponding to members 2 and 3 meeting at joint 3. In the traditional method of analysis, $\theta_{21} = \theta_{22} = \theta_2$, and $\theta_{32} = \theta_{33} = \theta_3$.

Since the degrees of freedom corresponding to the fixed joints 1 and 4 are zero, the unknown active degrees of freedom are only 8 corresponding to joints 2 and 3 and the problem can be reduced to a system of 8 equations and 8 unknowns:

$$< \Delta > = < u_2, v_2, \theta_{21}, \theta_{22}, u_3, v_3, \theta_{32}, \theta_{33} > \tag{6.41}$$

which can also be written as:

$$< \Delta > = < \Delta_4, \Delta_5, \Delta_6, \Delta_7, \Delta_8, \Delta_9, \Delta_{10}, \Delta_{11} > \tag{6.42}$$

We now write explicitly the numerical values of the various matrices in which we have used, as discussed previously, the joint stiffness value and damping constant as,

$$k = \frac{5EI}{L} = \frac{5 \times 7.17 \times 10^{10} \times 117 \times 10^{-9}}{0.381} = 110165 \text{ N.m} \tag{6.43}$$

$$C = \sqrt{\frac{4}{3} MLEI} \qquad = 33 \text{ N.m.sec} \tag{6.44}$$

The reduced global mass, damping and stiffness matrices are:

$$[M] = \begin{bmatrix} 0.179817 & 0 & 0.00509198 & 0 & 0.0425243 & 0 & 0 & 0 \\ 0 & 0.179817 & 0 & 0.00509198 & 0 & 0.0328044 & -0.0030089 & 0 \\ 0.00509198 & 0 & 0.000352735 & 0 & 0 & 0 & 0 & 0 \\ 0 & 0.00509198 & 0 & 0.000352735 & 0 & 0.0030089 & -0.000264551 & 0 \\ 0.0425243 & 0 & 0 & 0 & 0.179817 & 0 & 0 & 0.00509198 \\ 0 & 0.0328044 & 0 & 0.0030089 & 0 & 0.179817 & -0.00509198 & 0 \\ 0 & -0.0030089 & 0 & -0.000264551 & 0 & -0.00509198 & 0.000352735 & 0 \\ 0 & 0 & 0 & 0 & 0.00509198 & 0 & 0 & 0.000352735 \end{bmatrix} \tag{6.45}$$

$$[C] = \begin{bmatrix} 0 & 0 & 0 & 0 & 0 & 0 & 0 & 0 \\ 0 & 0 & 0 & 0 & 0 & 0 & 0 & 0 \\ 0 & 0 & 33 & -33 & 0 & 0 & 0 & 0 \\ 0 & 0 & -33 & 33 & 0 & 0 & 0 & 0 \\ 0 & 0 & 0 & 0 & 0 & 0 & 0 & 0 \\ 0 & 0 & 0 & 0 & 0 & 0 & 0 & 0 \\ 0 & 0 & 0 & 0 & 0 & 0 & 33 & -33 \\ 0 & 0 & 0 & 0 & 0 & 0 & -33 & 33 \end{bmatrix} \tag{6.46}$$

$$[K] = \begin{bmatrix} 47354400 & 0 & 346976 & 0 & -45533000 & 0 & 0 & 0 \\ 0 & 47354400 & 0 & 346976 & 0 & -1821400 & 346976 & 0 \\ 346976 & 0 & 198297 & -110165 & 0 & 0 & 0 & 0 \\ 0 & 346976 & -110165 & 198297 & 0 & -346976 & 44065.9 & 0 \\ -45533000 & 0 & 0 & 0 & 47354400 & 0 & 0 & 346976 \\ 0 & -1821400 & 0 & -346976 & 0 & 47354400 & -346976 & 0 \\ 0 & 346976 & 0 & 44065.9 & 0 & -346976 & 198297 & -110165 \\ 0 & 0 & 0 & 0 & 346976 & 0 & -110165 & 198297 \end{bmatrix} \tag{6.47}$$

Note that $[K^J]$ has been included in the above global stiffness matrix $[K]$ where,

$$[K^J] = \begin{bmatrix} 0 & 0 & 0 & 0 & 0 & 0 & 0 & 0 \\ 0 & 0 & 0 & 0 & 0 & 0 & 0 & 0 \\ 0 & 0 & 110165 & -110165 & 0 & 0 & 0 & 0 \\ 0 & 0 & -110165 & 110165 & 0 & 0 & 0 & 0 \\ 0 & 0 & 0 & 0 & 0 & 0 & 0 & 0 \\ 0 & 0 & 0 & 0 & 0 & 0 & 0 & 0 \\ 0 & 0 & 0 & 0 & 0 & 0 & 110165 & -110165 \\ 0 & 0 & 0 & 0 & 0 & 0 & -110165 & 110165 \end{bmatrix} \tag{6.48}$$

These matrices are substituted in the system of equations:

$$\lambda^2[M]\{\phi\} + \lambda[C]\{\phi\} + [K]\{\phi\} = \{0\} \tag{6.49}$$

The above eigenvalue problem was solved by using 3 different programs namely, NASTRAN, and programs constructed by the author using Mathematica and MatLab. The results are shown in Table 6.1. Note that NASTRAN cannot model the damping in the fashion accounted for in this thesis. The frequencies from NASTRAN were obtained only as reference values for the standard case of no damping and rigid joints. For presentation of the results in the tables below, the eigenvalue λ is changed to $\omega = \lambda/i$ $= \omega_d + i\zeta\omega$.

ω NASTRAN (Hz)	ω Mathematica (Hz)	ω MatLab (Hz)
390.80	$361.70 + 15.03i$	$361.67 + 15.03i$
1612.84	$1614.98 + 28.62i$	$1615.0 + 28.63i$
2718.95	$2910.84 + 00.00$	$2910.8 + 00.00$
2857.30	$3029.45 + 30.64i$	$3029.5 + 30.66i$
4083.43	$4093.1 + 83.38i$	$4093.1 + 83.42i$
4298.60	$5171.75 + 93.65i$	$5171.7 + 93.69i$

Table 6.1: Frequency comparison of 2-D frame using different programs.

As expected, the differences between frequency values $\omega = \omega_d + i\zeta\omega$ obtained by MatLab and Mathematica are negligible. It is apparent that the damped frequencies ω_d computed by these constructed programs are higher than the undamped frequencies obtained by NASTRAN, except for the first frequency. The reason for such results follows.

The above FE idealization of one element per member is rather crude and the frequencies (except perhaps the first one or two) cannot be expected to be accurate. This inaccuracy is evident from a comparison of the above NASTRAN frequencies with the analytically exact frequencies obtained in Chapter 5, and listed in Table 5.1. Therefore, in the interest of obtaining more accurate frequencies, a finer mesh consisting of five elements per member was employed. Fig. 6.3 shows the division of the members into elements, and the numbering of the degrees of freedom. The total number of active degrees of freedom is 44 including the 2 extra degrees of freedom of rotation at joints 5 and 10.

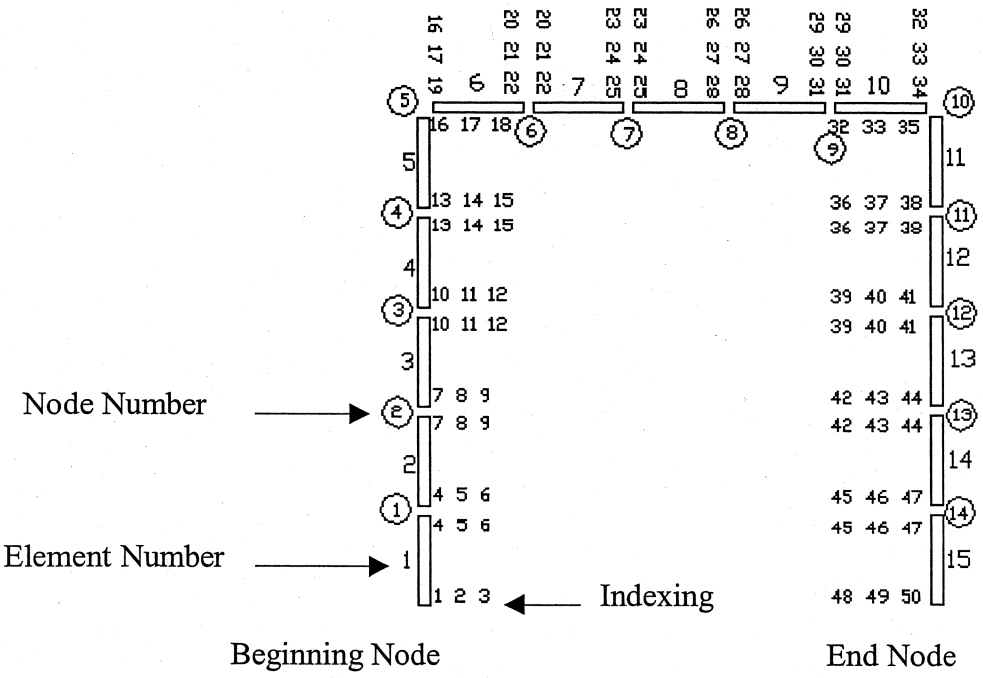

Fig. 6.3: One-storey one-bay frame of Chapter 4 with 5 elements per member.

The following table shows the frequencies obtained for the finer model.

1	2	3	4	5
NASTRAN (Hz)	MatLab (Hz)	MatLab (Hz)	MatLab (Hz)	% Increase
$k^{\mathrm{J}} = \infty$	$k^{\mathrm{J}} =$ large, $C = 0$	$k^{\mathrm{J}} = 5EI/L$, $C = 0$	$k^{\mathrm{J}} = 5EI/L$, $C = 33$	$\frac{(\omega_d - \omega)}{\omega} \times 100$
389.79	389.81	$353.97, -9.19\%$	$360.89 + 14.89i$	$+1.95\%$
1421.20	1421.44	$1362.9, -4.12\%$	$1412.2 + 22.02i$	$+3.62\%$
2287.65	2289.29	$2114.1, -7.65\%$	$2271.7 + 55.84i$	$+7.45\%$
2506.49	2506.71	$2355.4, -1.51\%$	$2493.4 + 44.34i$	$+5.86\%$
2757.38	2764.34	$2764.3, -0.00\%$	$2764.3 + 0.01i$	$+0.00\%$
3590.94	3601.13	$3425.2, -4.88\%$	$3589.3 + 45.65i$	$+4.79\%$
5008.35	5037.48	$5034.3, -0.06\%$	$5037.4 + 0.60i$	$+0.06\%$
5759.66	5770.99	$5660.3, -0.02\%$	$5770.0 + 11.01i$	$+1.94\%$
7310.71	7360.71	$6696.5, -1.92\%$	$7350.0 + 90.54i$	$+9.76\%$
7830.97	7872.67	$7596.6, -3.50\%$	$7869.2 + 31.60i$	$+3.59\%$

Table 6.2: Frequency comparison using 15 elements (5 elements per member).

For a more extensive comparison 10 frequencies (rather than 5) are listed in this table. Evidently, the first five are significantly changed for this finer model in comparison to Table 6.1, except for the first one. For this finer model, the undamped NASTRAN

frequencies are very close to the analytically obtained frequencies of Table 5.1 for each of the ten frequencies.

The frequencies from the MatLab program were obtained in 3 ways by assigning joint stiffness values and joint damping values: (1) $k^{\mathrm{J}} = \infty$, $C = 0$, (2) $k^{\mathrm{J}} = 5EI/L$, $C = 0$ and, (3) $k^{\mathrm{J}} = 5EI/L$, $C = 33$. It is to be noted that, as expected, the frequencies for the first case are almost the same, albeit very slightly higher than the NASTRAN frequencies. The slight differences result from the fact that NASTRAN uses a lumped mass procedure for determining the mass matrices (as opposed to the consistent mass matrix used in the present formulation). This comparison therefore validates the correctness of the MatLab program for the standard case of free (undamped) vibrations of frame with rigid joints. The MatLab values for the above three cases were verified by Mathematica program using the method presented in Chapter 2, which, as pointed out before, is based on a different method of extraction of eigenvalues.

Column 3 of the table shows the effect of finite joint stiffness only, when the two joints 5 and 10 of the frame, Fig. 6.3, are assigned a finite stiffness $k^{\mathrm{J}} = 5EI/L$ and there is no damping. The frame is now weakened in its stiffness, and correspondingly, as expected, the natural frequencies are lower than those in column 2 of Table 6.2 for the case of rigid joints. The most affected frequency is the first one, lower by 9.19% than that for the rigid jointed frame column 2.

When damping is introduced, the frequencies are rendered complex as listed in column 4 of the above table, with an oscillatory part ω_d and a damping attenuation part $\omega\zeta$. The comparison is made between the damped frequency and the undamped frequency for the same values of the joint stiffnesses. The percentage differences of the oscillatoy parts are shown in column 5. One finds that the rotational damping has increased the oscillatory parts of the complex frequencies. They are all positive meaning that the damped frequencies ω_d are higher than the undamped ones ω (column 4 versus columns3).

Additionally, the effect of damping is evident by the presence of the damping factor which is indicated by the imaginary parts. It is interesting to note that the damping factor does not change uniformly from mode to mode. For example, the damping factor for the third mode is quite high, whereas for the fifth mode it is almost zero. This means that while the third mode is attenuated very significantly in each cycle of vibration, the fifth

mode amplitude remains virtually unchanged. The reason for this peculiar behaviour will be explained subsequently.

Now, a parametric study is made for the effect of the rotational damping, as it is increased from $C = C_r = 33$ units to $C = 3C_r = 99$ units, keeping the joint rotational stiffness as $5EI/L$. Table 6.3 is obtained by analyzing the above structure using one element per member (i.e. 3 elements structure) with an increase in rotational damping for each run. The table shows that the higher the damping the higher is the associated frequency.

$C_r = 33$	$1.5C_r = 49.5$	$2C_r = 66$	$3C_r = 99$
$\omega = \omega_d + \zeta\omega i$	$\omega = \omega_d + \zeta\omega i$	$\omega = \omega_d + \zeta\omega i$	$\omega = \omega_d + \zeta\omega i$
$361.67i - 15.03$	$367.93i - 18.31$	$373.56i - 18.97$	$380.95i - 16.90$
$1615i - 28.63$	$1620.6i - 20.37$	$1622.7i - 15.64$	$1624.2i - 10.60$
$2910.8i - 00.00$	$2910.8i - 00.00$	$2910.8i - 00.00$	$2910.8\,i - 00.00$
$3029.5i - 30.66$	$3032.2i - 20.69$	$3033.2i - 15.59$	$3033.9i - 10.42$
$4093.1i - 83.42$	$4100.4i - 56.25$	$4103.0i - 42.35$	$4104.9i - 28.31$
$5171.7i - 93.69$	$5175.2i - 62.4$	$5176.4i - 46.81$	$5177.3i - 31.20$

Table 6.3: Frequency results of a one-storey one-bay frame with 1 element per member.

A similar parametric study is now made for the refined model of the same frame with 5 elements per member, Fig. 6.3. The resulting complex frequencies are shown in Table 6.4

$C_r = 33$	$1.5C_r = 49.5$	$2C_r = 66$	$3C_r = 99$
ω(Hz)	$\omega = \omega_d + \zeta\omega i$	$\omega = \omega_d + \zeta\omega i$	$\omega = \omega_d + \zeta\omega i$
$360.89i - 14.89$	$367.09i - 18.15$	$372.67i - 18.81$	$379.99i - 16.77$
$1412.2i - 22.02$	$1417.0i - 15.96$	$1418.9i - 12.34$	$1420.3i - 8.41$
$2271.7i - 55.84$	$2281.2i - 39.00$	$2284.7i - 29.73$	$2287.2\,i - 20.05$
$2493.4i - 44.34$	$2500.6i - 30.90$	$2503.2i - 23.54$	$2505.1i - 15.87$
$2764.3i - 0.01$	$2764.3i - 00.00$	$2764.3i - 00.00$	$2764.3i - 00.00$
$3589.3i - 45.65$	$3595.7i - 31.46$	$3598.1i - 23.88$	$3599.8i - 16.05$
$5037.4i - 0.60$	$5037.4i - 0.41$	$5037.4i - 0.31$	$5037.5i - 0.21$
$5770.0i - 11.01$	$5770.5i - 7.37$	$5770.7i - 5.54$	$5770.9i - 3.70$
$7350.0i - 90.54$	$7355.9i - 60.76$	$7358.0i - 45.67$	$7359.5i - 30.50$
$7869.2i - 31.60$	$7871.1i - 21.20$	$7871.8i - 15.93$	$7872.3i - 10.64$

Table 6.4: Frequency results of a one-storey one-bay frame with 5 elements per member.

From the above table, Table 6.4, one finds that as the damping is increased, the oscillatory part of every frequency also increases. This is to be expected. Since, theoretically, when the damping is very large, the relative rotational velocities are rendered very low, almost equal to zero regardless of the finite joint stiffnesses. Hence, the relative rotation is also rendered zero. This, in turn, means that the joint is rendered rigid (although in a quasi static motion, the finite joint stiffness will allow relative rotation of the members meeting at the joint). Hence, as the damping approaches a large value ($C_r = \infty$) at all joints, the oscillatory part of every frequency must approach the corresponding undamped frequency of the rigid jointed frame and the damping part must approach zero (column 2 of Table 6.2). This statement can be proved rigorously from the equations of motions by putting $C_r = \infty$ for all joints where relative rotation is allowed. The entries in Table 6.4 show this trend convincingly. It is also apparent that the higher frequencies approach their undamped values faster than the lower frequencies.

The variation of the oscillatory part of each of the first ten damped frequencies as functions of rotational damping are plotted below, Fig. 6.4.

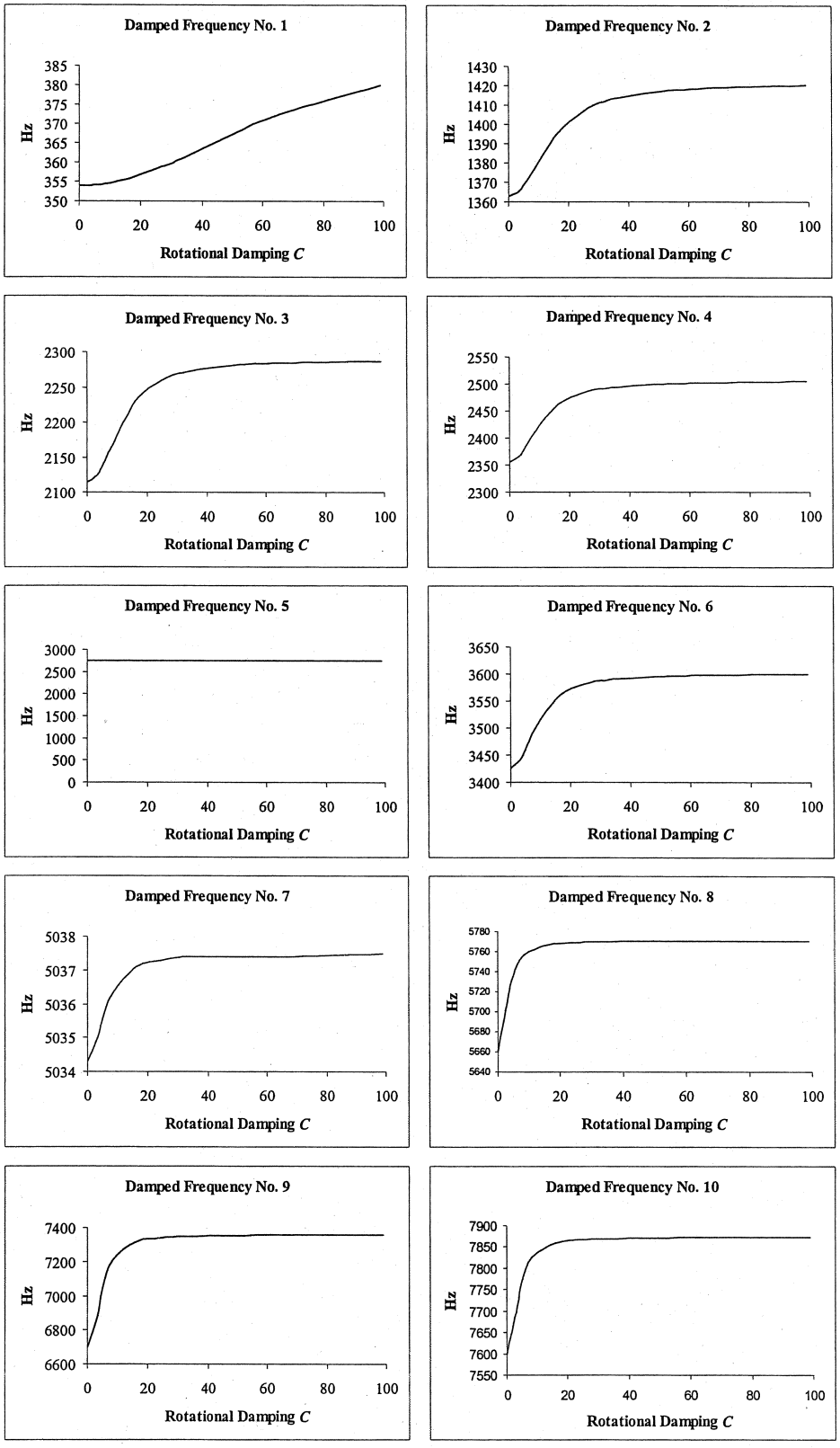

Fig. 6.4: Frequency vs rotational damping for first 10 frequencies for $k^J = \frac{5EI}{L}$

These plots, drawn for values of the rotational damping ranging from 0 to 99 units and $k = \frac{5EI}{L}$, reinforce the conclusions drawn before from Table 6.4. With the exception of the first frequency, the frequencies approach their asymptotic values at relatively low rotational damping.

For joint stiffnesses lower than the above value, $0 < k < \frac{5EI}{L}$, and no damping, $C = 0$, the frequencies can be expected to be lower than those shown in column 3 of Table 6.4. The damped frequencies in such a case will have a larger range of variation before they approach their asymptotic limits, column 2 of Table 6.4. The plots of frequency versus rotational damping for such a case will therefore be similar in appearance to Fig. 6.4. Conversely, for joint stiffnesses $k > \frac{5EI}{L}$, the range of variation of the frequencies will be lower than the ones shown in Fig. 6.4.

The mode shapes of the first five modes, as obtained from NASTRAN, are shown in Fig. 6.5. The mode shapes for the damped cases can be expected to be very similar to those obtained by NASTRAN and, therefore, not shown. From these figures, it is clear that the first four modes involve significant bending at the joints, hence the frequencies of these modes can be expected to be significantly affected by joint rotational damping. In contrast, the fifth mode involves mostly the axial movement of the two columns, with almost no bending. Table 6.2 confirms this observation; the fifth frequency indeed remains constant regardless of the increase in the joint rotation damping. Similar explanation appears responsible for the small effect of damping on the frequencies of the seventh and the eighth modes. Modes other than those mentioned in the preceding do involve significant bending and show sensitivity to joint rotation damping.

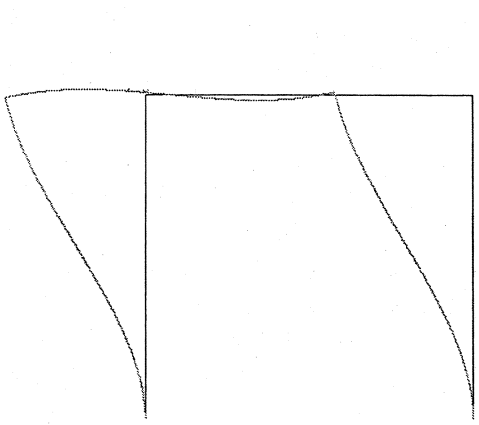

(a) Mode 1

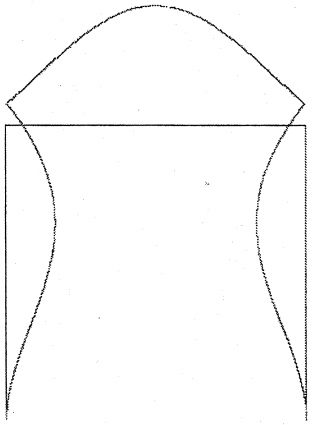

(b) Mode 2

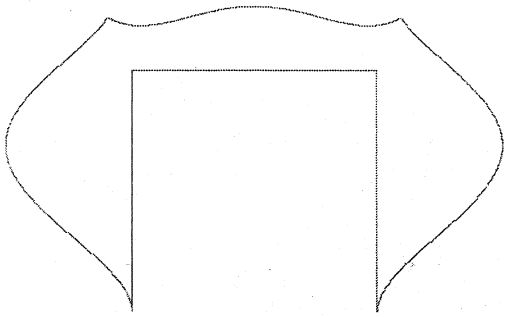

(c) Mode 3

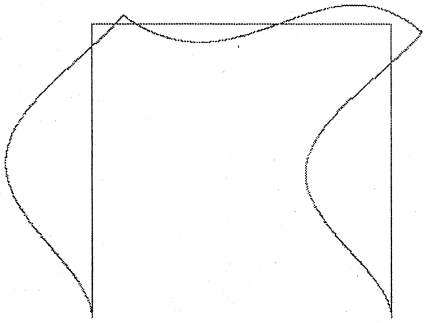

(d) Mode 4

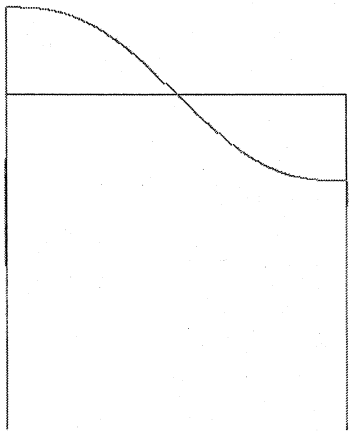

(e) Mode 5

Fig. 6.5: NASTRAN mode shapes using 15 elements idealization.

6.4 Example 2: Two-storey one-bay frame

The MatLab program is general enough to analyze any plane frame with finite joint stiffness and rotational joint damping. As an illustration of the use of this program, two other frames with different configurations were analyzed. Figure 6.6 shows the first of the two frames, a two-storey one-bay frame.

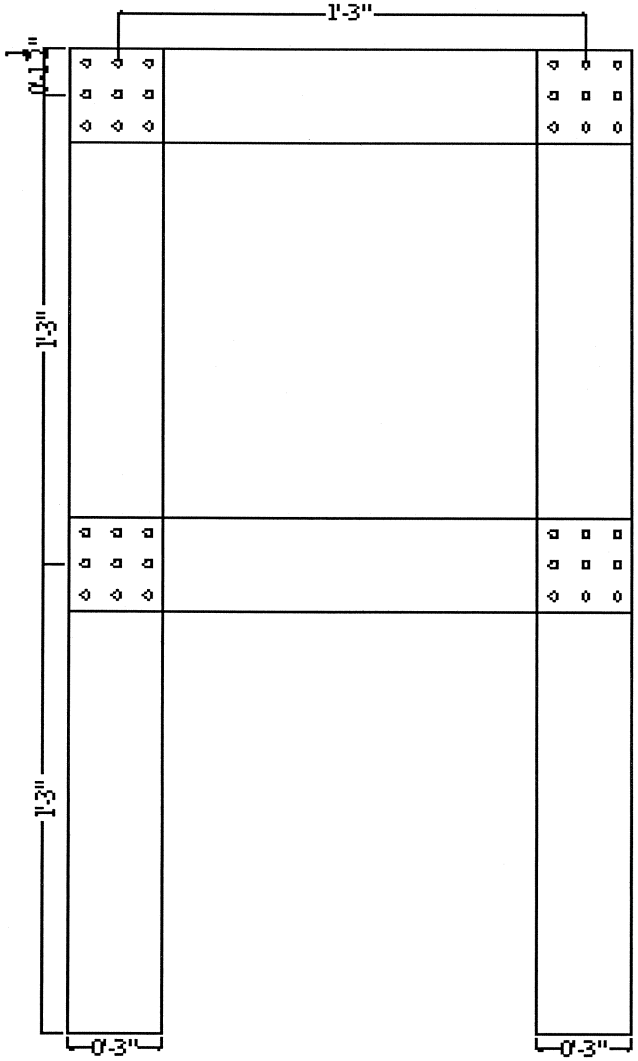

Fig. 6.6: Two-storey one-bay frame.

The joints of the frame are defined by data in Table 6.5. This table identifies the nodes, which have rotational dampers and finite joint stiffness. It also enumerates the extra degrees of freedom at such joints.

Node No.	x coord	y coord	k, C	Extra dof
1	0	0	N	
2 to 5	0	incr 0.381/5	N	
6	0	0.381	Y	2
7 to 10	0	incr 0.381/5	N	
11	0	0.762	Y	1
12	0.381	0	N	
13 to 16	0.381	incr 0.381/5	N	
17	0.381	0.381	Y	2
18 to 21	0.381	incr 0.381/5	N	
22	0.381	0.762	Y	1
23 to 26	incr 0.381/5	0.381	N	
27 to 30	incr 0.381/5	0.762	N	

Table 6.5: Joint data for frame of Fig. 6.7.

The member connectivity, first node i second node j, and the associated degrees of freedom are listed in Table 6.6 for each member. In general, the members can have different properties, but for this example problem they are taken to be the same for all members and therefore not listed for individual members. These common properties are the same as for the previous one-storey one-bay frame. The rotational stiffness and the rotational damping values for joints allowing relative rotation are also taken to be the same for all sets of joints as in the previous example, namely, $k = 5EI/L = 110165$ N.m and $C = \sqrt{\frac{4}{3}MLEI} = 33$ N.m.sec. Table 6.6 corresponds to Fig. 6.7, wherein the numbering of the degrees of freedom is shown explicitly.

Memb	i	j	DOFi	DOFj		Memb	i	j	DOFi	DOFj
1	1	2	1, 2, 3	4, 5, 6		16	17	18	50, 51, 53	54, 55, 56
2	2	3	4, 5, 6	7, 8, 9		17	18	19	54, 55, 56	57, 58, 59
3	3	4	7, 8, 9	10, 11, 12		18	19	20	57, 58, 59	60, 61, 62
4	4	5	10, 11, 12	13, 14, 15		19	20	21	60, 61, 62	63, 64, 65
5	5	6	13, 14, 15	16, 17, 18		20	21	22	63, 64, 65	66, 67, 68
6	6	7	16, 17, 19	20, 21, 22		21	6	23	16, 17, 69	70, 71, 72
7	7	8	20, 21, 22	23, 24, 25		22	23	24	70, 71, 72	73, 74, 75
8	8	9	23, 24, 25	26, 27, 28		23	24	25	73, 74, 75	76, 77, 78
9	9	10	26, 27, 28	29, 30, 31		24	25	26	76, 77, 78	79, 80, 81
10	10	11	29, 30, 31	32, 33, 34		25	26	17	79, 80, 81	50, 51, 82
11	12	13	35, 36, 37	38, 39, 40		26	11	27	32, 33, 83	84, 85, 86
12	13	14	38, 39, 40	41, 42, 43		27	27	28	84, 85, 86	87, 88, 89
13	14	15	41, 42, 43	44, 45, 46		28	28	29	87, 88, 89	90, 91, 92
14	15	16	44, 45, 46	47, 48, 49		29	29	30	90, 91, 92	93, 94, 95
15	16	17	47, 48, 49	50, 51, 52		30	30	22	93, 94, 95	66, 67, 96

Table 6.6: Degrees of Freedom for 2 Storey 1 Bay Frame.

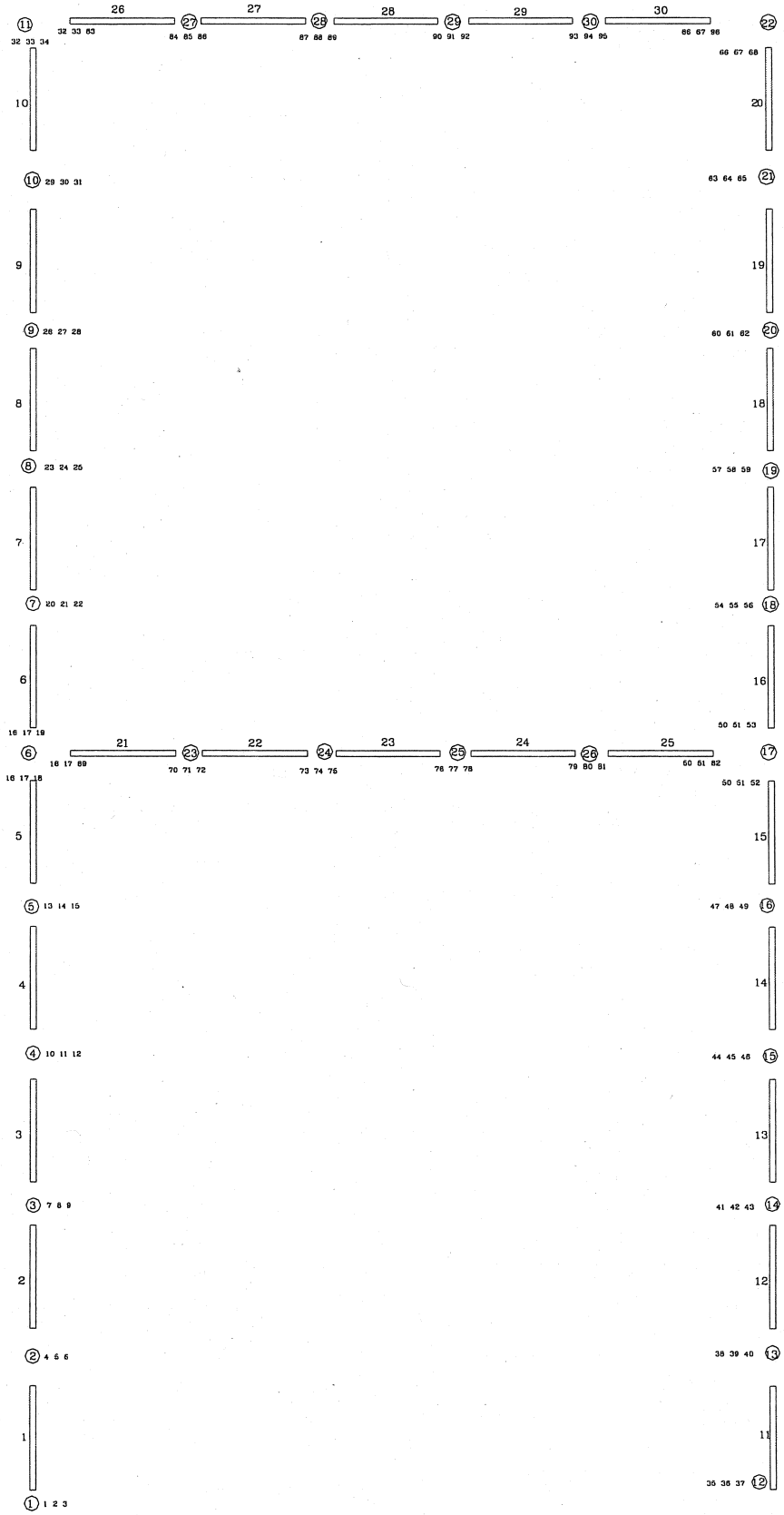

Fig. 6.7: Two-storey one-bay frame with 5 elements per member (96 DOF).

The frequencies of this frame are determined by using NASTRAN with $k = \infty$ and $C = 0$, and also by the constructed MatLab program for the three combinations of k and C. These latter frequencies are listed in columns 2, 3 and 4 of the table below. Comparing columns 1 and 2, it is clear that the values for all 10 frequencies are almost identical, with small positive and negative differences. Here, therefore, the NASTRAN does not always give a frequency lower than the constructed MatLab program. This comparison again provides a validation for the constructed MatLab program.

1	2	3	4	5
NASTRAN (Hz)	MatLab (Hz)	MatLab (Hz)	MatLab (Hz)	% Increase
$k = \infty$	$k =$ large, $C = 0$	$k = 5EI/L$, $C = 0$	$k = 5EI/L$, $C = 33$	$\frac{(\omega_d - \omega)}{\omega} \times 100$
178.59	178.50	159.97, $-$ 10.4%	$160.92 - 4.31i$	0.59
593.00	592.78	521.49, $-$ 12.02%	$548.97 - 37.01i$	5.27
1130.09	1130.00	1099.20, $-$ 2.73%	$1122.10 - 13.67i$	2.08
1325.86	1325.50	1301.50, $-$ 1.81%	$1321.30 - 9.27i$	1.52
1523.12	1523.70	1511.10, $-$ 0.83%	$1521.10 - 5.07i$	0.66
2068.02	2067.20	1920.10, $-$ 7.11%	$2051.40 - 47.40i$	6.84
2110.78	2111.00	1949.10, $-$ 7.67%	$2102.10 - 34.92i$	7.85
2431.85	2432.40	2121.00, $-$ 12.8%	$2396.80 - 114.04i$	13.00
2740.99	2741.60	2466.70, $-$ 10.03%	$2724.00 - 71.55i$	10.43
3036.92	3036.20	2757.20, $-$ 9.19%	$3022.20 - 64.30i$	9.61

Table 6.7: Frequency comparison using 30 elements (5 elements per member).

When relative rotation is permitted at the junction joints with joint rotational stiffness $k = 5EI/L$, and with zero joint damping, then the frequencies become those shown in column 3 of Table 6.7. As expected, due to finite rotational stiffnesses at the junction joints, these frequencies are always smaller than when these joints are assumed to be rigid, columns 1 and 2.

A parametric study similar to the one done previously is performed for the effect of the rotational damping, for the above frame. Table 6.8 shows the changes in the complex frequencies as the rotational joint damping is increased. The trends indicated by the listed results and the conclusions that follow are entirely similar to those for the previous one-bay one-storey frame. For the limiting case of large damping ($C = \infty$), the frequencies approach the values for the rigid-joint frame listed in column 2 of Table 6.7.

$C_r = 33$	$1.5C_r = 49.5$	$2C_r = 66$	$3C_r = 99$
ω(Hz)	$\omega = \omega_d + \zeta\omega i$	$\omega = \omega_d + \zeta\omega i$	$\omega = \omega_d + \zeta\omega i$
$160.92i - 4.31$	$162.02i - 6.15$	$163.4i - 7.63$	$166.58i - 9.39$
$548.97i - 37.01$	$565.12i - 36.99$	$574.92i - 32.85$	$584.02i - 24.87$
$1122.1i - 13.67$	$1125.9i - 10.58$	$1127.6i - 8.40$	$1128.9\,i - 5.84$
$1321.3i - 9.27$	$1323.4i - 6.83$	$1324.3i - 5.31$	$1325.0i - 3.64$
$1521.1i - 5.07$	$1522.4i - 3.81$	$1522.9i - 2.98$	$1523.3i - 2.06$
$2051.4i - 47.4$	$2059.9i - 33.37$	$2063.0i - 25.52$	$2065.4i - 17.25$
$2102.1i - 34.92$	$2106.8i - 24.22$	$2108.6i - 18.43$	$2109.9i - 12.42$
$2396.8i - 114.04$	$2416.2i - 79.18$	$2423.2i - 60.22$	$2428.3i - 40.55$
$2724.0i - 71.55$	$2733.6i - 49.07$	$2737.1i - 37.17$	$2739.5i - 24.95$
$3022.2i - 64.3$	$3029.8i - 43.86$	$3032.6i - 33.16$	$3034.6i - 22.23$

Table 6.8: Frequency results of a one bay two storey frame.

The NASTRAN mode shapes of the frame corresponding to the above frequencies are shown in Fig. 6.8. It is found that most of these mode shapes show significant bending of the beams and columns except for the fifth mode, where there is no significant bending of the columns, but only their axial deformation. Correspondingly, the fifth frequency in the above table remains unaffected, regardless of the rotational damping amount.

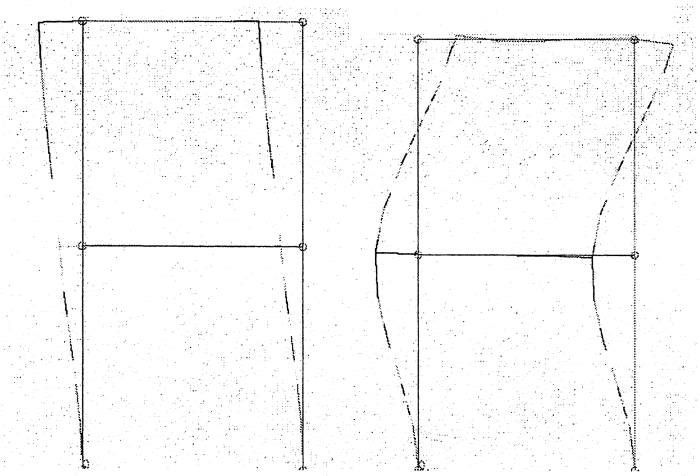

Mode 1. Mode 2.

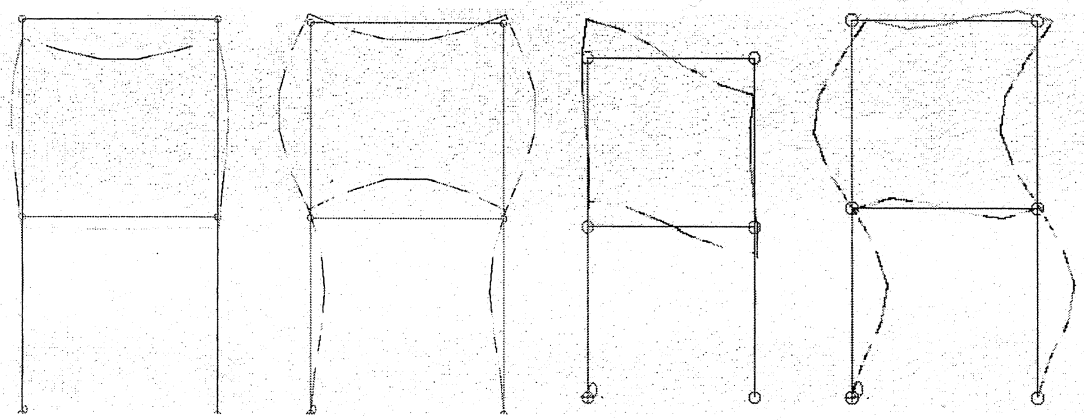

Mode 3. Mode 4. Mode 5. Mode 6.

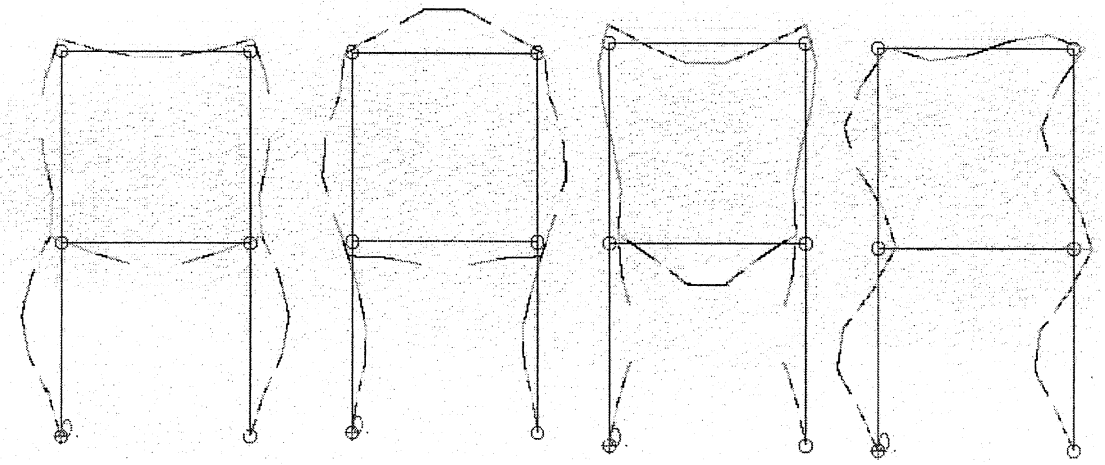

Mode 7. Mode 8. Mode 9. Mode 10.

Fig 6.8: NASTRAN mode shapes of the 2-storey 1-bay frame.

6.5 Example 3: Two-storey two-bay frame

To illustrate the generality of the program, a more complex frame was investigated. Like the previous frame it consists of 2 storeys, but now with 2 bays. The complexity arises from the asymmetry of the structure. Here, there are four members meeting at joint C. A blown up view of details at joints A, B and C are shown in Fig. 6.9.

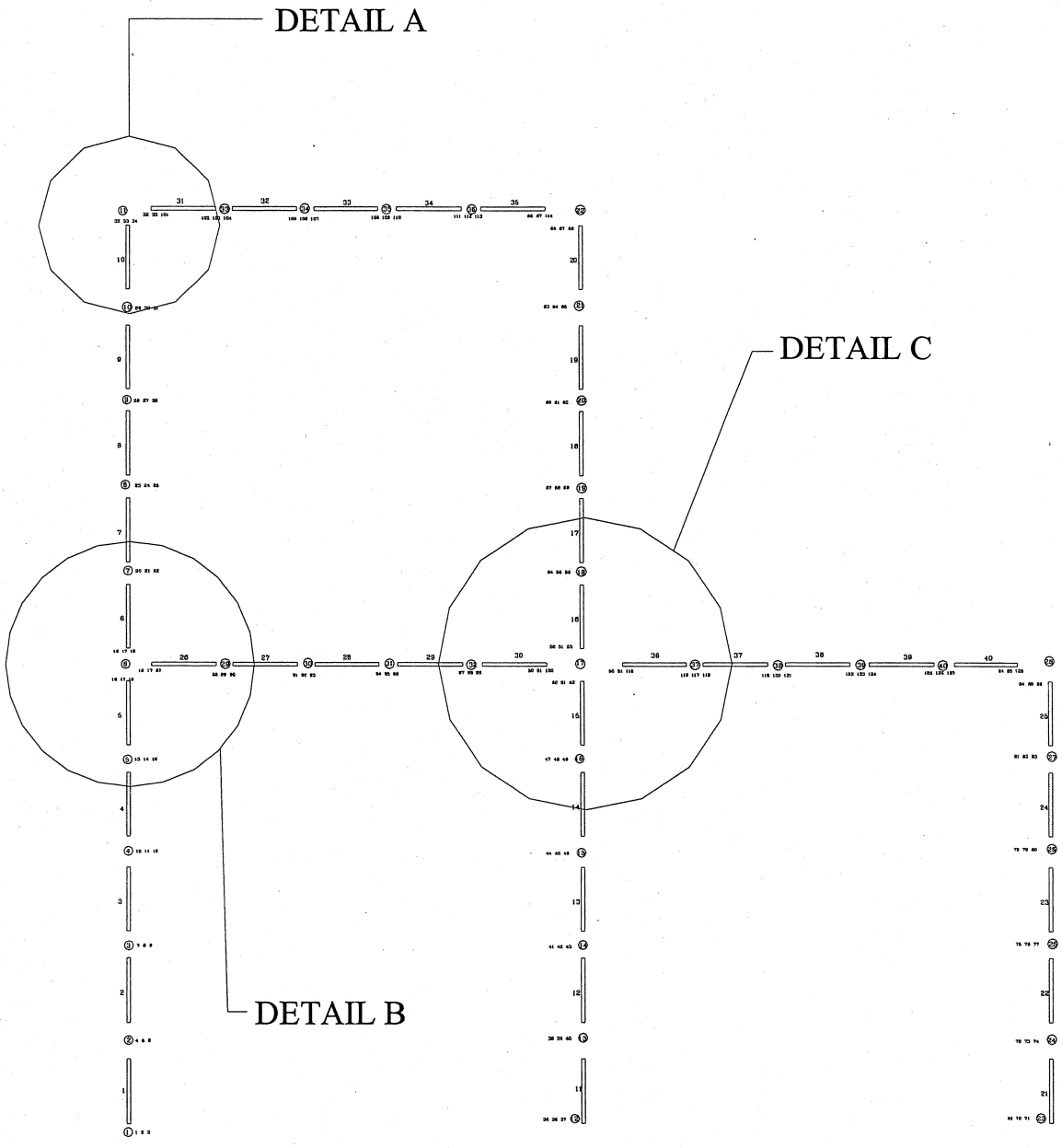

Fig. 6.9: Two-storey one-bay frame with 5 elements per member (128 DOF).

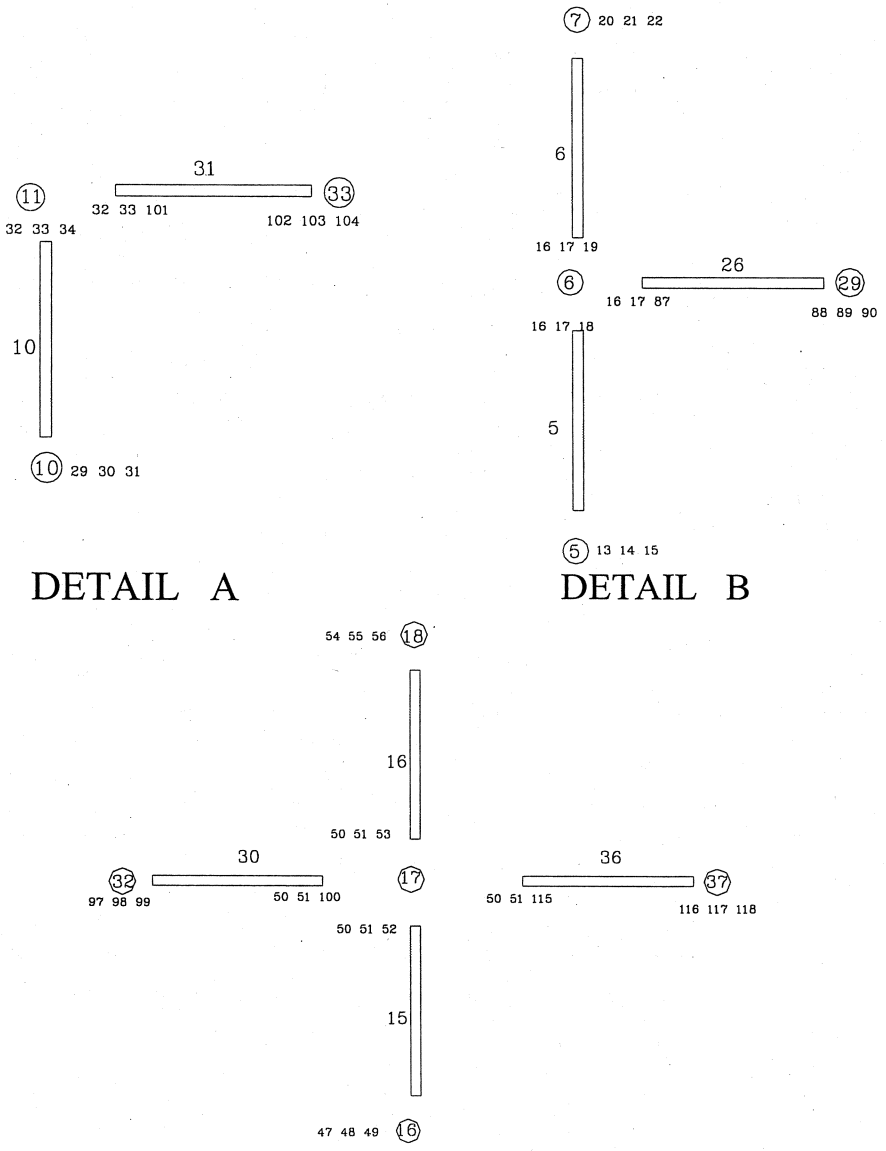

Fig 6.10: Numbering of the DOF at joints A, B and C.

The joint details shown in Figs. 6.10 are rotational joints with damping. They indicate clearly the jumps in the numbering of the degrees of freedom because of the different rotations of the members meeting at such a joint.

This frame has the same material properties and member dimensions as those of the previous examples. Similar to the previous examples, NASTRAN results were obtained by considering the joints to be rigid and without damping. The MatLab results were

obtained for different cases of joint stiffness and damping values similar to those analyzed previously and indicated in the table below:

1	2	3	4	5
NASTRAN (Hz)	MatLab (Hz)	MatLab (Hz)	MatLab (Hz)	% Increase
$k = \infty$	$k =$ large, $C = 0$	$k = \frac{5EI}{L}, C = 0$	$k = \frac{5EI}{L}$, $C = 33$	$\frac{(\omega_d - \omega)}{\omega} \times 100$
206.3	203.91	182.55, $-$ 10.48%	$183.94 - 5.57i$	0.76
527.9	526.39	464.22, $-$ 11.81%	$484.25 - 30.95i$	4.31
1106.0	1095.60	1063.80, $-$ 2.90%	$1086.90 - 14.38i$	2.17
1344.0	1362.30	1332.30, $-$ 2.20%	$1357.70 - 10.79i$	1.91
1414.8	1406.50	1376.10, $-$ 2.16%	$1401.90 - 10.72i$	1.87
1725.3	1625.10	1531.80, $-$ 6.09%	$1612.40 - 32.96i$	5.26
1925.6	1725.00	1674.80, $-$ 2.91%	$1719.60 - 15.33i$	2.67
2106.1	2086.80	1941.90, $-$ 6.94%	$2071.00 - 46.48i$	6.65
2344.6	2292.00	2030.90, $-$ 11.39%	$2270.20 - 83.06i$	11.78
2474.4	2464.70	2254.30, $-$ 8.54%	$2444.10 - 61.95i$	8.42

Table 6.9: Frequency comparison using 40 Elements (5 elements per member).

For validation of the MatLab program, frequency values with large k are compared with those from NASTRAN in which case k is infinite. The finite value of k renders the MatLab frequencies lower than those from NASTRAN. The largest difference is in frequency number 7, being about 10% lower than the NASTRAN value. For a value of k which is much lower in comparison to that used in column 2, the MatLab program gives as expected even lower frequency values as shown in column 3.

Column number 4 in the above table gives the frequencies for the same value of the joint stiffness $k = \frac{5EI}{L}$, but with joint rotational damping included. The damping renders the frequencies to be complex with a damping part and an oscillatory part. It can be seen that all the oscillatory parts of the frequencies are now higher than the undamped frequencies, column 3, due to rotational joint damping.

The effect of damping is not significant on the first frequency, being only slightly higher (183.94 Hz) than the undamped frequency (182.55 Hz). The second damped frequency shows a more significant increase of 4.3% (484.25 Hz vs. 464.22 Hz). Frequencies 3,4 and 5 again show only a smaller increase, within 2%. The higher frequencies, namely the 6^{th}, 8^{th}, 9^{th} and 10^{th} are significantly higher than their undamped counterparts as evident

in Table 6.9. In comparison, the 7th frequency shows a much lower increase, which is rather surprising because it does not fit the trend. A possible reason might be that the associated mode shape may not involve significant rotation of the frame joints.

A parametric study for this more complex structure was conducted by varying the rotational damping values in the same fashion as done previously. The frequency results are shown below in Table 6.10. These results exhibit the same characteristics as those observed before for the previous two frames. The frequencies always increase with the increase of rotational damping and reach their ultimate asymptotic values, column 2, when the damping is infinite.

$C_r = 33$	$1.5C_r = 49.5$	$2C_r = 66$	$3C_r = 99$
ω(Hz)	$\omega = \omega_d + \zeta\omega i$	$\omega = \omega_d + \zeta\omega i$	$\omega = \omega_d + \zeta\omega i$
$183.94i - 5.57$	$185.52i - 7.82$	$187.48i - 9.51$	$191.59i - 11.14$
$484.25i - 30.95$	$498.02i - 32.93$	$507.38i - 30.41$	$516.77i - 23.84$
$1086.9i - 14.38$	$1091.1i - 11.25$	$1092.9i - 8.98$	$1094.4i - 6.27$
$1357.7i - 10.79$	$1360.0i - 7.83$	$1361.0i - 6.06$	$1361.6i - 4.13$
$1401.9i - 10.72$	$1404.3i - 7.81$	$1405.2i - 6.06$	$1405.9i - 4.14$
$1612.4i - 32.96$	$1619.1i - 23.57$	$1621.6i - 18.13$	$1623.5i - 12.31$
$1719.6i - 15.33$	$1722.4i - 10.89$	$1723.5i - 8.36$	$1724.3i - 5.67$
$2071.0i - 46.48$	$2079.4i - 32.77$	$2082.6i - 25.07$	$2084.9i - 16.95$
$2270.2i - 83.06$	$2282.4i - 56.68$	$2286.7i - 42.81$	$2289.7i - 28.67$
$2444.1i - 61.95$	$2455.0i - 43.80$	$2459.1i - 33.56$	$2462.2i - 22.72$

Table 6.10: Frequency results of a 2-storey 2-bay frame with 5 elements per member.

An examination of the mode shapes obtained from NASTRAN analysis, Fig. 6.11 shows that mode shape 7 does not involve significant rotation. In comparison, mode shapes 8, 9, and 10 show extensive rotations of joints and consequently higher effect of rotational damping.

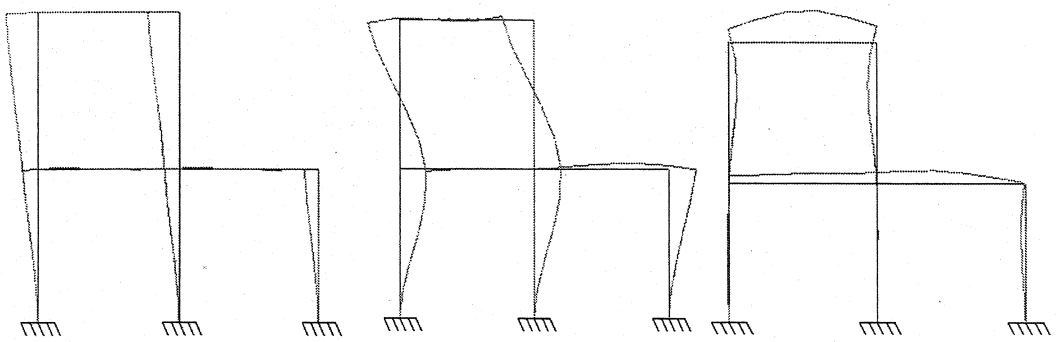

a – Mode 1. b – Mode 2. c – Mode 3.

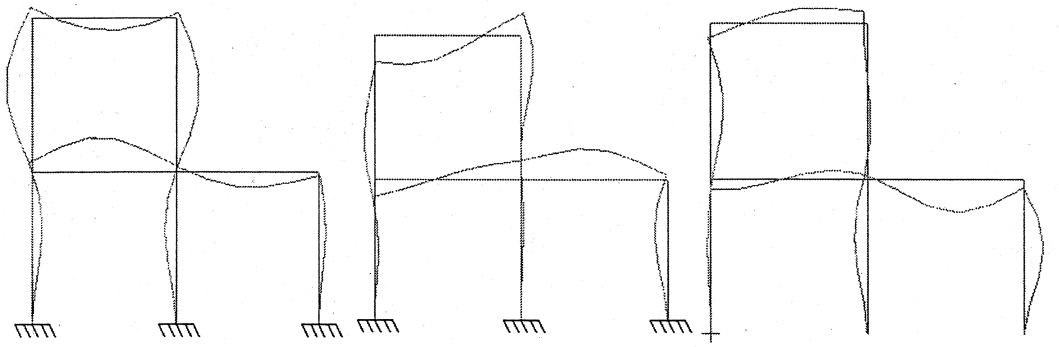

d – Mode 4. e – Mode 5. f – Mode 6.

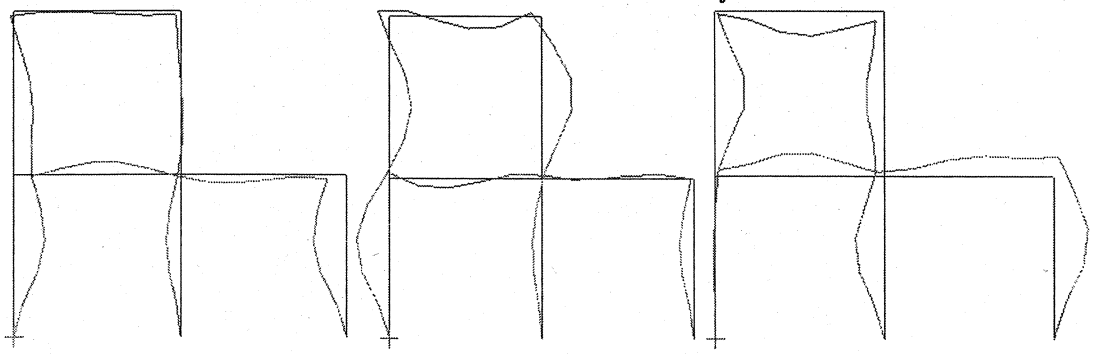

g – Mode 7. h – Mode 8. i – Mode 9.

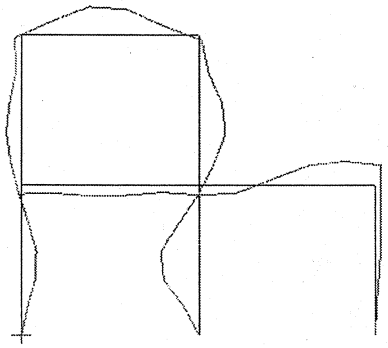

j – Mode 10.

Fig. 6.11 : NASTRAN mode shapes of the 2-storey 2-bay frame.

6.6 The MatLab Program

The MatLab Program mentioned above and used in the calculation of the frequencies of the three frames, was constructed by the author by assembling the subroutines provided in Reference [19]. Extensive modifications were necessary to include joint damping and finite joint stiffness in the main program. A flow chart and the listing of the program are provided in Appendix A.

The information has to be prepared before it is entered into the program. The numbering of (1) joints, (2) elements, and (3) degrees of freedom have to be chosen. This requires taking into account the extra degrees of freedom which are associated with joints allowing rotations. This numbering, for example, has been shown in Fig. 6.7 for the 2 storey 2 bay frame.

The main program starts with the control information. These include the number of elements, nodes per elements, total number of nodes of the system and, total number of degrees of freedom in the system. Then, nodal coordinates (x, y) are specified.

Next the material properties are entered, namely, Young's Modulus, the cross-section area, moment of inertia of the members and, mass density of the material. Now, since this is a program that takes into account the rotational stiffness and rotational damping, it is necessary to include their values. Different spring constants and different damping constants may be used for joints with 2 members, 3 members or 4 members. These constants are chosen by the user. Then, nodal connectivity for each member is read and the degrees of freedom associated with the boundary conditions are specified.

Before assembly, different matrices are initialized to zero according to their proper dimensions. The assembly is started by looping over first the members and second over the joints. Member stiffness and mass matrices are computed and assembled and put into the corresponding global stiffness matrix $[K]$ and global mass matrix $[M]$ in accordance with the degrees of freedom associated with the ends of the member.

Rotational stiffness matrix is computed and added to the global stiffness matrix $[K]$ appropriately according to the rotational degrees of freedom at the joint. Simultaneously, rotational damping matrix is constructed and added to the global rotational damping matrix $[C]$

again according to the rotational degrees of freedom at the joint. Note that matrix $[C]$ is quite sparse containing only the terms due to rotational joint damping. On the other hand, $[K]$ and $[M]$ are banded matrices. The assembly is done with the help of the subroutine called Asm1 for members as well as joints. Boundary conditions are then applied to reduce the size of the global matrices by deleting the rows and columns corresponding to the constrained degrees of freedom. The reduced $[K]$, $[M]$ and $[C]$ for the system are now ready for solving the quadratic eigenvalue problem (QEP):

$$\lambda^2[M]\{\phi\} + \lambda[C]\{\phi\} + [K]\{\phi\} = \{0\} \tag{6.50}$$

to find the eigenvalues λ and the corresponding mode shapes ϕ. The MatLab program provides this facility through the "polyeig" command. The command gives the complex eigenvalues and the associated mode shapes.

When the system is undamped, one may use the simpler command "eig" for solving the generalized eigenvalue problem (GEP):

$$[K]\{\phi_1\} = \mu[M]\{\phi_1\} \tag{6.51}$$

which gives frequencies $\omega = \dfrac{\sqrt{\mu}}{2\pi}$. The frequencies are sorted in the ascending order by using the command "sort".

6.7 Summary of the chapter

In this chapter we have presented the eigenvalue analysis of plane frames in which joints allow relative rotations of members meeting at the joints. Thus, joints do not necessarily have infinite stiffness, but may have different finite values specified by the analyst. The relative rotation can be hindered by rotational damping present at the joint. The damping of the structure is modeled by assigning damping constants at the selected joints.

Three frames of increasing complexity were chosen for analysis. The analyses were performed by using the finite element method. Programs were constructed using the (1) Mathematica software and (2) MatLab software. These programs incorporated the finite rotational stiffness and rotational damping of the joints. NASTRAN finite element code was also used, but since it does not allow for inclusion of rotational damping it could not be used for the analysis of these frames. It was used only for the verification of the

undamped cases of the Mathematica and MatLab results. For all three frames, the first 10 frequencies of the in-plane vibration were determined by assigning different values of stiffness and damping constants.

As expected when the joint rotations are permitted by virtue of finite joint stiffnesses, the frequencies are lower than when joints are assumed to be rigid. It is found that when rotational damping is introduced at joints allowing relative rotations, the frequencies increased. As the rotational damping increases, the frequencies continue to increase, but not indefinitely. They reach their maximum values which are those corresponding to the frequencies of a rigid jointed frame. The increase in frequencies is not uniform, but is dependent upon the mode shapes. The most effect is seen on those frequencies which are associated with mode shapes that involve significant bending.

Finally, the constructed MatLab program was described (Appendix A). This program can be used for analysing other plane frames with rotational joint damping.

CHAPTER 7

CONCLUSION

This thesis has been based on the premise that it is important to take into account rotational joint damping of aerospace structures in a realistic way for an accurate dynamic analysis, especially as it relates to the updating of finite element models in conjunction with the experimental data.

The significance of the concept was demonstrated in chapter 3 where rotational damping was first introduced and compared with translational damping. It was shown that the effect of rotational damping is significant and is not confined only to low frequency modes. This chapter provides the proof of the concept of rotational joint damping having a significant influence on the frequency of free vibration.

The practical proof of this concept was attempted by conducting dynamic modal testing on a simple frame. The experiment was designed to determine the effect of joint damping on frequencies. The experiment was successful. However, only two frequencies could be determined as the structure proved to be quite stiff for the frequency range of the measuring equipment.

Exact undamped frequencies for the tested frame were obtained by the transfer matrix method. These frequencies served as benchmarks for later calculations by the constructed MatLab and Mathematica programs, as well as, the NASTRAN code.

The final chapter formulates the theoretical concepts for use in the FE method. Three frames of different configurations were considered using the constructed MatLab programs. Different rotational joint stiffness and rotational damping constants were used to determine the effect of joint damping. It was found that in all cases the rotational joint damping affected the frequencies significantly. It was observed that the higher percentage difference was found in the higher frequencies. The effect of rotational joint damping was found to be dependent on the nature of the associated mode shapes. The effect on the frequency was highest for modes with significant bending. As a corollary, it must also be said that the effect of damping was less in modes dominated by translational motion.

Traditionally, in updating the analyst is concerned with matching the first few frequencies, say 5 frequencies, and finds it difficult to match higher frequencies. This difficulty may now be overcome by including appropriate rotational joint damping which will affect the higher frequencies more than the lower ones. Of course, this option of updating can be used in conjunction with other updating options. This gives a flexibility to the analyst to tune the FE model to correspond to its experimental behaviour. This method of updating should be used, especially if the analyst realizes the NASTRAN mode shapes show a lot of bending.

7.1 Proposal For Further Research

- A thorough experimental investigation should be undertaken to determine the stiffness of different types of joints and also the damping constants associated with these joints under different types of bolts and torques.

- The methodology presented in this thesis can be extended to 3D frames.

REFERENCES

1. Beards, C.F., Williams J.L. (1977). "The Damping of Structural Vibration By rotational Slip In Joints", Journal of Sound and Vibration, Vol. 53, No. 3, pp. 333-340.

2. Beards, C.F. (1985)."Damping In Structural Joints", Shock Vib. Dig.17, pp.17-20.

3. Tedesco, J. W., McDougal, W. G. and Ross, C.A. *Structural Dynamics Theory and Applications,* Addison Wesley Longman, Inc., 1998.

4. Bishop, R.E.D. and Gladwell, G.M.L. (1963). "An Investigation into the Theory of Resonance Testing", Philosophical Transactions of the Royal Society of London,Vol. 255 A.1055, pp. 241-280.

5. Ewins, D. J. *Modal Testing: Theory and Practice*, Research Studies Press Ltd., England, John Wiley & Sons Inc., 1984.

6. Mia, N.M.M. and Montalvao e Silva, J.M. *Theoretical and Experimental Modal Analysis*, Research Studies Press Ltd., England, John Wiley & Sons Inc., New York, 1996.

7. Avitable, P., Foster, T, and O'Callahan, J. (1994)."Comparison of Reduction Vs. Expansion For Orthoganality Checks", Proc. SPIE Vol. 2251, Proceedings of the 12th International Modal Analysis Conference (IMAC), Honolulu, Hawaii, Jan. 31-Feb. 3, p. 225.

8. Breitfeld, T. (1996). "A Method for Identification of a Set of Optimal Measurement Points for Experimental Modal Analysis", The International Journal of Analytical and Experimental Modal Analysis, Vol.11, No.1, pp. 1-9.

9. Avitable, P., Pechinsky, F. (1994). "Coordinate orthoganality check (CORTHOG)", 12th International Modal Analysis Conference (IMAC), Honolulu, Hawaii, Jan. 31-Feb. 3, pp. 753-760.

10. Friswell, M.I. and Mottershead, J.E. *Finite Element Model Updating in Structural Dynamics*, Kluwer Academic Publishers, 1995.

11. Zheng, W. (1996). "Modal Test for Finite Element Model Validation of Space Structures", CASI Conference on Astronautics - Towards the Next Century in Space, 9th, Proceedings; 12-15 Nov. 1996, pp. 254-261.

12. CADA X software, version 3.4. CADA X is a registered trademark of LMS Engineering Innovation, Researchpark Z1, Interleuvenlaan 68, 3001 Leuven, Belgium, Tel: +32 16 384 200, Fax: +32 16 384 350.

13. Biggs, J. M. *Introduction to Structural Dynamics*, McGraw Hill, Inc., 1964.

14. PATRAN 90.3/MSC NASTRAN 70.7. MSC Software Corporation, 2 MacArthur Place, Santa Ana, CA 92707 USA, Tel: (714) 540-8900, Fax: (714) 784-4056.

15. MATLAB, version 5.3.1 for students. MATLAB is a registered trademark of The Math Works, Inc. 24 Prime Park Way, Natick, MA 01760, Tel: (508) 647-7000, Fax (508) 647-7001.

16. Mathematica 4.0 for students. Mathematica is a registered trademark of The Wolfram Research, 100 Trade Center Drive, Champaign, IL 61820-7237 USA, Tel : (217)-398-0700, Fax: (217)-398-0747.

17. Pestel and Leckie. *Matrix Methods in Elastomechanics,* McGraw-Hill Book Company, 1963.

18. Cook, R. D., Malkus, D. S., Plesha, M. E. and Witt, R.J. *Concepts and Applications of Finite Element Analysis*, 4th addition. John Wiley & Sons, 2002.

19. Kwon, Y. W. and Bang, H. *The Finite Element Method using MatLab*, CRC Press, Inc. 1997.

BIBLIOGRAPHY

Armstrong, D.M., Sibbald, A., Fairfield, C.A. and Forde, M.C. 1995 "Modal Analysis for Masonry Arch Bridge Spandrell Wall Separation Identification", NDT & E international ISSN 0963-8695, Vol. 28 No.6, pp. 377-386.

Avitable, P. and Foster, T.J. 1995 "Evaluation of Degree of Freedom Based Vector Correlation Methods" IMAC 14, pp.1-9.

Balasubramanian, P., Jagadeesh, J.G., Suhas, H.K. and Ramamurti, V. 1994 "Modal Methods for the Analysis of Cyclic Symmetric Structures", Computer & Structures, Vol. 50 No. 1, pp. 67-77.

Bert, C.W. 1973 "Material Damping: An Introductory Review of Mathematical Models, Measures and Experimental Techniques" Journal of Sound and Vibration, Vol. 29 (2), pp. 129-153.

Bruzzone L.E. and Molfino R.M. 2006 "A Geometric Definition Of Rotational Stiffness And Damping" International Journal of Robotics and Automation, Vol. 21, No. 3.

De Clerck, J.P. and Avitable, P. 1995 "Development of Several New Tools for Pre-Test Evaluation" IMAC 14, pp. 1-5.

Den Hartog, J.P., 1930 "Forced Vibrarions with Combined Viscous and Coulomb Damping" Phil.Mag.,9 pp. 801-817.

Deo, A. and Walker I.D. 1993 "Overview of Damped Least-Squares Methods for
Dossing, O. 1995 "Going Beyond Modal Analysis, Or IMAC In A New Key", The International Journal of Analytical and Experimental Modal Analysis, Vol.10 (2), pp. 69-83.

Earles, S.W.E 1966 "Theorectical Estimation of the Frictional Energy Dissipation in a Simple Lap Joint" Journal Mechanical Engineering Science, Vol. 8 No.2, pp. 207-214.

Ehrich, F.F., 1992, " Handbook of Rotordynamics" , USA, McGRAW-HILL Inc., pp.2.1-2.25.

Inman, D.J., 1990 "Matching Analytical Models With Experimental Modal Data In Mechanical Systems", Control and Dynamic Systems. Vol. 37, pp. 327 - 363.
Inverse Kinematics of Robot Manipulators" Journal of lntelligent and Robotic Systems Vol. 14, pp. 43-68.

Karpel, M. and Ricci, S. 1997 "Experimental Modal Analysis of Large Structures by Substructuring", Mechanical Systems and Signal Processing, Vol. 11(2), pp. 245-256.

Kozin, F. and Natke, H.G. 1986 "System Identification Techniques", Structural Safety, Vol. 3, pp. 269-316.

Lin, R.M., Lim, M.K. and Du, H. 1995 "Improved Inverse Eigensesitivity Method for Structural Analytical Model Updating" Journal of Vibration and Acoustics, Vol. 117, pp. 192-193.

Maia, N.M.M., Silva, J.M.M. and Ribeiro, A.M.R 1994 "A New Concept in Modal Analysis: The Characteristic Response Function (CRF)", The International Journal of Analytical and Experimental Modal Analysis, Vol.9 (3), pp. 191-202.

Mitsugu, A., Yuji, Y. et al 2003 "Development of active-damping bridges and its application to triple high-rise buildings" JSME international journal. Series C, Mechanical systems, machine elements and manufacturing, vol. 46, no3, pp. 854-860.

Okubo, N. 1994 "Modal Analysis - Toward Virtual Design", The International Journal of Analytical and Experimental Modal Analysis, Vol.9 (2), pp. 71-76.

Pandey, A.K. and Biswas, M. 1995 "Damage Diagnosis of Truss Structures by Estimation of Flexibility Change", The International Journal of Analytical and Experimental Modal Analysis, Vol.9 (2), pp. 104-117.

Penny, J.E.T., Friswell, M.I. and Garvey, S.D 1994 "Automatic Choice of Measurement Locations for Dynamic Testing" AIAA Journal, Vol. 32, No. 2, pp. 407-414.

Piedboeuf, J-C, Carufel, J. and Hurteau R. 2000 "Friction and Stick-Slip in Robots: Simulation and Experimentation" Multibody System Dynamics, Vol. 4, pp. 341-354.

Rei, O. and Tetsuro, T. 1999 "Effect of hysteresis damping to a high-rise building on vortex-induced oscillations. Response estimation due to equivalent damping and stiffness", Vol. no79, pp. 119-120.

Richardson, R.S.H 1976 "Vibration Damping by Friction in Stuctural Joints" Vibration and Noise Control Engineering Proceedings, pp. 117-118.

Richardson, R.S.H. and Nolle, H. 1977 "Energy Dissipation in Rotary Structural Joints" Journal of Sound and Vibration, Vol. 54 (4), pp. 577-588.

Schlesinger, A. 1979 "Vibration Isolation in The Presence of Coulomb Friction" Jounal of Sound and Vibration, Vol. 63 (2), pp. 213-224.

Slanik, M.L., Nemes, James, Potvin, M-J and Piedboeuf, J-C 2000 "Time Domain Finite ELement Simulations of Damped Multilayered Beams Using a Prony Series Representation" Mechanics of Time-Dependent Materials, Vol. 4, pp. 211-230.

Stabb, M. and Blelloch, P 1995 "Application of Flexibility Shapes to Sensor Selection" IMAC 13th, Nashville, TN, pp. 1255-1262.

Tadeo, A. T., Cavalca, K. L. 2003 "A comparison of flexible coupling models for updating in rotating machinery response" J. Braz. Soc. Mech. Sci.& Eng. vol.25 no.3 Rio de Janeiro.

Targoff, W.P. 1976 "Orthogonality Check and Correction of Measured Modes" AIAA Journal, Vol. 14 No.2, pp. 165-167.

Toshiya, S., Hiroshi et 2004 "Vibration Characteristics of High-rise Buildings with High-damping Stories" Reports of Technical Research Institute of Sumitomo Mitsui Construction Co., Ltd. Vol. no.2, p. 13.

Ungar, E.E 1964 "Energy Dissipation at Structural Joints; Mechanisms and Magnitudes" Air Force Flight Dynamics Lab. Rept. FDL-TDR-64-98, AD-607257.

Ungar, E.E. and Carbonell, J.R 1966 "On Panel Vibration Damping Due to Structural Joints" AIAA Journal, Vol. 4 No.8, pp. 1385-1390.

Wang H., Gao X.H., Jin M.H., Du L.B., Li T.Q., Liu H., "A Passive Robot System for Measuring Spacesuit Joint Damping Parameters", Proceedings of the 1003 IEEE International Conference on Robotics &Automation, Taipei, Taiwan, Sep. 14-19, 2003.

Williams, E.J. and Earles, S.W.E. 1974 "Optimization of the Response of Frictionally Damped Beam Type Structures With Reference to Gas Turbine Compressor Blading" Journal of Engineering for Industry, Trans.ASME, 96 pp. 471-476.

Xu, M., Marangoni, R. D., 1994, "Vibration Analysis of a Motor-Flexible Coupling-Rotor System Subject to Misalignment and Unbalance", Part I: Theorical model and analysis, Part II: Experimental validation. Journal of Sound and Vibration, Vol. 176, pp. 663-691.

APPENDIX A

FLOWCHART AND LISTING OF THE MATLAB PROGRAM

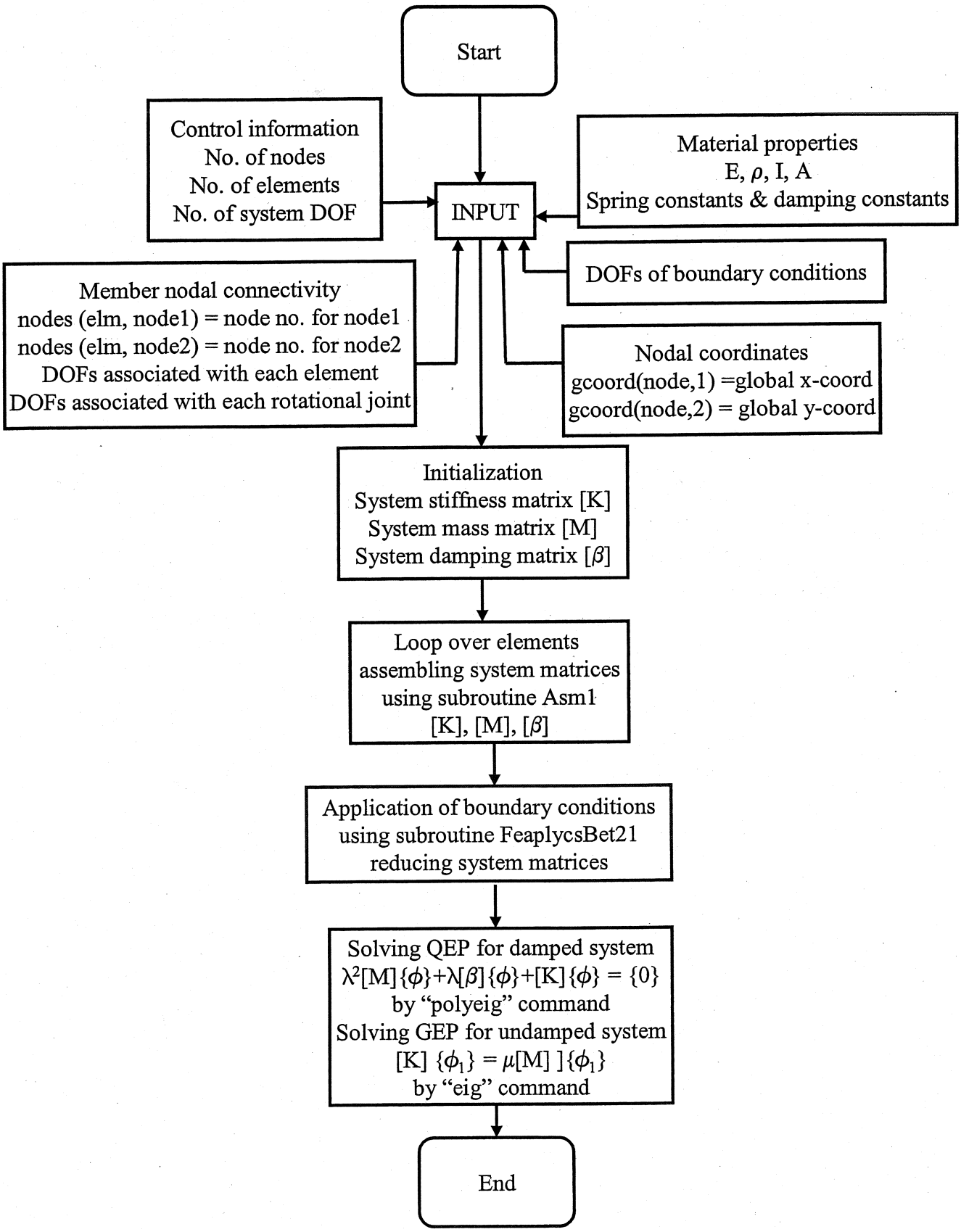

Fig. A.1 Flow Chart for the MatLab Program for a 2-Storey 2-Bay Frame

```
%-------------------------------------------------------------------------%
%   2 Storeys 2 Bays Frame                                                %
%   PLEASE REFER TO THE TEXT FOR EXPLANATIONS AND DIAGRAM                 %
% This program was assembled to find the natural frequencies for a        %
% 2-d frame using beam elements                                           %
% Problem description                                                     %
% Find the natural frequencies of a frame which is made of three columns  %
% and three beams of length of 15 in (0.381 m) each as described in the text %
% All members have                                                        %
% cross-sections of 3 in (0.0762 m) x 1/8 in (0.003175 m).                %
% The elastic modulus is 7.17 E10 Pa.                                     %
% The Frame has a mass density of 2767.99 Kg/m^3. 40 elements are used    %
% Rotational Stiffness and Rotational Damping are introduced into the sysem. %
% Variable descriptions                                                   %
%   x and y = global x and y coordiates of each node                      %
%   k = element stiffness matrix                                          %
%   kk = system stiffness matrix                                          %
%   m = element mass matrix                                               %
%   mm = system mass matrix                                               %
%   index1 = a vector containing system dofs associated with each element %
%   index2 = a vector containing system dofs associated with each         %
%    Rotational Joint with 2 members                                      %
%   index3 = a vector containing system dofs associated with each         %
%    Rotational Joint with 3 members                                      %
%   index4 = a vector containing system dofs associated with each         %
%    Rotational Joint with 4 members                                      %
%   bcdof = a vector containing dofs associated with boundary conditions  %
%                                                                         %
%                                                                         %
%-------------------------------------------------------------------------%
%                                                                         %
%       SPECIFYING CONTROL INFORMATION                                    %
%                                                                         %
%-------------------------------------------------------------------------%
%
%
clc;
nel=40;                 % number of elements
nnel=2;                 % number of nodes per element
ndof=3;                 % number of dofs per node, except rotational joints
nnode=(nnel-1)*nel;     % total number of nodes in system
sdof=128;               % total system dofs
%
%
%
%-------------------------------------------------------------------------%
%       SPECIFYING NODAL COORDINATES                                      %
%-------------------------------------------------------------------------%
%       The Nodal coordiantes specify the position of each                %
%       node of the element with respect to the global coordinate.        %
%       For example,                                                      %
%                                                                         %
%       gcoord(node,1) = Global x-coordinate                              %
%       gcoord(node,2) = Global y-coordinate                              %
%-------------------------------------------------------------------------%
%
%
gcoord(1,1)=0.0;            gcoord(1,2)=0.0;
gcoord(2,1)=0.0;            gcoord(2,2)=0.0762;
gcoord(3,1)=0.0;            gcoord(3,2)=0.1524;
```

```
gcoord(4,1)=0.0;          gcoord(4,2)=0.2286;
gcoord(5,1)=0.0;          gcoord(5,2)=0.3048;
gcoord(6,1)=0.0;          gcoord(6,2)=0.381;

gcoord(7,1)=0.0;          gcoord(7,2)=0.4572;
gcoord(8,1)=0.0;          gcoord(8,2)=0.5334;
gcoord(9,1)=0.0;          gcoord(9,2)=0.6096;
gcoord(10,1)=0.0;         gcoord(10,2)=0.6858;
gcoord(11,1)=0.0;         gcoord(11,2)=0.762;

gcoord(12,1)=0.381;       gcoord(12,2)=0.0;
gcoord(13,1)=0.381;       gcoord(13,2)=0.0762;
gcoord(14,1)=0.381;       gcoord(14,2)=0.1524;
gcoord(15,1)=0.381;       gcoord(15,2)=0.2286;
gcoord(16,1)=0.381;       gcoord(16,2)=0.3048;
gcoord(17,1)=0.381;       gcoord(17,2)=0.381;

gcoord(18,1)=0.381;       gcoord(18,2)=0.4572;
gcoord(19,1)=0.381;       gcoord(19,2)=0.5334;
gcoord(20,1)=0.381;       gcoord(20,2)=0.6096;
gcoord(21,1)=0.381;       gcoord(21,2)=0.6858;
gcoord(22,1)=0.381;       gcoord(22,2)=0.762;

gcoord(23,1)=0.762;       gcoord(23,2)=0.0;
gcoord(24,1)=0.762;       gcoord(24,2)=0.0762;
gcoord(25,1)=0.762;       gcoord(25,2)=0.1524;
gcoord(26,1)=0.762;       gcoord(26,2)=0.2286;
gcoord(27,1)=0.762;       gcoord(27,2)=0.3048;
gcoord(28,1)=0.762;       gcoord(28,2)=0.381;

gcoord(29,1)=0.0762;      gcoord(29,2)=0.381;
gcoord(30,1)=0.1524;      gcoord(30,2)=0.381;
gcoord(31,1)=0.2286;      gcoord(31,2)=0.381;
gcoord(32,1)=0.3048;      gcoord(32,2)=0.381;

gcoord(33,1)=0.0762;      gcoord(33,2)=0.762;
gcoord(34,1)=0.1524;      gcoord(34,2)=0.762;
gcoord(35,1)=0.2286;      gcoord(35,2)=0.762;
gcoord(36,1)=0.3048;      gcoord(36,2)=0.762;

gcoord(37,1)=0.4572;      gcoord(37,2)=0.381;
gcoord(38,1)=0.5334;      gcoord(38,2)=0.381;
gcoord(39,1)=0.6096;      gcoord(39,2)=0.381;
gcoord(40,1)=0.6858;      gcoord(40,2)=0.381;
```

```
%-------------------------------------------------------------------------%
%       SPECIFYING MATERIAL PROPERTIES                                    %
%-------------------------------------------------------------------------%
%                                                                         %
%The material properties to be entered in the computation are shown below:%
%                                                                         %
%-------------------------------------------------------------------------%
%
ell=0.381;
el=7.170548e+10;          %   elastic modulus
area=0.000241935;         %   cross-sectional area
xi=117.07e-9;             %   moment of inertia of cross-section
rho=2767.99;              %   mass density per volume
spr2=5*el*xi/ell;         %   Node Spring Connecting 2 members
spr3=5*el*xi/ell;         %   Node Spring Connecting 3 members
```

```
spr4=5*el*xi/ell;                    %   Node Spring Connecting 4 members
b2=sqrt(4/3*rho*ell^2*area*xi*el) ; %   Rotational Damper between 2 members
b3=sqrt(4/3*rho*ell^2*area*xi*el) ; %   Rotational Damper between 3 members
b4=sqrt(4/3*rho*ell^2*area*xi*el) ; %   Rotational Damper between 4 members
%
%   Notice that the Rotational spring values spr2=spr3=spr4 are left intentionally
%   with the same value of 5EI/L. The user may choose to input different values
%   for each. Similarly, the Rotational damper values b2=b3=b4
%   where b2=Sqrt(4/3*rho*ell^2*area*xi*el)
%
%
%-------------------------------------------------------------------------------%
%  SPECIFYING NODAL CONNECTIVITY                                                %
%-------------------------------------------------------------------------------%
% The Nodal coonectivity specifies the nodal numbering of the system            %
% with respect to the elements connected to them.                               %
%                                                                               %
% nodes(Element no.,node 1 of element) = first  Global Node Number of the Element %
% nodes(Element no.,node 2 of element) = second Global Node Number of the Element %
%-------------------------------------------------------------------------------%
%
nodes(1,1)=1;       nodes(1,2)=2;
nodes(2,1)=2;       nodes(2,2)=3;
nodes(3,1)=3;       nodes(3,2)=4;
nodes(4,1)=4;       nodes(4,2)=5;
nodes(5,1)=5;       nodes(5,2)=6;
nodes(6,1)=6;       nodes(6,2)=7;
nodes(7,1)=7;       nodes(7,2)=8;
nodes(8,1)=8;       nodes(8,2)=9;
nodes(9,1)=9;       nodes(9,2)=10;
nodes(10,1)=10;     nodes(10,2)=11;

nodes(11,1)=12;     nodes(11,2)=13;
nodes(12,1)=13;     nodes(12,2)=14;
nodes(13,1)=14;     nodes(13,2)=15;
nodes(14,1)=15;     nodes(14,2)=16;
nodes(15,1)=16;     nodes(15,2)=17;
nodes(16,1)=17;     nodes(16,2)=18;
nodes(17,1)=18;     nodes(17,2)=19;
nodes(18,1)=19;     nodes(18,2)=20;
nodes(19,1)=20;     nodes(19,2)=21;
nodes(20,1)=21;     nodes(20,2)=22;

nodes(21,1)=23;     nodes(21,2)=24;
nodes(22,1)=24;     nodes(22,2)=25;
nodes(23,1)=25;     nodes(23,2)=26;
nodes(24,1)=26;     nodes(24,2)=27;
nodes(25,1)=27;     nodes(25,2)=28;

nodes(26,1)=5;      nodes(26,2)=29;
nodes(27,1)=29;     nodes(27,2)=30;
nodes(28,1)=30;     nodes(28,2)=31;
nodes(29,1)=31;     nodes(29,2)=32;
nodes(30,1)=32;     nodes(30,2)=17;

nodes(31,1)=11;     nodes(31,2)=33;
nodes(32,1)=33;     nodes(32,2)=34;
nodes(33,1)=34;     nodes(33,2)=35;
nodes(34,1)=35;     nodes(34,2)=36;
nodes(35,1)=36;     nodes(35,2)=22;
```

```
nodes(36,1)=17;      nodes(36,2)=37;
nodes(37,1)=37;      nodes(37,2)=38;
nodes(38,1)=38;      nodes(38,2)=39;
nodes(39,1)=39;      nodes(39,2)=40;
nodes(40,1)=40;      nodes(40,2)=28;

%-------------------------------------------------------------------------%
%  SPECIFYING BOUNDARY CONDITIONS                                         %
%-------------------------------------------------------------------------%
%   The following input shows the dof to be restrained, for example       %
%   the first dof to be restrained bcdof(1)=1. Note that the value in     %
%   bracket bcdof(i) is a numeration that will be used in the subroutine  %
%   "feaplycsBet21"                                                       %
%   In refering to the Fig. pertaining to this example, one can see that  %
%   these dof are those of the column supports                            %
%                                                                         %
%-------------------------------------------------------------------------%
%
bcdof(1)=1;   % transverse deflection at node is constrained
bcdof(2)=2;   % axial displacement at node is constrained
bcdof(3)=3;   % slope at node is constrained

bcdof(4)=35;  % transverse deflection at another node is constrained
bcdof(5)=36;  % axial displacement at another node is constrained
bcdof(6)=37;  % slope at another node is constrained

bcdof(7)=69;  % transverse deflection at different node is constrained
bcdof(8)=70;  % axial displacement at different node is constrained
bcdof(9)=71;  % slope at different node is constrained
%
%
%-------------------------------------------------------------------------%
%  MATRIX INITIALIZATION                                                  %
%-------------------------------------------------------------------------%
%
k=zeros(sdof,sdof);  %  initialization of element stiffness matrix
m=zeros(sdof,sdof);  %  initialization of element mass matrix
kk=zeros(sdof,sdof); %  initialization of system stiffness matrix
mm=zeros(sdof,sdof); %  initialization of system mass matrix
bet=zeros(sdof,sdof);%  initialization of system damping matrix
kn=zeros(sdof,sdof); %  initialization of the reduced system stiffness matrix
mn=zeros(sdof,sdof); %  initialization of the reduced system mass matrix
ms2=zeros(2,2);          %   initialization of the 2x2 massless spring matrix
ms3=zeros(3,3);          %   initialization of the 3x3 massless spring matrix
ms4=zeros(4,4);          %   initialization of the 4x4 massless spring matrix
index1=zeros(6,1);       %   initialization of index1 vector
index2=zeros(2,1);       %   initialization of index2 vector
index3=zeros(3,1);       %   initialization of index3 vector
index4=zeros(4,1);       %   initialization of index4 vector
```

```
%
%
%-------------------------------------------------------------------------%
%                                                                         %
%                            LOOP FOR ELEMENTS                            %
%                                                                         %
%-------------------------------------------------------------------------%
%                                                                         %
%   The following steps will lead the reader on how the program progresses %
%                                                                         %
%-------------------------------------------------------------------------%


for iel=1:nel       % loop for the total number of elements

nd(1)=nodes(iel,1);  % 1st connected node for the (iel)-th element
nd(2)=nodes(iel,2);  % 2nd connected node for the (iel)-th element

x1=gcoord(nd(1),1); y1=gcoord(nd(1),2); % coordinate of 1st node
x2=gcoord(nd(2),1); y2=gcoord(nd(2),2); % coordinate of 2nd node

leng=sqrt((x2-x1)^2+(y2-y1)^2);          % element length

if (x2-x1)==0;       % compute the angle between the local and global axes
   beta=pi/2;
 if (y2-y1)<0;
    beta=-pi/2;
    end
else
beta=atan((y2-y1)/(x2-x1));          % elemental angle calculations
end

%   The assembling process takes both into account. It associates the
%   elements or joints with the corresponding dof. Index1 indicates the
%   dof for the elements. Index2 is for a rotational joint with 2 Elm.
%   Index 3 is for a rotational joint with 3 Elm.
%   Index 4 is for a rotational joint with 4 Elm as indicated before.

if iel==1;
        index1=[1 2 3 4 5 6];
elseif iel==2;
        index1=[4 5 6 7 8 9];
elseif iel==3;
        index1=[7 8 9 10 11 12];
elseif iel==4;
        index1=[10 11 12 13 14 15];
elseif iel==5;
        index1=[13 14 15 16 17 18];
elseif iel==6;
        index1=[16 17 19 20 21 22];
elseif iel==7;
        index1=[20 21 22 23 24 25];
elseif iel==8;
        index1=[23 24 25 26 27 28];
elseif iel==9;
        index1=[26 27 28 29 30 31];
elseif iel==10;
        index1=[29 30 31 32 33 34];
elseif iel==11;
        index1=[35 36 37 38 39 40];
```

```
elseif iel==12;
        index1=[38 39 40 41 42 43];
elseif iel==13;
        index1=[41 42 43 44 45 46];
elseif iel==14;
        index1=[44 45 46 47 48 49];
elseif iel==15;
        index1=[47 48 49 50 51 52];
elseif iel==16;
        index1=[50 51 53 54 55 56];
elseif iel==17;
        index1=[54 55 56 57 58 59];
elseif iel==18;
        index1=[57 58 59 60 61 62];
elseif iel==19;
        index1=[60 61 62 63 64 65];
elseif iel==20;
        index1=[63 64 65 66 67 68];
elseif iel==21;
        index1=[69 70 71 72 73 74];
elseif iel==22;
         index1=[72 73 74 75 76 77];
elseif iel==23;
         index1=[75 76 77 78 79 80];
elseif iel==24;
        index1=[78 79 80 81 82 83];
elseif iel==25;
        index1=[81 82 83 84 85 86];
elseif iel==26;
        index1=[16 17 87 88 89 90];
elseif iel==27;
        index1=[88 89 90 91 92 93];
elseif iel==28;
        index1=[91 92 93 94 95 96];
elseif iel==29;
        index1=[94 95 96 97 98 99];
elseif iel==30;
        index1=[97 98 99 50 51 100];
elseif iel==31;
        index1=[32 33 101 102 103 104];
elseif iel==32;
        index1=[102 103 104 105 106 107];
elseif iel==33;
        index1=[105 106 107 108 109 110];
elseif iel==34;
        index1=[108 109 110 111 112 113];
elseif iel==35;
        index1=[111 112 113 66 67 114];
elseif iel==36;
        index1=[50 51 115 116 117 118];
elseif iel==37;
        index1=[116 117 118 119 120 121];
elseif iel==38;
        index1=[119 120 121 122 123 124];
        index2=[34 101]; % In here starts the assembly of the rotational joints with :
elseif iel==39;
        index1=[122 123 124 125 126 127];
        index2=[68 114];
elseif iel==40;
        index1=[125 126 127 84 85 128];
```

```
        index2=[86 128];
        index3=[18 19 87];        % Index 3 for a 3 elm joint
        index4=[52 53 100 115];   % Index 4 for a 4 elm joint
      end

    %   The "feframe2Beam" subroutine is invoked to compute element stiffness matrix

    [k,m]=feframe2Beam(el,xi,leng,area,rho,beta,1);

    ks2=springBeam2(spr2);  % creating rotational stiffness for 2 members

    ks3=springBeam3(spr3);  % creating rotational stiffness for 3 members

    ks4=springBeam4(spr4);  % creating rotational stiffness for 4 members

    bb2=dampBeam2(b2);      % creating rotational damping for 2 members

    bb3=dampBeam3(b3);      % creating rotational damping for 3 members

    bb4=dampBeam4(b4);      % creating rotational damping for 4 members

    % assemble the system stiffness matrix

    kk=Asm1(iel,kk,k,index1,ks2,index2,ks3,index3,ks4,index4);

    % assemble system mass matrix

    mm=Asm1(iel,mm,m,index1,ms2,index2,ms3,index3,ms4,index4);

    % assemble element damping matrices into system matrix

    bet=Damping1D(iel,bet,bb2,index2,bb3,index3,bb4,index4);
end
%-------------------------------------------------------------------------%
%                                                                         %
%   SOLUTION OF THE EIGENVALUE PROBLEM FOR THE DAMPED AND UNDAMPED SYSTEMS    %
%                                                                         %
%-------------------------------------------------------------------------%
% Applying the boundary conditions by invoking the subroutine "feaplycsBet21"
%
[kn,mn,betn]=feaplycsBet21(kk,mm,bet,bcdof);
%
% solving the eigenvalue problem of DAMPED SYSTEM using the "polyeig" command.
%
[X,fsol]=polyeig(kn,betn,mn);
%
fsol=fsol/(2*pi);                    % converting frequency to Hz.
%
sort(fsol)
%
[kn,mn]=feaplycsBeam(kk,mm,bcdof);  % apply the boundary conditions
%
% solving the eigenvalue problem of UNDAMPED SYSTEM using the "eig" command.
%
fsol=eig(kn,mn);                     % solve the matrix equation of undamped system
%
fsol=sqrt(fsol)/(2*pi);
%
sort(fsol)
```

```
%-------------------------------------------------------------------------%
%  BEAM ELEMENT SUBROUTINE  "feframe2Beam"                                %
%-------------------------------------------------------------------------%
function [k,m]=feframe2Beam(el,xi,leng,area,rho,beta,ipt)                  %
%-------------------------------------------------------------------------%
%  Purpose:                                                               %
%     Stiffness and mass matrices for the 2-d frame element               %
%     nodal dof {u_1 v_1 theta_1 u_2 v_2 theta_2}                         %
%                                                                         %
%  Synopsis:                                                              %
%     [k,m]=feframe2(el,xi,leng,area,rho,beta,ipt)                        %
%                                                                         %
%  Variable Description:                                                  %
%     k - element stiffness matrix (size of 6x6)                          %
%     m - element mass matrix (size of 6x6)                               %
%     el - elastic modulus                                                %
%     xi - second moment of inertia of cross-section                      %
%     leng - element length                                               %
%     area - area of beam cross-section                                   %
%     rho - mass density (mass per unit volume)                           %
%     beta - angle between the local and global axes                      %
%            is positive if the local axis is in the ccw direction from   %
%            the global axis                                              %
%     ipt = 1 - consistent mass matrix                                    %
%         = 2 - lumped mass matrix                                        %
%         = 3 - diagonal mass matrix                                      %
%-------------------------------------------------------------------------%
% stiffness matrix at the local axis

a=el*area/leng;
c=el*xi/(leng^3);
kl=[a    0           0            -a     0          0;...
    0    12*c        6*leng*c      0    -12* c      6*leng*c;...
    0    6*leng*c    4*leng^2*c    0    -6*leng*c   2*leng^2*c;...
    -a   0            0             a     0          0;...
    0   -12*c       -6*leng*c      0     12*c      -6*leng*c;...
    0    6*leng*c    2*leng^2*c    0    -6*leng*c   4*leng^2*c];

%    rotation matrix

r=[ cos(beta)   sin(beta)   0   0           0          0;...
    -sin(beta)  cos(beta)   0   0           0          0;...
        0           0           1   0           0          0;...
        0           0           0   cos(beta)   sin(beta)  0;...
        0           0           0  -sin(beta)   cos(beta)  0;...
        0           0           0   0           0          1];

% stiffness matrix at the global axis

k=r'*kl*r;

% consistent mass matrix

if ipt==1

    mm=rho*area*leng/420;
    ma=rho*area*leng/6;
    ml=[2*ma  0           0            ma    0           0;...
        0     156*mm      22*leng*mm   0     54*mm      -13*leng*mm;...
        0     22*leng*mm  4*leng^2*mm  0     13*leng*mm -3*leng^2*mm;...
```

```
        ma     0             0              2*ma   0              0;...
        0      54*mm         13*leng*mm     0      156*mm        -22*leng*mm;...
        0     -13*leng*mm -3*leng^2*mm      0     -22*leng*mm     4*leng^2*mm];

% lumped mass matrix

elseif ipt==2

    ml=zeros(6,6);
    mass=rho*area*leng;
    ml=mass*diag([0.5  0.5  0  0.5  0.5  0]);

% diagonal mass matrix

else

    ml=zeros(6,6);
    mass=rho*area*leng;
    ml=mass*diag([0.5  0.5  leng^2/78  0.5  0.5  leng^2/78]);
end
    % mass in the global system
    m=r'*ml*r;
```

```
%-------------------------------------------------------------------%
% ROTATIONAL JOINT STIFFNESS  SUBROUTINE springBeam2                %
%-------------------------------------------------------------------%
function [ks2]=springBeam2(spr2)

%   [ks2] is the Rotational Spring Matrix of a node
%   connecting two members
%   spr2 is the numerical value of 5EI/L

ks2=[spr2 -spr2;...
    -spr2 spr2];


%-------------------------------------------------------------------%
% ROTATIONAL JOINT STIFFNESS  SUBROUTINE springBeam3                %
%-------------------------------------------------------------------%
function [ks3]=springBeam3(spr3)

%   [ks3] is the Rotational Spring Matrix of a node
%   connecting three members
%   spr3 is the numerical value of 5EI/L

ks3=[2*spr3 -spr3  -spr3;...
      -spr3 2*spr3 -spr3;...
      -spr3 -spr3  2*spr3];


%-------------------------------------------------------------------%
% ROTATIONAL JOINT STIFFNESS  SUBROUTINE springBeam4                %
%-------------------------------------------------------------------%
function [ks4]=springBeam4(spr4)

%   [ks4] is the Rotational Spring Matrix for a node
%   connecting four members
%   spr4 is the numerical value of 5EI/L

ks4=[3*spr4 -spr4  -spr4    -spr4;...
     -spr4 3*spr4 -spr4 -spr4;...
      -spr4 -spr4  3*spr4   -spr4;...
        -spr4   -spr4     -spr4 3*spr4];
```

```
%-------------------------------------------------------------------------%
%   ROTATIONAL JOINT DAMPING SUBROUTINE dampBeam2                         %
%-------------------------------------------------------------------------%
function [bb2]=dampBeam2(b2)

%   [bb2] is the Rotational Damping Matrix of a node
%   connecting two members
%   b2 is the numerical value of sqrt(4/3*rho*ell^2*area*xi*el)

bb2=[b2 -b2;...
  -b2 b2];

%-------------------------------------------------------------------------%
%   ROTATIONAL JOINT DAMPING SUBROUTINE dampBeam3                         %
%-------------------------------------------------------------------------%
function [bb3]=dampBeam3(b3)

%   [bb3] is the Rotational Damping Matrix of a node
%   connecting three members
%   b3 is the numerical value of sqrt(4/3*rho*ell^2*area*xi*el)


bb3=[2*b3 -b3  -b3;...
    -b3 2*b3 -b3;...
    -b3 -b3  2*b3];


%-------------------------------------------------------------------------%
%   ROTATIONAL JOINT DAMPING SUBROUTINE dampBeam4                         %
%-------------------------------------------------------------------------%
function [bb4]=dampBeam4(b4)

%   [bb4] is the Rotational Damping Matrix of a node
%   connecting four members
%   b4 is the numerical value of sqrt(4/3*rho*ell^2*area*xi*el)


bb4=[3*b4 -b4  -b4  -b4;...
    -b4 3*b4 -b4    -b4;...
    -b4 -b4  3*b4   -b4;...
     -b4 -b4  -b4   3*b4];
```

```
%-------------------------------------------------------------------%
%    SYSTEM MATRIX ASSEMBLY SUBROUTINE Asm1                         %
%-------------------------------------------------------------------%
function [kk]=Asm1(iel,kk,k,index1,ks2,index2,ks3,index3,ks4,index4)
%-----------------------------------------------------------
%  Purpose:
%     Assembly of element matrices into the system matrix
%
%  Synopsis:
%     [kk]=Asm1(iel,kk,k,index1,ks2,index2,ks3,index3,ks4,index4)
%
%  Variable Description:
%    kk - system matrix
%    k  - element matrix
%    index1 - d.o.f. vector associated with an element
%       ks2 -   stifness matrix associated with a joint connecting two elements
%       index2  -   d.o.f. vector associated with a  joint connecting two elements
%       ks3 -   stifness matrix associated with a joint connecting three elements
%       index3  -   d.o.f. vector associated with a  joint connecting three elements
%       ks4 -   stifness matrix associated with a joint connecting four elements
%       index4  -   d.o.f. vector associated with a  joint connecting four elements
%-----------------------------------------------------------
edof1 = length(index1);
for i=1:edof1
    ii=index1(i);
       for j=1:edof1
            jj=index1(j);
            kk(ii,jj)=kk(ii,jj)+k(i,j);
        end
 end
    if iel >=38;    % Note at this element value indexing2 starts
    edof2=length(index2);
    for i=1:edof2
    ii=index2(i);
         for j=1:edof2
            jj=index2(j);
          kk(ii,jj)=kk(ii,jj)+ks2(i,j);
        end
    end
  end
    if iel ==40;        % Note at this element value indexing3 and 4 start
    edof3=length(index3);
    for i=1:edof3
        ii=index3(i);
            for j=1:edof3
                jj=index3(j);
                kk(ii,jj)=kk(ii,jj)+ks3(i,j);
        end
    end
        edof4=length(index4);
          for i=1:edof4
                ii=index4(i);
                for j=1:edof4
                    jj=index4(j);
                    kk(ii,jj)=kk(ii,jj)+ks4(i,j);
                    end
                end
        end
```

```
%-------------------------------------------------------------------------%
%BOUNDARY CONDITIONS SUBROUTINE "feaplycsBet21"                           %
%-------------------------------------------------------------------------%
%                                                                        %
function [kn,mn,betn]=feaplycsBet21(kk,mm,bet,bcdof)                     %
%                                                                        %
%-------------------------------------------------------------------------%
%  Purpose:                                                              %
%     Apply constraints to eigenvalue matrix equation                    %
%     [kk]{x}=lamda[mm]{x}                                               %
%                                                                        %
%  Synopsis:                                                             %
%     [kn,mn,betn]=feaplycsBet21(kk,mm,bet,bcdof)                        %
%                                                                        %
%  Variable Description:                                                 %
%     kk - system stiffness matrix before applying constraints           %
%     kn - system stiffness matrix after applying constraints            %
%     mm - system mass matrix before applying constraints                %
%     mn - system mass matrix after applying constraints                 %
%       bet - system damping matrix before applying constraints          %
%       betn - system damping matrix after applying constraints          %
%    bcdof - a vector containging constrained d.o.f                      %
%-------------------------------------------------------------------------%

mn = mm;
kn = kk;
betn = bet;

n=length(bcdof);
sdof =size(kk,1);

  for i=1:n
  c=bcdof(i);    %   The subroutine reads the values of the bcdof(i) from
  for j=1:sdof   %   the main program and transforms them to 0 values in the
    kn(c,j)=0;% kn and bet matrices. The mn is transformed into 1 values
    kn(j,c)=0;% to retain the possibility of solving the matrix equation.
    mn(c,j)=0;
    mn(j,c)=0;
    bet(j,c)=0;
    bet(c,j)=0;
    end
  mn(c,c)=1;
end
```